Development of a Hygrothermal Simulation Tool (HAM-BE) for Building Envelope Study

Qinru Li

A Thesis

in the

Department

of

Building, Civil and Environmental Engineering

Presented in Partial Fulfillment of the Requirements

for the Degree of Doctor of Philosophy (Building Engineering)

at

Concordia University

Montréal, Québec, Canada

December, 2008

Your file Votre référence
ISBN: 978-0-494-63355-7
Our file Notre référence
ISBN: 978-0-494-63355-7

ABSTRACT

Development of a hygrothermal simulation tool (HAM-BE) for building envelope study

Qinru Li, 2008

Concordia University, 2008

To prevent the building envelope from moisture-related damages, it is essential to predict the building envelope's hygrothermal performance through a scientific approach, and further to improve the design and construction. In this thesis, an advanced numerical tool (HAM-BE) was developed to simulate the combined heat, air and moisture (HAM) transport in the building envelope. The state of the art knowledge of heat and mass transfer in building materials was applied. The major features of HAM-BE are: multi-dimensional and transient coupling of heat and moisture transport; air convection integrated in hygrothermal simulation through Darcy-Boussinesq approximation; heat transfer mechanisms of conduction and convection of sensible and latent heat; moisture transport mechanisms of vapor diffusion, capillary suction and air convection; material database of common building materials in North America; experimental settings or hourly weather data as boundary conditions; and setting moisture loading inside the materials or along the surfaces of the building envelope's hidden or exposed components to simulate the wetting process. A commercial finite element solver was chosen to solve the governing partial differential equations (PDEs) of hygrothermal transport. This approach provided building science researchers the flexibility to build, modify, and

maintain their modeling work efficiently. Validation of HAM-BE included inter-model comparison with benchmarking cases of the HAMSTAD project and comparison between numerical simulation with data of the Collaborative Research and Development (CRD) project measured by fellow students under the supervision of Drs Fazio and Rao. Through validation work, HAM-BE was proven to have great potential as an accurate and reliable research tool for the building envelope study.

As the extension of the CRD investigation, parametric study was carried out to estimate the drying performance of wood-frame walls under the climatic conditions of Montreal and Vancouver. It is demonstrated that the climate condition has the most significant influence to the drying process of the wet components in wall assemblies. The drying process occurs mainly in the summer season, and is largely restrained in the winter season. To improve outward drying, the cladding materials should have high vapor permeance, especially the sheathing membrane. The sheathing board with higher vapor permeance also facilitates drying. Under the investigated climates, the polyethylene vapor barrier at the warm side of the wall is not beneficial, rather restricts the possibility of inward drying.

Acknowledgements

The research presented in this thesis was carried out at the Centre of Building Study, in the Department of Building, Civil and Environmental Engineering, Concordia University, under the supervisor of Prof. Paul Fazio. His valuable instructions and helpful advices are greatly appreciated. His dedication and passion in the research work always inspired me in the course to complete the thesis.

I would also like to express my deep gratitude to my colleagues. Special thanks are due to Dr. Jiwu Rao, who has dedicated his expertise and patience in the review of this thesis. His detailed and constructive comments provided important support to this thesis. Dr. Hua Ge encouraged me to pursue this PhD program and also devoted warm help for my study. Dr. Qian Mao and Dr. Arslan Alturkistani, provided the experimental data of wall assemblies to evaluate the numerical model. Yang Wu, supplied the material properties from his laboratory measurement. I have also benefited from numerous discussions with other researchers: Dr. Miljana Horvat, Dr. Weimin Wang, and Xiangjin Yang. Their expertise in various fields enriched my knowledge base.

Finally, I would like to thank my wife Bo Lu, daughter Grace and son LeCheng for their understanding and support.

The financial support from Dr Paul Fazio, NSERC, and Concordia University is gratefully acknowledged.

Table of Contents

List of Figures ix

List of Tables xvi

Abbreviations xvii

Nomenclature xix

1 Introduction 1

1-1 Context of the research project 1

1-2 Knowledge gap 2

1-3 Objectives 3

1-4 Methodology 5

1-5 Outline of the thesis 8

2 Literature Review 10

2-1 Building envelope and moisture-related failure 10

2-2 Application of hygrothermal modeling in building envelope study 16

2-3 Survey of hygrothermal tools in building envelope study 19

3 Numerical Model of HAM-BE 26

3-1 Moisture retention curve of building material 27

3-1-1 moisture storage in building material 27

3-1-2 Analytical equations for moisture retention curve 30

3-2 Moisture transfer mechanisms in building envelope 36

3-2-1 Numerical equations of moisture transport 38

3-2-2 Moisture transfer under isothermal condition 47

3-2-3 Moisture transfer under non-isothermal conditions 48

3-3 Heat transport in building envelope..... 49
3-4 Air transport in building envelope..... 52
3-5 Material properties for hygrothermal modeling..... 56
3-6 Boundary conditions of hygrothermal modeling..... 61
3-6-1 Moisture flow through exterior surface..... 62
3-6-2 Heat flow through exterior surface..... 63
3-6-3 Moisture flow through interior surface..... 67
3-6-4 Heat flow through interior surface..... 67
3-7 Conservation equations of combined heat and moisture transport..... 69
3-8 Implementation of HAM-BE in COMSOL environment..... 75
3-8-1 Coefficient Form of governing equations of HAM-BE..... 75
3-8-2 Procedure of HAM-BE modeling..... 79
4 Evaluation of HAM-BE 84
4-1 Inter-model comparison against HAMSTEAD benchmarks 84
4-1-1 Case of "Insulated Roof" 86
4-1-2 Case of "Analytical Solution" 90
4-1-3 Case of "Response Analysis" 94
4-1-4 Case of "Capillary-active Insulation" 100
4-2 Validation with experimental data of full-scale walls 102
4-2-1 Introduction of the full-scale wall experiment 102
4-2-2 Comparisons between simulated and measured moisture profiles of sheathing board 115
5 Investigaiton of Wood-frame Walls' Drying Performance 129
5-1 Analysis of wall panels' drying performance under CRD experimental conditions 130
5-1-1 Calculation of RHT index 130
5-1-2 Analysis wall panels' drying performance based on RHT index 135

5-2 Investigation of wood-frame walls' drying performance exposed to climatic data of Montreal and Vancouver 137
5-2-1 Modeling of wall panels' drying performance under hourly weather data 139
5-2-2 Analysis based on numerical simulation 144
5-3 Guidelines for moisture control in wood-frame wall 171
6 Conclusion, Contribution and Future Work 182
6-1 Conclusion and Contribution 182
6-2 Future Work 185
References 188

List of Figures

Figure1.1 Section view of wood-frame wall panels..... 5

Figure 2.1 Integration of numerical modeling and experimental method in hygrothermal study of building envelopes..... 19

Figure 3.1 Moisture retention curve of a porous material 30

Figure 3.2 Moisture retention curve of plywood board 36

Figure 3.3 Vapor permeability of spruce 41

Figure 3.4 Moisture diffusivity of spruce 45

Figure 3.5 Liquid permeability of plywood board 47

Figure 4.1 Construction detail of benchmarking case "insulated roof" 87

Figure 4.2 Total moisture content of load bearing material in the first year 87

Figure 4.3 The heat flow from interior side to the wall in the first year 88

Figure 4.4 Total moisture content in load bearing material of the 5th year 89

Figure 4.5 Total moisture content in insulation material of the first year 89

Figure 4.6 Total moisture content in insulation material of the 5th year 90

Figure 4.7 Construction detail of benchmarking case "analytical case" 91

Figure 4.8 Moisture content across the sample (15.5cm to 18.5cm) after 100 hours 91

Figure 4.9 Moisture content across the sample (2cm to 4cm) after 300 hours 92

Figure 4.10 Moisture content across the sample (1.5cm to 4.5cm) after 1000 hours 92

Figure 4.11 Moisture content across the sample (7.5cm to 13cm) after 300 hours 93

Figure 4.12 Moisture content across the sample (16cm to 20cm) after 300 hours 93

Figure 4.13 Moisture content across the sample after 100, 300 and 1,000 hours 94

Figure 4.14 Construction detail of benchmarking case "response analysis" 95

Figure 4.15 Boundary loads of Benchmark case "response analysis": Outdoor and indoor temperatures 95

Figure 4.16 Boundary loads of Benchmark case "response analysis": vapor pressure and Wind-driven rain 96

Figure 4.17 Moisture profile across the two layer wall after 24 hours of simulation 96

Figure 4.18 Moisture profile across the two layer wall after 48 hours of simulation 97

Figure 4.19 Moisture profile across the two layer wall after 54 hours of simulation 97

Figure 4.20 Moisture content on outer surface during the simulation period 98

Figure 4.21 Moisture content on inner surface during the simulation period 98

Figure 4.22 Temperature on outer surface during the simulation period 99

Figure 4.23 Temperature on inter surface during the simulation period 99

Figure 4.24 Construction detail of benchmarking case "Capillary active inside insulation material" 100

Figure 4.25 Relative humidity profiles across brick/mortar/insulation wall at the end of simulation 101

Figure 4.26 Moisture content profiles across brick/mortar/insulation wall at the end of simulation 101

Figure 4.27 Moisture profiles with and without capillary conductivity 102

Figure 4.28 Floor plan of the test hut 104

Figure 4.29 Vertical section of the test hut 105

Figure 4.30 Locations of gravimetric samples (SH), moisture content pins (MC) and thermocouples (TC) on the wall panels 106

Figure 4.31 Configurations of tested wall panels 107

Figure 4.32 a) 3D view of the water tray 110

Figure 4.32 b) Load cell equipment 110

Figure 4.33 Location of water tray/load cell in the tested wall panels 110

Figure 4.34 Graphic plot of temperature (contour lines) and relative humidity (colored surface) of full-height wall assemblies 117

Figure 4.35 Measured and simulated moisture content at different heights of the sheathing board, design configurations of the wall (Panel No. 5&17): wood siding, OSB sheathing and polyethylene vapor barrier 119

Figure 4.36 Measured and simulated moisture content at different heights of the sheathing board, design configurations of the wall (Panel No. 6&18): stucco finish, OSB sheathing and polyethylene vapor barrier 119

Figure 4.37 Measured and simulated moisture content at different heights of the sheathing board, design configurations of the wall (Panel No. 7&19): wood siding, plywood sheathing and polyethylene vapor barrier 120

Figure 4.38 Measured and simulated moisture content at different heights of the sheathing board, design configurations of the wall (Panel No. 8&20): stucco, plywood sheathing and polyethylene vapor barrier 120

Figure 4.39 Measured and simulated moisture content at different heights of sheathing board, design configurations of the wall (Panel No. 9&21): wood siding, fiberboard and vapor barrier 121

Figure 4.40 Measured and simulated moisture content at different heights of sheathing board, design configurations of the wall panel (Panel No. 10&22): stucco, fiberboard sheathing and vapor barrier 121

Figure 4.41 Measured and simulated moisture content at different heights of sheathing board, design configurations of the wall (Panel No. 11 & 23): wood siding, OSB sheathing, and no vapor barrier 122

Figure 4.42 Measured and simulated moisture content at different heights of sheathing board, design configurations of the wall (Panel No. 12 & 24): Stucco, OSB sheathing and no vapor barrier 122

Figure 4.43 Measured and simulated moisture content at different heights of sheathing board, design configurations of the wall (Panel No. 13&25): wood siding, plywood sheathing and no vapor barrier 123

Figure 4.44 Measured and simulated moisture content at different heights of sheathing board, design configurations of the wall (Panel No. 14&26): stucco, plywood sheathing and no vapor barrier 123

Figure 4.45 Measured and simulated moisture content at different heights of sheathing board, design configurations of the wall (Panel No. 15&27): wood siding, fiberboard sheathing and no vapor barrier 124

Figure 4.46 Measured and simulated moisture content at different heights of sheathing board, design configurations of the wall (Panel No. 16&28): stucco, fiberboard sheathing and no vapor barrier 124

Figure 5.1 Averaged temperature and RH of the sheathing board, to calculate the RHT index 133

Figure 5.2 RHT indices of CRD wall assemblies 135

Figure 5.3 Wall assemblies with wet sheathing as moisture load 141

Figure 5.4 Outdoor and indoor temperatures for Montreal 142

Figure 5.5 Outdoor and indoor temperatures of Vancouver 142

Figure 5.6 Outdoor/indoor vapor pressure of Montreal 143

Figure 5.7 Outdoor and indoor vapor pressure of Vancouver 143

Figure 5.8 Drying of wet sheathing of stucco wall under Montreal and Vancouver climate data, simulated by HAM-BE 146

Figure 5.9 Drying of wet sheathing of wood siding walls under Montreal and Vancouver climate data, simulated by HAM-BE 146

Figure 5.10 Climatic map of North America 148

Figure 5.11 Monthly Drying Indices of Montreal and Vancouver 150

Figure 5.12 Drying of wet sheathing under Montreal climate 152

Figure 5.13 Drying of wet sheathing under Vancouver climate 152

Figure 5.14 Vapor permeance of stucco wall's components 157

Figure 5.15 Vapor permeance of wood siding wall's components 157

Figure 5.16 Comparison of building components' vapor permeance of two cladding types 158

Figure 5.17 Vapor permeance of wood siding wall with exterior insulation sheathing 160

Figure 5.18 Drying of wet sheathing under Montreal climate, with or without EPS 160

Figure 5.19 Drying of wet sheathing of stucco wall with and without polyethylene VB under Montreal climate 164

Figure 5.20 Drying of wet sheathing of wood siding wall with and without polyethylene VB under Montreal climate 164

Figure 5.21 Drying of wet sheathing of stucco walls with and without polyethylene VB under Vancouver climate 165

Figure 5.22 Drying of wood siding walls with and without polyethylene VB under Vancouver climate 165

Figure 5.23 High and medium levels of indoor vapor pressure used in HAM-BE modeling 167

Figure 5.24 Drying of wet sheathing of wood siding wall affected by indoor humidity level 167

Figure 5.25 Drying of wet sheathing in wood siding walls under Montreal climate, comparison between OSB, plywood and FB 169

Figure 5.26 Drying of sheathing in stucco walls under Montreal climate, comparison between OSB, Plywood and FB 170

Figure 5.27 Drying of wet sheathing in stucco wall under Vancouver climate, comparison between OSB, Plywood and FB 170

Figure 5.28 Drying of wet sheathing in wood siding wall under Vancouver climate, comparison between OSB, Plywood and FB 171

List of Tables

Table 2.1 Moisture sources and defending methods for building envelopes 15

Table 3.1 One to one correspondence between relative humidity and capillary pressure 33

Table 3.2 Heat, air and moisture transfer mechanisms of HAM-BE 55

Table 3.3 Material properties and corresponding measurement methods 57

Table 4.1 Configurations of the wall panels in the experiment 108

Table 4.2 Boundary condiotns and moisture load of the CRD experiment 111

Table 4.3 Material properties used in numerical simulation 112

Table 4.4 Possible causes of deviation between experiment and numerical simulation 126

Table 5.1 Values of RHT indices of wall panels from numerical simulation 134

Table 5.2 Simulation cases to investigate the influence of weather condition 145

Table 5.3 Categories of building materials' vapor permeance 154

Table 5.4 Vapor permeance of building materials in wood-frame walls 155

Table 5.5 Simulation settings to investigate the influence of exterior insulation board 159

Table 5.6 Simulation settings to investigate the performance of vapor barrier under Montréal and Vancouver climates 162

Table 5.7 Features of sheathing membranes 178

Abbreviations

ASHRAE: American Society of Heating, Refrigerating and Air-Conditioning Engineers

ASTM: American Society for Testing and Materials

CHAMPS: Combined Heat, Air, Moisture, and Pollutants Transport in Building Environmental Systems

CMHC: Canada Mortgage and Housing Corporation

CRD: Collaborative Research & Development project

CWC: Canadian Wood Council

DI: Drying Index

EIFS: Exterior Insulation and Finish System

EPS: Expanded polystyrene sheathing

FEM: Finite Element Method

FB: Fiberboard

GUIs: Graphic user interfaces

HAM: Heat, Air and Moisture

HAM-BE: Heat, Air, and Moisture transport in Building Envelope

HAMSTAD: Heat, Air, and Moisture Standards Development

IAQ: Indoor air quality

IEA:	International Energy Agency
IRC:	Institute for Research in Construction
MC:	Moisture Content
MEWS:	Moisture Management for Exterior Wall Systems
NRC:	National Research Council of Canada
OSB:	Oriented Strand Board
PDEs:	Partial differential equations
RH:	Relative Humidity
RHT:	Relative Humidity and Temperature
SBPM:	Spun bonded polyolefin membrane with crinkled surface
VB:	Vapor Barrier
VOC:	Volatile Organic Compound
WRB:	Weather Resistant Barrier
WUFI:	Wärme und Feuchte instationär - Transient Heat and Moisture

Nomenclature

Latin letters

D_w (m^2/s) liquid diffusivity of porous material

$g = 9.81$ (m/s^2) acceleration due to gravity

g ($kg/m^2 \cdot s$) flow of moisture

k_a ($kg/m \cdot s \cdot Pa$) air permeability of material

K_l (s) liquid water permeability

L_v (J/kg) enthalpy of evaporation/condensation

m ($kg/m^2 \cdot s$) moisture flow rate

$M_w = 0.018$ (kg/mol) molar water mass

p_a (Pa) air pressure

P_c (Pa) capillary pressure

P_{sat} (Pa) saturated water vapor pressure

P_v (Pa) partial water vapor pressure

q (W/m^2) heat flow rate

Q_m ($kg/m^3 \cdot s$) moisture source

Q_h (W/m^3) heat source

R_v ($J/kg \cdot K$) gas constant for water vapor

t (s) time

T (K) temperature

T^{eq} (K) equivalent temperature

u (%, kg(moisture)/kg(dry material)) moisture content by mass

w (kg/m^3) moisture content in mass of volume

v (m/s) air velocity

Greek letters

α ($W/m^2 \cdot K$) surface heat transfer coefficient

$\beta (1/K)$ thermal expansion coefficient of air

$\beta_p (kg/m^2 \cdot s \cdot Pa)$ surface vapor transfer coefficient

$\delta_p (kg/m \cdot s \cdot Pa)$ water vapor permeability

η_a $(kg/m\ s)$ dynamic viscosity of air

λ $(W/m \cdot K)$ thermal conductivity

μ (-) vapor resistance factor of material

$\mu_a (kg/m \cdot s)$ dynamic viscosity of air

ξ (-) moisture storage capacity

$\rho (kg/m^3)$ density of material

$\varphi (\%)$ relative humidity

ϕ (-) driving potential in transport equations

Subscript

a	air	*m*	moisture
dry	dry condition	*n*	normal direction
e	exterior side of building envelope	*surf*	surface
en	enthalpy heat	*sat*	saturation state
h	heat	*w*	water
i	interior side of building envelope	*wet*	wet condition
l	liquid	*v*	vapor

1 Introduction

1-1 Context of the research project

Wood-frame buildings dominate the low-rise dwelling/commercial buildings in North America. They are light-weight, easily built, durable and environmentally friendly. However, they also can be susceptible to moisture-related damage if not well designed and built. To comply with the strict requirements of energy use, currently building envelopes are built with thick insulation and airtight approach. This practice has reduced significantly the building envelope's tolerance to moisture intrusion. Moreover, to pursue fast construction and reduced cost, new materials and building envelope systems were implemented with insufficient consideration given to design details to cope with the moisture loads on the envelope. The moisture sources can be interstitial condensation of vapor diffusion, cold condensation of air leakage, wetting during construction and ground water; but the primary source leading to the premature damage is rain penetration (Rousseau 1999). Rain water can pass through poorly designed/constructed interface details on the claddings, reach the materials at the back of the claddings and sometimes accumulate in the stud cavities. In various locations across Canada and the States, building failures due to moisture damages were reported (Kudder & Erdly 1998, Barrett

1998, Karagiozis 2003). In the benchmarking survey completed by CMHC, Rousseau (1999) investigated 37 houses with moisture problems, which included cladding systems of stucco, wood siding and vinyl siding. Ninety percent of the problems were related to details between wall components.

The possible moisture-related building envelope failures include stain of drywall, reduced thermal resistance of insulation materials, deformation of envelope's components, rust/ corrosion of metal fasters, and fungi growth and deterioration of indoor air quality (IAQ). The most severe threaten is the rot of organic materials by decay fungi.

1-2 Knowledge gap

To improve the durability of the building envelope in its service life, it is necessary to predict the precise hygrothermal response of the specific building envelope under the climate condition where it is erected. This work requires the scientific method developed from multi-discipline knowledge of heat/mass transfer, accurate measurement of material properties, collection and analysis of climate loads and also construction practices. However, the current building envelope design is driven more by "rule of thumb" rather than scientific principles. There is insufficient information from scientific analysis to support design improvements and revisions to the building code; also, there is lack of reliable tool for accurate assessment of the envelope performance and local guidelines for

the choice of material and structure details for different climate zones in Canada.

In the past two decades, numerical modeling has proliferated and drawn growing attention as an efficient method to study hygrothermal performance of building envelopes. Various numerical tools have been published (Rode 1990, Kunzel 1995, Hens 1996, Burch 1997, Karagiozis 1999, Hagentoft 2002ab, Salonvaara 2004, Janssen et al. 2007) and successful applications reported (Kunzel 1998, Beaulieu et al. 2001, Hens 2002, Karagiozis 2002). However, most hygrothermal tools were originated from research projects with diverse purposes and interests. Significant differences among them exist as: the choice of moisture state variables, the transfer mechanisms included in the conservation equations, the handling of material properties and boundary conditions, and the degree of validation. Also, due to different choices of numerical methods and programming languages, availability and ease of use, extensibility by programmers and users, and/or interchangeability are less certain. This situation was described by Rode (2006) as follows: "generally however, such tools are not in the public domain, and may only have been partly documented and validated. The models are scarcely maintained, and can very often be operated only by the person(s) who developed them".

1-3 Objectives

The objectives of this thesis include the development of an advanced numerical tool for hygrothermal modeling and application of the numerical tool to investigate the

hygrothermal behavior of several types of wood-frame wall systems under the climatic conditions of selected locations in Canada.

The hygrothermal tool developed can handle transient and multi-dimensional heat, air and moisture (HAM) transport in multi-layer building envelopes. It can treat mixed vapor-liquid flow accurately: to apply material properties of common building materials in North America; to couple severe meteorological phenomena including solar radiation, long-wave radiation, precipitation and wind as the boundary condition; and to set moisture source at the boundary of building components or inside the building materials to simulate internal moisture load. Moreover, the numerical tool should be easy to operate and flexible to be modified/extended for various research projects.

With the hygrothermal tool, the hygrothermal performance of wood-frame walls with various design configurations under specific climate zones have been investigated through numerical simulation. The structure of walls reflects the common practice of Canadian residential construction. The studs are 2X6 or 2X4 lumbers, with fibrous insulation filled in the stud cavities. Sheathing boards are nailed at the exterior side of the studs, and gypsum boards are nailed at the interior side of the studs. The exterior claddings of the wall panels were wood siding on furring with spun bonded polyolefin membrane with crinkled surface and 3 coating stucco with 2 layer asphalt impregnated papers (Figure 1.1). The moisture sensitive components are the wood frame and the wooden sheathing boards. The parameters investigated include the locations, types of claddings: wood siding or stucco; the type of sheathing boards: oriented strand board

(OSB), plywood or fiberboard; and the presence and absence of polyethylene vapor barrier.

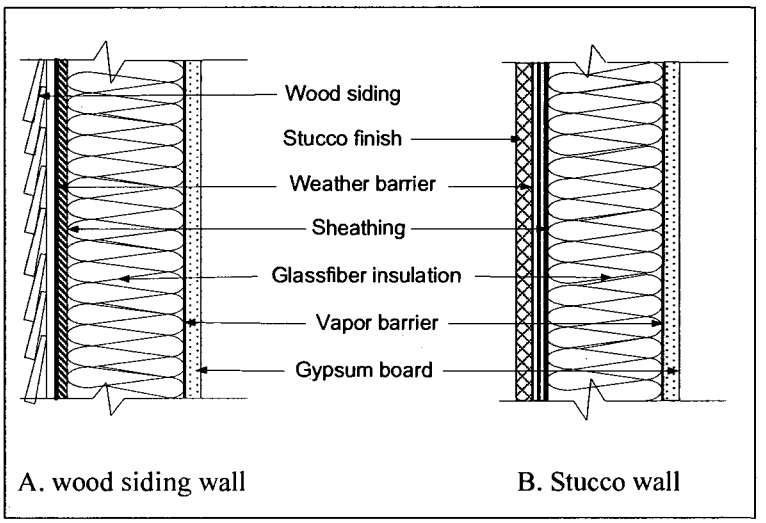

Figure 1.1 Section view of wood-frame wall panels (Fazio et al. 2006a)

1-4 Methodology

A numerical tool to predict combined heat, air, and moisture (HAM) transport in building envelopes, (abbreviated as HAM-BE) was developed by making use of commercial finite element software, COMSOL-MULTIPHYSICS (COMSOL for short hereafter) (COMSOL 2007), to solve the governing partial differential equations (PDEs) of hygrothermal transport. HAM-BE is a research tool for simulating transient HAM responses in multi-layer and multi-dimensional building envelope systems. State of the art knowledge of heat and mass transfer in building materials is applied. The heat transfer

mechanisms are conduction and convection of sensible and latent heat. The moisture transfer mechanisms are vapor diffusion driven by water vapor pressure gradient, vapor flow with air convection and liquid flow driven by capillary pressure gradient. Buoyancy flow in fibrous insulation filled stud cavities is treated by the Darcy-Boussinesq approximation. The material properties used in HAM-BE are drawn from laboratory measurements of thermal conductivity, thermal capacity, sorption isotherm, water retention, vapor permeability, liquid diffusivity and air permeability. The material properties are expressed as analytical or interpolation functions of moisture state variables. The boundary conditions of HAM-BE can be hourly data of meteorological parameters, including temperature, water vapor pressure, solar radiation, wind speed, and precipitation; or specific settings. Moreover, HAM-BE has the capacity to set moisture sources inside the material or along the surface of the building envelope's hidden or exposed components to simulate the wetting process.

COMSOL as a commercial PDEs solver provides equation-based models and fully coupled multi-physics modeling in 2D and 3D; also, it can work together with MATLAB/SIMULINK for extended modeling. The user can define the entire simulation target through user-friendly GUIs (graphic user interfaces); or through a script file. The user avoids elaborate work in implementing and verifying the solution algorithm and input/output interfaces, and can thus focus on the physical model of his/her research. Hosted by the COMSOL, HAM-BE has the flexibility for the user to

build/modify/extend models; moreover, the modeling work can be easily maintained and transferred between different projects or research groups.

To verify the presented numerical tool, including its governing equations, material data, boundary setting and their integration, and also to test the accuracy and efficiency of COMSOL as a modeling environment, two tasks were carried out. First one is the inter-model comparison with the benchmarks of the HAMSTAD project. The EU initiated the HAMSTAD project (Heat Air and Moisture Standards Development) to develop a standardized HAM modeling procedure to replace the less accurate Glaser method (Hagentoft 2002a, b). As one major contribution of the project, five benchmarking cases were developed to validate the existing and future hygrothermal tools (Adan et al. 2003). The second part validation is to compare with data of a laboratory experiment of full-size wall panels measured by fellow students under the supervision of Drs Fazio and Rao. Thirty-one full-size wall assemblies with various design configurations were constructed as the enclosure of a two-story test hut built within a large environmental chamber (Fazio et al. 1997, 2006a, 2007). A specially-designed water tray glued on a load cell was located on the top surface of the bottom plate of each wall assembly and served as the internal moisture loading. Moisture evaporating from the tray would move into the space of the stud cavity, be absorbed in part by surrounding materials, and transport in part to outside of the assembly. In tailoring HAM-BE for this experiment, wall assemblies are modeled by 2D vertical sections cross the exterior to interior of the assembly. The hygrothermal properties used in simulation were derived from material data from

dedicated measurements of the same materials used in the experiments (Wu et al. 2008). The moisture loading of the internal water tray in a wall assembly was modeled by a constant-moisture-flow boundary condition at the bottom of the stud cavity, while the flux value was taken as the measured water evaporation rate of the water tray. The comparisons focused on the temporal moisture content (MC) profiles at three heights of the sheathing. The predicted moisture contents produced by HAM-BE were compared with moisture contents measured by gravimetric samples at selected locations close to the centerline of sheathing.

In both the validation tasks, HAM-BE presents satisfactory reliability and accuracy to predict the hygrothermal performance of building envelopes. The influences of the weather loads and design configurations to the drying performance of wood-frame wall systems are investigated through parametric analysis by numerical simulation. Guidelines of design strategy and material selection are summarized based on the numerical simulation.

1-5 Outline of the thesis

This thesis composes of six chapters. Chapter 1 introduces the need to prevent failures of wood-frame buildings due to moisture accumulation, the application of hygrothermal modeling in building envelope study, the requirement of accurate prediction of building envelopes' drying performance and the advanced numerical tool, the objectives and

method of the thesis. Chapter 2 summarizes the defense strategies against moisture penetration implemented in wood-frame building envelope systems, and research activities and the current status of hygrothermal modeling. The numerical model of the HAM-BE, based on the state of the art theory of combined heat and mass transport in porous materials, is developed in Chapter 3. Chapter 4 presents the validation work to verify the presented numerical tool through inter-model comparison and comparison with the measured data of experiment of large-scale wall assemblies carried out by Dr. Fazio's team. Chapter 5 describes the parametric analysis of selected wood-frame wall systems' drying performance under certain moisture load based on numerical modeling, and design guidelines of better moisture management. Chapter 6 concludes the work of this thesis and proposes possible work to extend the research.

2 Literature Review

2-1 Building envelope and moisture-related failure

Building envelope protects the indoor environment from severe outdoor surroundings, and was defined by Watt (1999) as an enclosure that "buffers or filters external conditions for internal needs". The building envelope has multi-layer components to control transfer of heat, air, moisture, noise and light, and also to provide privacy and aesthetic sense.

In North America, wood is a traditional and popular material for building frames and building envelopes. The application of wood as building materials can be traced back to the early immigrants who brought building skill from Europe and combined it with the vernacular forest resources. From then until present, "Wood is by far the preferred building material for residential construction in North America, and is becoming increasingly popular in commercial and industrial construction" (CWC 2007). Moreover, wooden materials are widely used for interior partitions, floors, foundations and exterior/interior finishes. The invention of engineered wood products, like oriented strand board (OSB), plywood, fiberboard, glued beam, laminated veneer lumber (LVL) and so on, extend the utility of wood resource; and have been applied widely in the building industry.

The residential building envelopes constructed by traditional methods and materials could had excellent durability without moisture problems because the cavities between wood studs usually were not filled with insulation materials and the frames were not wrapped by moisture-resistant membranes, e.g. polyethylene sheet, felt paper, weather resistance barrier (WRB) and housewrap. The building envelope systems had high vapor permeance to release moisture absorbed or accumulated during a rain. After the 1970s' energy crisis, with the pursuit of low energy consumption in building systems and also comfortable indoor environments of temperature, sunlight, and flexibility of building styles, building envelopes have increasingly been built with thick insulation and airtight approach. The well-insulated envelope results in improved thermal performance and reduced energy demand. However, this change also significantly reduces the moisture tolerance of the building envelope system and also affects the moisture balance between the system and the outdoor/indoor surroundings. The challenge to the practice of air/moisture-tight design is the increasing moisture-related problems, since moisture intrusion has less chance to dry out from an air and vapor tight envelope. It seems that as the airtightness and insulation level increases so does the risk of moisture-related failures. A 1998 survey of residential buildings in the metropolitan area of Seattle (ORNL 2001) revealed that about 70% of surveyed multi-family residential buildings reported moisture damage. The problem is not limited to Seattle. Atlanta, Wilmington, and other high-humidity areas also report growing problems from moisture damage to buildings (Hen et al. 2007).

The moisture sources with respect to the building envelope can come from indoor,

outdoor and accidental sources. The indoor sources are mainly the raised indoor humidity level from the occupants and their behaviors, such as the moisture generation in manufacture process for industrial buildings, and cocking and washing for residential buildings. The outdoor sources are the humid air, precipitation in the forms of rain or snow, and ground water around the foundation. The accidental sources include usage of wet materials, wetting during construction (construction dampness), pipe leakage and flooding. In all the possible sources, rain penetration is identified as the most prominent one. The exterior moisture, mostly from direct rain penetration, is a contributing factor in 91% of moisture-related problems (Tom 2001). Pushed by wind pressure, rain drops can pass the joints/penetration/interfaces on the cladding and result in partial or thorough penetration of the building envelope. Most reported rain penetrations were related to the details on the exterior façades, such as the joints, doorways, balconies, and especially windows. "The water was found to enter the wall assemblies at interface details, primarily at windows, at the perimeter of decks, balconies and walkways, and at saddle locations. The problems with these details were found to be related to aspects of the design and construction rather than operations or maintenance, or the materials themselves." (Rousseau 1996). "35% to 48% of newly installed windows were found to leak through the window unit itself, through joints between the window and the rough opening, or both." "100% of installed residential windows examined after years in service were found to leak either through the window unit itself or at points of attachment to the building" (Journal of Light Construction 2003).

Moisture accumulation in building envelopes can cause various type degrading and deterioration. The building components can be discolored or stained. The insulation materials can lose their thermal resistance and result in increasing energy consumption (Gaur & Bansal 2002, Mendes et al 2003). Fluctuating change of moisture content and temperature can cause deformation of wooden materials. Under suitable temperature and moisture content level, mildew and mold can grow on the surfaces of organic building materials and the distribution of spores can cause health risks of disorder, asthma, dizziness and even lethal asphyxia to occupants (McNeel et al. 2003, Haverinen & Vahteristo et al. 2003, Husman 2004, Fazio et al. 2005). Decay fungi can deteriorate building materials, and even cause collapse of the structures (Carll & Highley 1999).

Building designers and builders of Canadian construction industry face the challenges from various climatic conditions to construct comfortable, healthy, energy efficient and most importantly, durable buildings. The eastern and middle regions of Canada have a long cold and humid winter and high-precipitation summer, while the pacific coast region is warm and rainy. Faced with such distinct natural features, localized design guidelines should be developed. The usage of composite boards (mainly the OSB, plywood and fiberboard) increases uncertainties and requires systematic investigations and more suitable standards for design and construction (Bomberg & Onysko 2002). Moreover, new cladding systems with improved thermal performance, vapor and air resistance, e.g. pre-manufactured structural insulated panel, insulated concrete forms and Exterior Insulation Finish Systems (EIFS), were introduced in the market on a regular basis; it

requires the corresponding design guide and efficient construction method.

Hazleden and Morris (1999) summarized the characteristics that building envelopes must have to prevent moisture-related damage as the 4Ds: deflection of rain by the cladding, drainage after rain water penetrates the exterior surface, drying of wet components, and durability of building materials. Since it is not practical to build and maintain the building envelope absolutely moisture-tight during its entire service life, the envelope should have certain moisture tolerance or drying capacity to properly cope with situations when water may penetrate the cladding and even accumulate in the stud cavity. In such cases the moisture content (MC) of the building materials surrounding the penetrated water should remain below threshold MC values deemed to induce damage while the drying of the moisture is in progress. Moreover, research has discovered that the moisture exchange between interior and exterior surroundings of a building has the function to maintain a healthy and comfortable indoor environment and reduce energy consumption (Annex 41, 2005). Therefore, to keep the moisture contents of building envelope's components at the safe level and avoid extreme moisture accumulation is critical to the durability of the building envelope system and should be thoroughly considered in the design of the system's configuration and selection of materials. The moisture sources and the responding methods to defend against its penetration in building practice are listed in Table 2.1.

Table 2.1 Moisture sources and defending methods for building envelopes

	Moisture resource	Defense means
1	Wind driven rain	1. Rain avoiding design by building geometry and orientation 2. Overhangs to reduce rain exposure 3. Rain screen principle: pressure equivalence, drainage, capillary break and ventilation 4. Flashings around interface details, e.g. windows, balcony, doors, joints etc. 5. Two-stage sealant
2	Air leakage	1. continuity of air barrier 2. control of indoor air pressure
3	Snow	1. Slope roof 2. Insulated roof and air-vapor barrier above ceiling
4	Ground water	1. Drainage system around foundation 2. Capillary break covering below-grade walls 3. direct runoff water away by slope
5	Indoor source: people and appliances	1. Breathable walls 2. Ventilation and dehumidification equipment 3. Vapor barrier to control vapor diffusion 4. Air barrier to eliminate air leakage
6	Construction dampness	1. Avoiding wet materials 2. Site cover of unfinished structure 3. Drying before wrapping the frame 4. Electric heater instead of water-generation heater

Investigation of hygrothermal performance of the building envelope requires multi-discipline knowledge from the theory of heat mass transfer, measurement technique of material properties, data collection and analysis of climate loads and also construction practice. However, current building envelope design is driven more by "rule of thumb" rather than scientific principles. There is insufficient information from scientific analysis to support design improvements and revisions to the building code. Moreover, there is lack of reliable tools for accurate assessment of the building envelope's performance; there is also a lack of local guidelines for the choice of material and structure details for different climate zone in Canada. Huge restoration cost and occurring litigations due to moisture-related building failures (Barrett 1998, Karagiozis & Desjarlais 2003) has prompted a growing research interest of the heat and moisture transport in envelope's components and the development of practical defending methods.

2-2 Application of hygrothermal modeling in building envelope study

In the study of building envelopes' hygrothermal performance (specially drying performance), experimental methods have been applied in various research projects. Salonvaara (Salonvaara et al. 1998) investigated the drying performance of wood-frame walls with wood sidings. Lawton (Lawton et al. 1999) applied water injection tubes at

the top of the insulated stud cavities as the moisture source in the experiment of stucco-clad walls' drying performance. Hazleden and Morris (2001) investigated drying performance of wood-frame walls with built-in moisture content in the building components. Van Straaten (2003) measured ventilation and drying performance of vinyl siding and brick clad by field experiment. Teasdale-St-Hilaire et al. (2003) carried out a series of experiments to apply water-contained blocks or water injection tubes to simulation rain infiltration and estimated the drying performance of wood-frame walls. Fazio et al. (2006a, b; 2007) developed the test method to estimate the relative drying performance of wood-frame walls by applying the internal moisture source inside the stud cavity and carried out a large-scale laboratory experiment of 31 wall panels with different configurations (Alturkistani et al. 2008).

The ongoing Annex 41 Project (Whole Building Heat, Air and Moisture Response (MOIST-EN)) aims to achieve the knowledge of whole building heat, air and moisture balance and its effects on indoor environment, energy consumption, and the envelope's durability. The tasks are twofold. Part 1 is to study the physics principles of heat, air, moisture response in whole building. Part 2 is to study whole building HAM response to indoor comfort, envelope durability, and energy consumption. (Hens 2003; Woloszyn & Carsten, 2007)

In the past twenty years, numerical modeling tools have been developed with improving accuracy and proliferated in the study of building envelopes' hygrothermal performance. Compared to experimental method, validated numerical modeling is low cost,

time-saving and has great predictability and controllability. Based on heat and mass conservation in the representative elementary volume of the building materials, the governing equations of the hygrothermal modeling tools can be solved by resorting to various numerical methods, e.g. finite different, finite volume and finite element methods. The material properties used by hygrothermal tools can be obtained from laboratory measurements of pore volume distribution, sorption isotherm, water retention, vapor permeability, liquid absorption, air permeability, thermal conductivity/specific capacity, and so on. The boundary conditions of a hygrothermal tool can be specific settings of the experiment or climatic data recorded by meteorological stations.

Since hygrothermal tools were built with a series of presumptions or simplifications, the accuracy and scope of application of a hygrothermal tool need to be verified through theoretical analysis and laboratory or field experiments. After validation, hygrothermal tools can be used as "virtual laboratory" for extensive parametric analysis in the range of appropriate application. Both the experimental and numerical methods can be applied to increase the understating of building envelopes' hygrothermal behavior and further develop guideline to improve the current design and construction practice. Meanwhile, the construction practice can raise new requirement and set objectives for the development of experimental and numerical modeling approaches. The relation between numerical modeling, the required knowledge base, and design and construction practice can be illustrated in Figure 2.1.

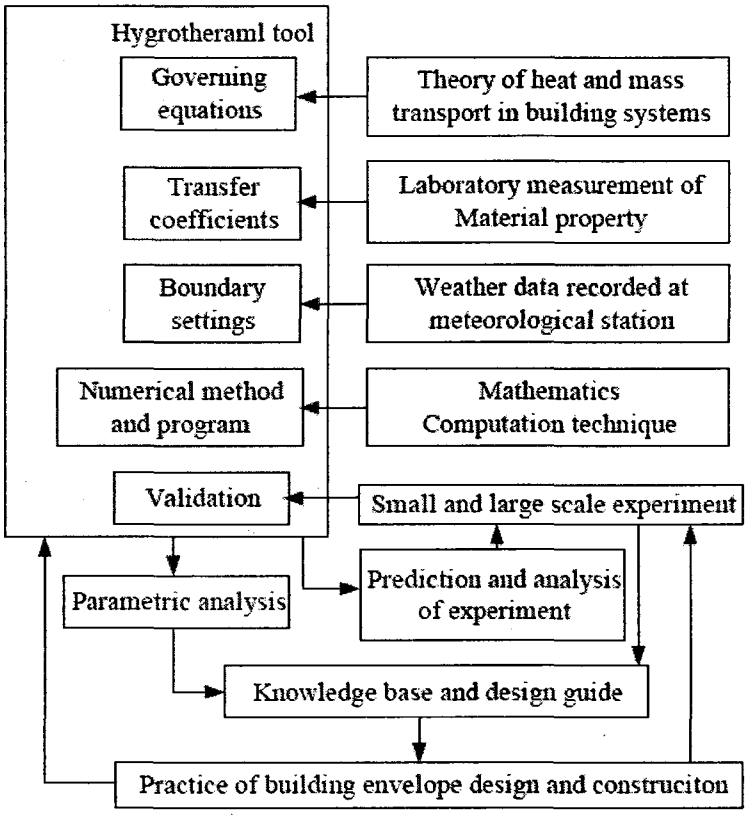

Figure 2.1 Integration of numerical modeling and experimental method in hygrothermal study of building envelopes

2-3 Survey of hygrothermal tools in building envelope study

Simple calculation tools to predict inner condensation at the interface of multi-layer building envelope have been developed based on the "Dew Point" or "Glaser Method" (TenWolde 1994), such as CONDENSE (Gowri 1990, Rivard 1993, Gerbasi 2005). CONDENSE is user-friendly and it was successful in introducing designers to a quantitative analysis of moisture and temperature conditions in the building envelope. However, the application of the simple calculation tools is quite limited, since these tools

treated the heat/moisture transport in building envelopes as one dimension, steady-state and linear process. No consideration was given to transient coupling of heat and mass (moisture and air) transport, hygroscopic features of porous materials, moisture-dependent material properties, and complex boundary conditions.

The transient, nonlinear (the material properties of heat/moisture transport are moisture dependent) hygrothermal tools are based on the energy and mass conservation of the representative elementary volume. With the development of numerical computation techniques, the coupled heat and mass transport in building envelopes, expressed as partial differential equations, can be calculated more accurately and efficiently. On the other hand, they require operators with extensive knowledge in building science.

In the Doctoral thesis of Carsten Rode (1990), a transient and nonlinear numerical model to calculate coupling heat and mass transfer in building envelope was developed. The one-dimensional model applied vapor diffusion and liquid suction as moisture transfer mechanisms. The hysteresis phenomenon of moisture storage in porous materials was included in the format of moisture isotherm curve. Burch and Chi (1997) published a free download software MOIST to simulate hygrothermal transport through building envelope. The MOIST is also a one-dimensional hygrothermal model and no consideration of air flow is included. The material database of MOIST contains common building materials in North America. The weather file covers major cities of North America and an indoor climate model also was provided. The MOIST provided graphic interfaces for model operation. Moreover, the user can define material properties through

simplified equations. After the initial publication, no update of the model was done in recent years.

Kunzel (1995) presented a hygrothermal model for building envelope in his Doctoral thesis, and later developed the WUFI program in the IBP (Institute of Building Physics, German). The first published WUFI was one-dimensional and applied relative humidity as the driving potential of moisture transport. After its publication, WUFI was used in various research projects and received continuous update to include two-dimensional version. WUFI-ORNL is the American version of WUFI by cooperation between IBP and ORNL (Oak Ridge National Laboratory, USA), which has extensive material database and climate files for North America application. The free downloaded WUFI-ORNL is a 1D hygrothermal model and no air convection is considered. In WUFI-ORNL, simplified formats of material properties are applied and the model user also can input the material properties for particular interest. A weather generator also was provided to allow the user to define the exterior and interior boundary conditions in the acceptable formats of WUFI.

hygIRC is IRC's hygrothermal model for research purpose. It can do one-dimensional and two-dimensional simulation. Relative humidity and moisture content are applied as driving potentials for moisture transfer. hygIRC was used in the MEWS project to carry on extensive parametric analysis in the analysis of major cladding systems' drying performance under selected climatic conditions of North American cities. The 1D version of hygIRC is a free downloaded tool for interested researchers and engineers, and the 2D

version is not accessible to public users.

MOIST-EXPERT is the research-oriented hygrothermal model of ORNL, and not published. MOIST-EXPERT has advanced features of moisture transport driven by moisture and temperature gradients, and air convection; wind-driven rain as boundary condition; and temperature-dependent material properties. A series of research projects have been carried out with application of the tool (Karagiozis, 2002, 2005).

CHAMPS (CHAMPS 2006) is a newly released hygrothermal model, which is developed from the DELPHINE program (Grunewald 200a, b) and can be downloaded for non-commercial users. The model is a joint product of Building Energy and Environmental Systems Laboratory (BEESL), Syracuse University, U.S.A and Institute for Building Climatology (IBK), University of Technology Dresden (TUD), Germany. CHAMPS applies coupled heat, air, moisture and salt transport in building materials and has the capacity of multiple-dimensional simulation. As the advanced feature, CHAMPS can coupled VOC (Volatile Organic Compounds) transport with HAM transport through the building envelope. CHAMPS allows the user to input material properties and boundary conditions through pre-defined formats of CHAMPS.

To clarify the purpose and application of the hygrothermal tool, Hens (1996) categorized the existing hygrothermal tools into three types: simplified hygrothermal models, full models for research purpose and engineering models for universal designer and engineer in the final report of the Annex 24 project (Heat, Air and Moisture Transfer in Highly Insulated Building Envelopes). Grunewald et al. (2003) further illustrated this

categorization of hygrothermal tools. In the simplified hygrothermal models, the moisture transport potential is empirical, e.g. moisture content gradient and the moisture transfer coefficient is secondary, e.g. moisture diffusivity. The material properties are simplified as a series of fixed functions for every material. The research models apply moisture transport potentials based on thermodynamics, e.g. capillary pressure and other possible potentials, and primary moisture transfer coefficient, e.g. liquid permeability. The material properties are described by individual forms for best accuracy. The engineering model is a type of simplification of the research model. It also applies capillary pressure gradient and liquid permeability, but with fixed functions for material properties. The purpose of engineering models is to transform scientific knowledge (complicated but accurate determination of moisture transfer coefficients and material properties) to practice (efficient measurements to determine the material properties with acceptable accuracy).

The above listed hygrothermal tools are originated from research projects with diverse purposes and interests. Significant differences between these HAM tools exist as: the choice of driving potential of moisture transport, the determination and input formats of material properties, the heat and mass transfer mechanisms included in the conservation equations, the phenomena included in the boundary conditions and the degree of validation. Even some hygrothermal tools provide graphic user interfaces to allow users to draw the objects, select materials from material database and set boundary conditions. But the users cannot modify the essential settings of the tool, such as the conservation

equations, driven potential of moisture transfer and formats of material properties. Moreover, since those tools were coded with different choices of numerical methods and programming languages, the modeling work cannot be transferred between them. In some cases, the hygrothermal tools were not well maintained and documented due to switch of research interest and personnel relocation. This situation was described by Rode (2006) as follows: "generally however, such tools are not in the public domain, and may only have been partly documented and validated. The models are scarcely maintained, and can very often be operated only by the person(s) who developed them".

One approach to develop hygrothermal tools emerged, which made use of mature environments of commercial engineering software, in particular MATLAB/SIMULINK, such as International Building Physics Toolbox (IBPT or HAM-tool) (Kalagasidis 2002, 2004; Weitzmann et al. 2003) and HAMLab (Schijndel 2002, 2005; Schellen & Schijnde 2005). The development of International Building Physics Toolbox (IBPT or HAM-tool) applied MATLAB/SIMULINK to generate modular blocks to represent various components, such as building envelopes, indoor climate, HVAC, and climate. To take advantage of the input/output interfaces and ability to link different blocks in a system, the IBPT can be used for whole building energy/moisture simulation. But the published application only applied one-dimensional heat, air and moisture transport in building envelopes. The similar HAMLab tool used the modeling environment of MATLAB/SIMULINK/COMSOL for building envelopes and whole building simulation. The COMSOL (COMSOL 2007) is commercial software to handle partial differential

equations (PDEs) by finite element method. It has built-in models for engineering/scientific phenomena that can be described by PDEs and strong capacity to couple various physical/chimerical/structural processes. Due to the public access and wide application of those engineering software, this approach provides a modular and open-source modeling platform for building physics. Using the solving algorithm, input/output interfaces of the commercial engineering software, this approach has great potential to provide researchers with time-saving and easy-operational tools. Moreover, the modeling work in MATLAB/SIMULINK/COMSOL can be shared, transferred and extended between different research groups and projects. This approach may be limited by the scope and capacity of the environments. But the limitations are being lifted with further development of the commercial entities and increase in computational power.

3 Numerical Model of HAM-BE

A numerical tool to predict combined heat, air, and moisture transport in building envelopes, abbreviated as HAM-BE, is developed by making use of the commercial finite element software, COMSOL, to solve the governing partial differential equations (PDEs) of hygrothermal transport. HAM-BE is a research tool for simulating transient HAM responses in multi-layer and multi-dimensional building envelope systems. State of the art knowledge of heat and mass transfer in building materials is applied. The heat transfer mechanisms are conduction and convection of sensible and latent heat. The moisture transfer mechanisms are vapor diffusion driven by water vapor pressure gradient, vapor flow with air convection, and liquid flow driven by capillary pressure gradient. Buoyancy flow in fibrous insulation filled stud cavities is treated by the Darcy-Boussinesq approximation. The material properties used in HAM-BE are acquired from laboratory measurements of thermal conductivity, thermal capacity, sorption isotherm, water retention, vapor permeability, liquid diffusivity and air permeability. The material properties are expressed as analytical or interpolation functions of moisture state variables. The boundary conditions of HAM-BE can be hourly data of meteorological parameters including temperature, water vapor pressure, solar radiation, wind speed, and precipitation; or they can be specific settings.

This Chapter covers the mathematical model of the HAM-BE tool: the induction of transient and non-isotherm heat and moisture conservation equations, the formats of moisture retention curve and thermal/moisture conductivities, the boundary conditions integrated of surface vapor transmit, rain absorption, solar radiation and wind flow; and the adaptation of the mathematical model in the modeling environment of the COMSOL.

3-1 Moisture retention curve of building material

3-1-1 moisture storage in building material

Most building materials are porous and have the capability to absorb moisture from the surroundings. The size, shape and distribution of the micro-pores determine the moisture storage performance of the material.

Moisture absorption in porous materials can be defined as hygroscopic and over-hygroscopic regions, distinguished by the dominant moisture transfer mechanisms. The over-hygroscopic region can be further subdivided as capillary and over-capillary regions. In the hygroscopic region, the dominant moisture transfer mechanism is vapor transfer. The surfaces of micro-pores of the material absorb water molecules and an equilibrium state can be reached between the amount of moisture absorption with the moisture state variable (relative humidity or capillary pressure) of the surrounding air. With the accumulation of vapor molecules on the pores' surfaces, the surface tension cannot bond these vapor molecules tightly and the moisture moves in the form of

'surface diffusion'. Small pores become filled with water up to the critical moisture content. When the large pores of the material start filling with water, the dominant mechanism of moisture transport switches to capillary suction, and the hygroscopic region goes into capillary region. The moisture content of the material increases steeply in this region until free water saturation is reached. A rough assumption was applied in the early literature to suggest the critical moisture content equal to the equilibrium moisture content of 98% relative humidity (Rode 1990). Recent research has revealed that the critical moisture content is material dependent, and a fixed value of relative humidity for all materials is not appropriately accurate (Carmeliet & Roels 2002).

Capillary saturation is the maximum moisture content that can be reached in normal conditions since air entrapped in partial pores cannot be evacuated except by pressured suction in laboratory condition. The over-capillary region (or supersaturated region) ranges from capillary saturation until all pores are filled by water. In this region, relative humidity is always 100%, and the capillary pressure is zero. The dominant moisture transfer mechanisms are liquid diffusion and gravity flow. In the practical environment of building envelopes, the moisture content rarely reaches this region, and in the development of hygrothermal tool for building simulation, the over-capillary region is normally not considered. The theory and application of heat and mass transport in the supersaturated region are more often found in the field of soil engineering (Carmeliet & Roels 2002).

The process of moisture taken up by the material is defined as absorption (wetting) and

the process by which the material releases moisture is defined as desorption (drying). The difference between absorption and desorption is defined as the hygroscopic hysteresis. In the hygroscopic region, the relationship between the material's moisture content and the equilibrium humidity is named as sorption isotherm. But at high RH level, the sorption isotherm can not be measured accurately, since the dominant moisture transfer mechanism switches to capillary suction and the resulting equilibrium between moisture content and capillary pressure is named as water retention or suction curve (Bomberg et al 2002). In the presented thesis, the term 'moisture retention' is used to cover the material's moisture storage character in both the hygroscopic and the over-hygroscopic regions. The moisture retention curve links the moisture contents of the material and the corresponding values of capillary pressure. An example of moisture retention curve is shown in Figure 3.1. The moisture storage stages are defines as the regions of hygroscopic, over-hygroscopic, capillary saturation and maximum saturation (Carmeliet 2002). Since the value of the capillary pressure varies over several magnitudes from hygroscopic to over-hygroscopic range, the logarithmic value of capillary pressure is applied. The absolute value of differentiation of the moisture retention curve is defined as the moisture capability (Roels et al. 1999).

Not all materials have all of the three regions in their moisture storage curve. Some are hygroscopic but non-capillary and vice versa; or, some materials are non-hygroscopic and non capillary active. For example, some fibrous insulation materials, such as mineral wool, do not absorb moisture from ambient air; when temperature is below dew point,

water vapor condenses directly in the voids between the material's fibers.

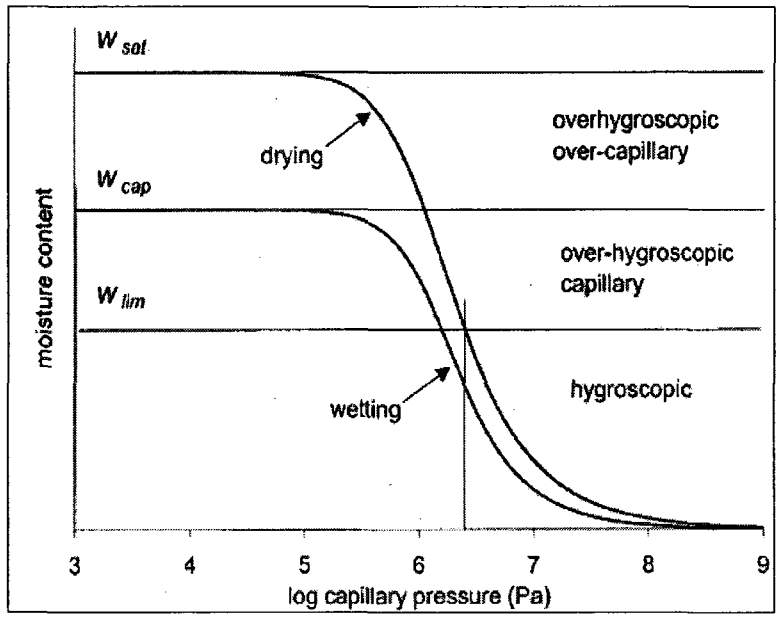

Figure 3.1 Moisture retention curve of a porous material (Carmeliet 2002)

3-1-2 Analytical equations for moisture retention curve

For hygrothermal modeling, the moisture retention curve can be expressed as analytical equations of moisture state variables, such as relative humidity or capillary pressure. The relative humidity (RH) is defined as the ratio of the actual vapor pressure and the saturation vapor pressure of the air, or the ratio of the vapor density and the saturated vapor density of the air.

$$\phi = \frac{P_v}{P_{sat}} = \frac{\rho_v}{\rho_{v,sat}} \tag{3.1}$$

where the above symbols, units in parenthesis and connotations are:

ϕ (-) relative humidity (RH)

P_v (Pa) partial pressure of vapor

$P_{sat}\,(Pa)$ saturated vapor pressure

$\rho_v\,(kg/m^3)$ vapor density

$\rho_{v,sat}\,(kg/m^3)$ saturated vapor density

The saturation vapor pressure is the function of temperature, assuming constant atmosphere pressure. Various equations exist and the one used by Kunzel (1995) is:

$$P_{sat} = 611 \cdot \exp\left(\frac{a \cdot T_0}{T_0 + T}\right) \tag{3.2}$$

where

$a = 22.44$ $T_0 = 272.44$ °C $T < 0$ °C

$a = 17.08$ $T_0 = 234.18$ °C $T \geq 0$ °C

In equilibrium condition, the gas phase pressure P_v and the liquid phase pressure P_l are satisfied by the Kelvin's relation.

$$P_l = P_{sat}(T) + R_v T \rho_l \ln \phi \tag{3.3}$$

where

$\rho_l\,(kg/m^3)$ density of water

$T\,(K)$ absolute temperature

$Rv = R/Mw$ Specific Gas Constant for Water Vapor

$R = 8314.34$ *(J/(kmol K))* Universal Gas Constant

$M_w = 18.0152$ *(kg/kmol)* Molar Mass of Water Vapor

Since the saturation vapor pressure P_{sat} is considerably smaller than the second term, it can be omitted and Eq3.3 can be rewritten as Eq3.4.

$$P_l = R_v T \rho_l \ln \phi \tag{3.4}$$

The pressure difference between surrounding air and liquid water is defined as the capillary pressure.

$$P_c = P_g - P_l \tag{3.5}$$

where P_g *(Pa)* refers to the pressure of the surrounding air, and the P_g is normally negligible in the context of building physics study. Therefore water liquid pressure is the negative value of capillary pressure, as shown in Eq. 3.6.

$$P_l = -P_c \tag{3.6}$$

therefore,

$$\ln \phi = -\frac{P_c}{\rho_l R_v T} \tag{3.7}$$

The RH and the one to one correspondent of capillary pressure are listed in Table 3.1.

Table 3.1 One to one correspondence between relative humidity and capillary pressure

Relative Humidity (-)	Capillary pressure (*Pa*)	Relative Humidity (-)	Capillary pressure (*Pa*)
0.1	3.117E+08	0.9	1.426E+07
0.2	2.179E+08	0.95	6.943E+06
0.3	1.630E+08	0.98	2.735E+06
0.4	1.240E+08	0.99	1.360E+06
0.5	9.383E+07	0.999	1.354E+05
0.6	6.915E+07	0.9999	1.354E+04
0.7	4.828E+07	0.99999	1.354E+03
0.8	3.021E+07	1	0

Different formulations are applied to the moisture retention curves. Kunzel (1995) recommends a simplified form of the BET equation with one fitting factor for both hygroscopic and capillary regions:

$$u(\phi\ ;\ b) = w_{sat}\frac{(b-1)\ \phi}{b-\phi} \tag{3.8}$$

where

$u\ (kg/kg)$ moisture content by mass

$w_{sat}\ (kg/m^3)$ saturation moisture content, which represents the maximum water

absorption of the material in normal condition

b (-) fitting factor determined from the moisture content at the relative humidity of 80%.

Another simplified form of the BET function, with three fitting factors, was used by Burch (1997) in the MOIST model and by Kumaran (1996) for the Annex 24 report.

$$w(\phi;\ a,b,c) = \frac{\phi}{a\phi^2 + b\phi + c} \tag{3.9}$$

where

w (kg/m^3) moisture content in mass of volume

a,b,c (-) fitting factors

Carmeliet and Roels (2002) sampled two porous materials: ceramic brick, which has a strong capillary and negligible hygroscopic behavior and calcium silicate, which is highly hygroscopic but less capillary active, to estimate the performance of different moisture storage equations through laboratory measurement. They concluded that the above simplified equations based on the BET model are only applicable in the hygroscopic region and not in the over-hygroscopic (capillary) region. Moreover, their research pointed out the modality (number of analytical sub-functions) as an important variable to accurately describe the measurement data. Bimodal curves are preferable to uni-modal curves, for bi-modal models include sufficient flexibility to model both

hygroscopic and over-hygroscopic regions. A more precise equation of moisture the retention curve is the van Genuchten type equation given by Durner (1994) with capillary pressure (P_c) as the moisture state variable.

$$w(P_c;\alpha,n,m) = w_{sat}\left[1+(\alpha P_c)^n\right]^{-m} \tag{3.10}$$

where

α, n, m (-) fitting factors

The bimodal equation of van Genuchten type is:

$$w(P_c;l_1,\alpha_1,n_1,m_1,l_2,\alpha_2,n_2,m_2) = w_{sat}l_1\left[1+(\alpha_1 P_c)^{n_1}\right]^{-m_1} + w_{sat}l_2\left[1+(\alpha_2 P_c)^{n_2}\right]^{-m_2} \tag{3. 11}$$

where

l_1, α_1, n_1, m_1, l_2, α_2, n_2, m_2 (-) fitting factors

However, to determine the fitting factors of a bimodal or even multi-modal equation, it requires more measured data than a uni-modal. It will be a heavy task to obtain those data for various building materials. Due to the limited material data, rather the capacity of the numerical model, in HAM-BE, the analytical equation of moisture retention curve is the uni-modal with the van Genuchten type equation. From the author's investigation, this uni-modal equation has acceptable accurate fitting results, in the scope of materials used in this study. One example of measured and fitted moisture retention curve of plywood was given in Figure 3.2.

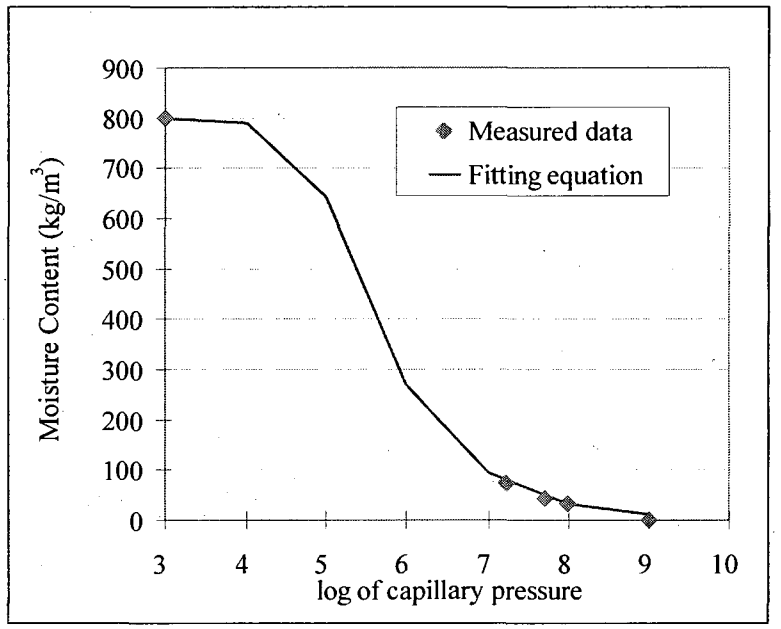

Figure 3.2 Moisture retention curve of plywood board, data source (Wu et al 2008)

3-2 Moisture transfer mechanisms in building envelope

One critical issue in the development of the hygrothermal tool is how to accurately calculate the moisture transport in porous building materials, including the choice of driving potential of moisture transport, the determination of corresponding transport coefficients and efficient method to measure the material properties. The effective method to calculate moisture flow in porous materials is to treat the vapor flow and liquid flow separately, as "phase-divided transport" (Funk & Wakili 2007). The moisture flow in porous materials can be in vapor or liquid phases and the mixture flow of vapor and liquid can be described as the sum of a series of products of moisture transfer

coefficients and gradients of driving potentials, shown in Equation 3.12.

$$q_{v+l} = \sum_{i=1}^{n} K_i \nabla \phi_i \qquad (3.12)$$

where

q_{v+l} total moisture flow of water vapor and liquid

$\nabla \phi_i$ driving potential of moisture flow, i =1,2 $\cdots$ n

∇ gradient vector, for 3 dimensional space: $\nabla f = \left(\frac{\partial f}{\partial x}, \frac{\partial f}{\partial y}, \frac{\partial f}{\partial z} \right)$

K_i corresponding moisture transfer coefficient to the driving potential

In most hygrothermal tools, the vapor flow is driven by water vapor pressure gradient and the corresponding moisture transfer conductivity is vapor permeability. For liquid flow, some hygrothermal tools chose moisture content gradient as the driving potential, but this choice was reported to be inaccurate for research purposes (Bomberg et al. 2002). The effort to verify the appropriate numerical model of moisture transport, especially liquid flow in building materials, and the determination of material properties, e.g. moisture retention and transfer coefficients, was carried out in the HAMSTAD project (Heat, Air and Moisture Standards Development) (Adan et al. 2003; Hagentoft et al. 2004). The application of water pressure gradient (or capillary pressure gradient) as the moisture driving potential and the determination of water retention curve and moisture conductivities were developed by Carmeliet & Roels (2001, 2002) and Carmeliet et al. (2004).

3-2-1 Numerical equations of moisture transport

In the development of HAM-BE, the minor moisture transfer mechanisms (effusion, electrokinesis, osmosis) were neglected in the expression; since in the determination of material properties from laboratory measurements, it is not necessary, also very difficult, to identify those insignificant transfer mechanisms separately. The measured moisture transfer conductivities include the effect of major and minor moisture transfer mechanisms. The two-phase moisture flow in porous materials cannot be divided as vapor flow and liquid flow strictly. But, an approximation to separate the total moisture flow into one vapor part and one liquid part is still helpful (so called as "phase-divided transport") (Funk & Wakili 2007). The considered moisture transfer mechanisms in HAM-BE are vapor flow in the forms of convection and diffusion, and liquid flow driven by capillary pressure.

a) Vapor flow

Vapor transfer (g_v) in porous material can be divided into convection part ($g_{v,c}$) and diffusion part ($g_{v,d}$).

$$g_v = g_{v,c} + g_{v,d} \tag{3.13}$$

Convective vapor flow

The convective vapor flow is the vapor migration with the air movement through the

porous materials. The forces of air convection can be the buoyancy force (stack effect), wind-induced pressure and mechanical force. The numerical expression of convective vapor flow through the building material is:

$$g_{v,c} = v \cdot \rho_v(\phi, T) \qquad (3.14)$$

where

$g_{v,c}$ (kg/m^2.s) convective vapor flow

v (m/s) air velocity

ρ_v (kg/m^3) water vapor density, it is dependent on temperature (T) and relative humidity (ϕ).

Diffusive vapor flow

The diffusive vapor flow is driven by mass fraction or concentration gradient. In the scope of building physics, the diffusive vapor flow can be expressed in the Fick's form: the representative transfer conductivity (vapor permeability) multiplied by the gradient of a state variable (water vapor pressure). The equation for diffusive vapor flow is written as Equation 3.15.

$$g_{v,d} = -\delta_p(w, T)\, \nabla P_v \qquad (3.15)$$

where

$g_{v,d}$ ($kg/m^2 \cdot s$) diffusive vapor flow

δ_p ($kg/m \cdot s \cdot Pa$) water vapor permeability

By adding Equation 3.14 and Equation 3.15, the vapor flow g_v can be expressed as Equation 3.16.

$$g_v = v\rho_v - \delta_p \nabla P_v \tag{3.16}$$

The water vapor permeability is closely related to the pore structure of the materials. Two pore structure models were set to describe the moisture transport in porous materials: serial-structured pore domains and parallel-structured pore domains (Grunewald & Bomberg 2003). The actual building materials consist of serial and parallel-structured pore sub-volumes. When water vapor passes through porous material, the vapor particles are bonded on the pores' surface by tension force. With accumulating of vapor particles, the surface tension cannot hold the particles tightly, and the particles start to move on the pore's surface. This phenomenon is called "surface diffusion", which is in fact in the form of liquid flow. This process raises the moisture flow gradually. The vapor permeability also increases with increase in temperature, but in most hygrothermal modeling, this influence is not considered due to relatively insignificance and also the lack of sufficient data.

The vapor permeability can be measured through the "cup method" (Mclean et al. 1992, Kumaran 1998). A test specimen of known area and thickness separates two environments that differ in relative humidity. Then the rate of vapor flow across the specimen, under steady-state conditions, is gravimetrically determined. The "dry cup" measurement is to put the sample between 50 % relative humidity and desiccant, the

measured vapor flow could be assumed as pure vapor flow. The "wet cup" measurement is to put the sample between the saturated air (100% relative humidity) and a relative humidity level higher than 50%, e.g. 75%. In this setting, the moisture flow contains not only vapor flow, but also surface diffusion (liquid flow). More accurate measurements of vapor permeability can be done through a series of cup measurements, with various settings of relative humidity cross the two side of the sample. Based on the measured data, the vapor permeability, as a function of relative humidity level of surroundings, can be obtained (Figure 3.3).

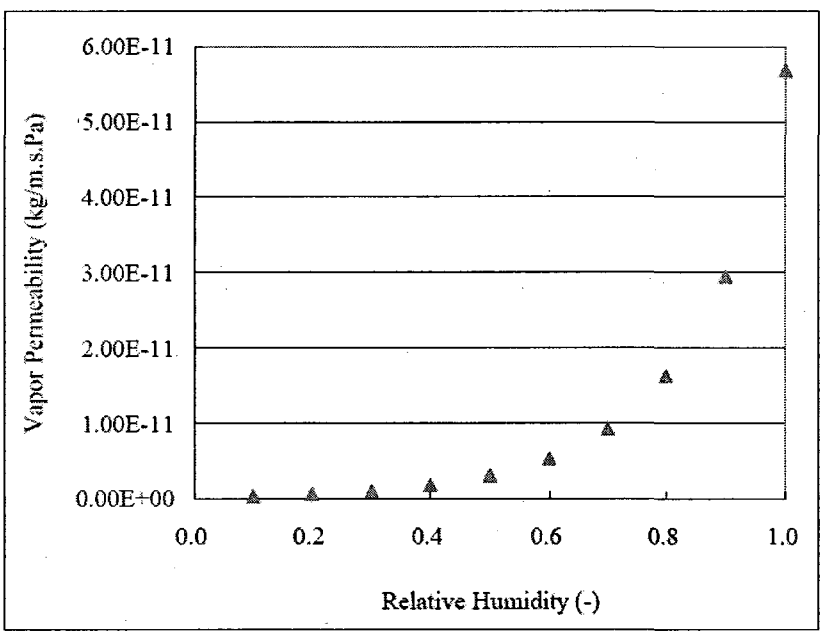

Figure 3.3 Vapor permeability of spruce, data source (Wu 2007)

As described, the "surface diffusion" is not vapor flow, rather liquid flow. Therefore, the measured vapor permeability under high relative humidity levels is not pure vapor flow, but the combination of vapor flow and liquid flow (surface diffusion). Since no practical measurement method can separate the vapor flow and liquid flow and the measured liquid conductivity also includes the contribution of surface diffusion, an assumption needs to be made to separate vapor flow and liquid flow artificially and to avoid overlap in the determination of liquid flow. Rode (1990) used a critical moisture content approach. Below the critical moisture content, the moisture flow is driven by the vapor pressure gradient and the vapor permeability as a function of relative humidity, are applied; above the critical moisture content, the liquid flow replaces the vapor flow and the vapor permeability goes down to zero. The critical moisture content is set at the equilibrium moisture content of 98% relative humidity.

However, to set the critical moisture content at the equilibrium value of 98% relative humidity is only a rough approximation. The critical moisture content is highly material dependent and some material can have liquid flow much lower than 98% relative humidity (Carmeliet & Roels 2001). Thus, another assumption was adapted to divide moisture flow as pure vapor flow and liquid flow including surface diffusion (Grunewald & Bomberg 2003). The vapor permeability measured through the "dry cup" method (relative humidity level of 20-30%) is assumed to be pure vapor flow; and the vapor permeability obtained from the "wet cup" method is accounted for in the determination of liquid permeability. This approach provides a more accurate description of the total

moisture flow (Adan et al 2004), and is applied in HAM-BE.

The vapor permeability of a building material can be expressed as Equation 3.17. The curve of this equation has a flat part through the major range of moisture content and has a steep part down near the saturation point.

$$\delta_p = \frac{M_w}{RT}\frac{26.1\cdot 10^{-6}}{\mu_{dry}}\cdot\frac{1-\frac{w}{w_{sat}}}{(1-p)\cdot(1-\frac{w}{w_{sat}})^2+p} \qquad (s) \qquad (3.17)$$

where

μ_{dry} (-) water vapor resistance factor of the material, $\mu_{dry} = \frac{\delta_{p,air}}{\delta_p}$

w_{sat} (kg/m^3) water content of free saturation

p (-) factor related to the proportion of pore sub-volume of the material

b) Liquid flow

The driving potential of liquid flow in porous material is capillary pressure and the flow is named "capillary suction". The essential mechanism of capillary suction is convection. In the context of building physics, it is sufficiently accurate to regard the liquid transport in the pore spaces as a diffusion phenomenon and the liquid flow also can be expressed in the Fick's form: a representative transfer conductivity driven by the gradient of a state variable (Hagentoft 2001). In some hygrothermal tools (Kunzel 1995, Burch 1997), "diffusivity method" was applied. The moisture content gradient was used to be the

driving potential of liquid flow, and the moisture diffusivity as the transfer conductivity, shown in Equation 3.18.

$$\boldsymbol{g}_l = -D_w(w,T)\ \nabla w \qquad (3.18)$$

where

$\boldsymbol{g}_l\ (kg/m^2 \cdot s)$ water liquid flux rate

$D_w\ (m^2/s)$ moisture diffusivity

$w\ (kg/m^3)$ moisture content, mass by volume

The moisture diffusivity is determined through water absorption measurement. One major surface of the specimen is placed in contact with liquid water. The increase in mass as a result of moisture absorption is recorded as a function of time. The data are analyzed using the Boltzmann transformation (Janz 1997) to derive the moisture diffusivity as a function of moisture content. An example of derived moisture diffusivity as function of moisture content is shown in Figure 3.4.

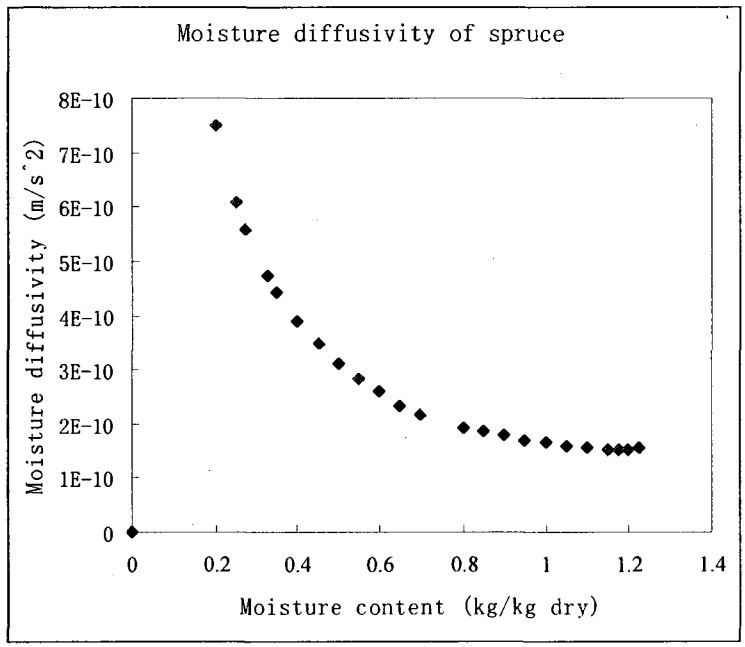

Figure 3.4 Moisture diffusivity of spruce, data source (Kumaran et al. 2002)

However, the application of moisture content as the driving potential of liquid flow is not sufficiently accurate for research purposes (Bomberg et al. 2002); since the moisture content is an empirical potential, instead of the thermodynamics potential, it cannot describe complicated phenomena in moisture transport, e.g. air entrapment, salt migration, and so on. Instead, the "permeability method" has proven to be the appropriate method for liquid flow (Carmeliet et al. 2004). In this method, the liquid flow is expressed in the Fick's form, with gradient of capillary pressure as the driving potential and liquid permeability as the moisture transfer conductivity, shown in Equation 3.19.

$$\begin{cases} \boldsymbol{g}_l = -D_w \nabla w = -D_w \dfrac{\partial w}{\partial P_c} \nabla P_c = K_l \nabla P_c \\ K_l = -D_w \dfrac{\partial w}{\partial P_c} \end{cases} \tag{3.19}$$

where

K_l ($kg/m \cdot s \cdot Pa$ or s) liquid permeability, which is a moisture transfer coefficient and highly moisture content dependent.

Based on Equation 3.19, an example of the liquid permeability is given in Figure 3.5. Also, the liquid permeability is temperature related, but is omitted in the presented hygrothermal tool.

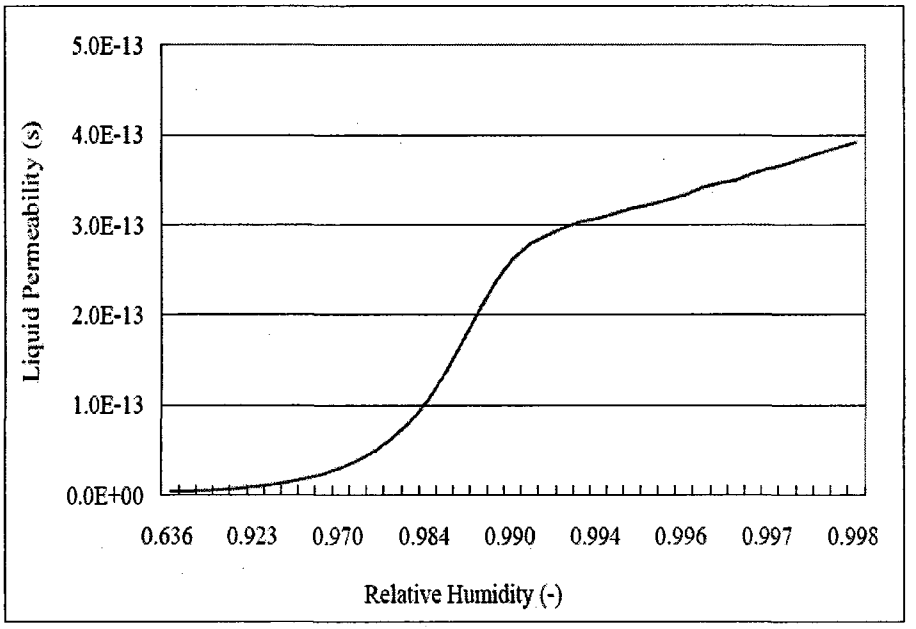

Figure 3.5 Liquid permeability of plywood board, data source (Wu 2008)

3-2-2 Moisture transfer under isothermal condition

The total moisture flow, including vapor and liquid phases, can be written as Equation 3.20, based on the above Equations 3.16 & 3.19.

$$\boldsymbol{g} = \boldsymbol{g}_v + \boldsymbol{g}_l = -\delta_p \nabla p_v + v\rho_v + K_l \nabla P_c \tag{3.20}$$

Under isothermal condition, temperature is constant, and the moisture conservation equation can be written as:

$$\frac{\partial w}{\partial t} = -\nabla\left(\boldsymbol{g}_l + \boldsymbol{g}_v\right) = \nabla(\delta_p \nabla p_v - \boldsymbol{v}\rho_v - K_l \nabla P_c) \tag{3.21}$$

3-2-3 Moisture transfer under non-isothermal conditions

Exposed to weather conditions and indoor conditions, the temperature gradient can be found across a building envelope. For example, the solar radiation can raise the surface temperature of the wall or roof, or in winter time, a large temperature difference exists between outdoors and indoors. The temperature gradient can drive moisture transport. If the temperature gradient is to be taken into account, there will be two independent state variables for the combined heat and moisture transport through a building envelope; one is the thermal state variable, temperature T, and the other is a moisture state variable. Therefore, the moisture conservation equation under isotherm condition needs to be adjusted.

To include the influence of temperature gradient, the moisture conservation equation has to be reconsidered, since $P_v = \phi P_{sat}$, and saturation vapor pressure P_{sat} is only dependent on temperature T, assuming constant atmosphere pressure. To denote P'_{sat} as the differential of the saturation vapor pressure, $P'_{sat} = \frac{d P_{sat}}{d T}$, the moisture conservation equation under non-isothermal condition can be written as:

$$\frac{\partial w}{\partial t} = \nabla(\delta_p P'_{sat} \nabla T + \delta_p P_{sat} \nabla \phi - v \rho_v - K_l \nabla P_c) \qquad (3.22)$$

3-3 Heat transport in building envelope

The heat transfer in building material can be divided into conduction part and convection part. The heat transfer by conduction is described by Fourier's law:

$$q_{cond} = -\lambda(w,T)\nabla T \qquad (3.23)$$

where

$q_{cond}\ (W/m^2)$ conductive heat flow

$\lambda\ (W/mK)$ thermal conductivity

Thermal conductivity is defined as the heat flux per unit temperature gradient in the direction perpendicular to an isothermal surface under steady-state conditions (Equation 3.24).

$$\lambda = \frac{Q\,L}{A\,\Delta T} \qquad (3.24)$$

where

$Q\ (W/m^2)$ heat flow rate across an area A

$L\ (m)$ thickness of test specimen

$\Delta T\ (K)$ temperature difference between the hot surface and the cold surface

Specific heat capacity is the measure of the heat energy required to increase the temperature of a unit quantity of a substance by one degree Celsius. The common used methods for testing the thermal conductivity and specific heat capacity for the building

materials are the Guarded-Hot-Plate Apparatus (ASTM 1997), and the Heat Flow Meter Apparatus (ASTM 1998).

Both temperature and moisture content can affect the thermal conductivity. The thermal conductivity increases with increasing temperature, but decreases with increasing moisture content of the material. Since temperature of a building envelope usually doesn't affect materials' thermal conductivities significantly, the influence of temperature can be neglected. Compared to temperature, the presence of moisture in porous materials has much more influence to the material's thermal conductivity. According to Kunzel (1995), the thermal conductivity of building materials can be expressed as a function of moisture content (Equation 3.25).

$$\lambda(w) = \lambda_w + (\lambda_d - \lambda_w)\frac{w_{sat} - w}{w_{sat}} \qquad (3.25)$$

where

λ_w (W/mK) heat conductivity of wet material

λ_d (W/mK) heat conductivity of dry material

w_{sat} (kg/m^3) saturation moisture content of the material

w (kg/m^3) moisture content of the material

The convective heat flow q_{conv} includes both sensible and latent heat carried by air and can be written as:

$$q_{conv} = v \rho_a c_{p,a} T + g_v \cdot (L_v + c_{p,v} T) + g_l c_{p,l} T$$

Since $g_v = v \rho_v - \delta_p \nabla P_v$ (Equation 3.16), the above equation can be expressed as:

$$q_{conv} = v \rho_a c_{p,a} T + (v \rho_v - \delta_p \nabla P_v)(L_v + c_{p,v} T) + g_l c_{p,l} T \qquad (3.26)$$

where

L_v (kJ/kg) enthalpy of evaporation/condensation

$c_{p,a}$ ($J/kg \cdot K$) dry specific heat of air

$c_{p,v}$ (kJ/kgK) specific heat capacity of water vapor

$c_{p,l}$ (kJ/kgK) specific heat capacity of water liquid

v (m/s) air velocity and calculated by Darcy-Boussinesq equation or Navier-Stokes equation, dependently the suitability of the case.

Neglecting the sensible heat carried by water liquid and water vapor, the convective heat flow can be approximated as:

$$q_{conv} = v \rho_a c_{p,a} T + L_v v \rho_v - L_v \delta_p \nabla P_v \qquad (3.27)$$

Based on Equations 3.23 and 3.27, the total heat flow through a building material can be expressed as:

$$q = q_{cond} + q_{conv} = -\lambda \nabla T + v \rho_a c_{p,a} T + L_v v \rho_v - L_v \delta_p \nabla P_v \qquad (3.28)$$

The energy conservation equation can be written as:

$$(c_p\rho + c_{p,l}w)\frac{\partial T}{\partial t} = -\nabla \boldsymbol{q} = \nabla(\lambda\nabla T + L_v\delta_p\nabla P_v - vL_v\rho_v - v\,\rho_a c_{p,a}T) \qquad (3.29)$$

where

c_p $(J/kg\cdot{}^oC)$ dry specific heat of building material.

3-4 Air convection in building envelope

Air transfer through building envelopes can be in two directions (exfiltration or infiltration) across the walls or across the roofs. Also, air circulation may occur in fibrous insulation material, e.g. low-density glass-fiber batt and mineral wool, and in air gaps and unfilled stud cavities. Uncontrolled air flow, especially air leakage, can have detrimental effects on the performance of a building (Hutcheon 1953), including heat loss, condensation by cooling surfaces, or frozen pipes by infiltration; and vapor condensation and ice dams by exfiltration of warm air. Air movement in building envelopes has been studied by (Quirouette et al. 1991, Okland 1998, Desmarais et al. 2000, Wang 2001, Janssens & Hens 2003, Sherman & Chan 2004).

The bulk of fluid motion of air is defined as advection. The random movement of molecules for conduction is also presented in the bulk flow. The combination of the random molecule movement and the bulk flow was defined as convection. Convection is induced by total pressure difference. Pressure difference can be produced by driving

forces like mechanical fans, wind, and temperature difference (stack effect). The air flow due to fans and wind is named as forced convection.

Air flow that has parallel streamlines is defined as laminar flow. Temperature differences could induce laminar flow in open-porous building materials and the resulting air velocity is as low as the millimeters per second level. Since the low air flow velocity, air flow in insulation material can be treated as laminar flow (Okland 1998). Turbulence flow is highly irregular and the motion of fluid having local velocities and pressures that fluctuate randomly. An indication of turbulent flow in the channel is that the Reynolds number is greater than 4000. The transition between laminar and turbulent flow is not exact and the flow regime for Reynolds numbers between 2300 and 4000 is called the transition zone (Kronvall 1980).

In most convection models including heat transfer, Boussinesq approximation is applied. The air properties are treated as constant, except that the air density in the gravity term still depends on temperature to induce natural convection effects. Boussinesq approximation has been verified to be appropriate in most cases.

The air density difference due to temperature gradient can be calculated through:

$$\rho_a - \rho_{a,o} = -\rho_a \beta (T - T_o) \qquad (3.30)$$

where

$\rho_a (kg/m^3)$ air density

$\rho_{a,o} (kg/m^3)$ air density at a certain reference temperature T_o

$\beta(1/K)$ thermal expansion coefficient of air

For the air flow caused by both the air pressure gradient and the buoyancy force, the Darcy-Boussinesq equation is used and is expressed as Equation 3.31.

$$\begin{cases} \boldsymbol{v} = -\dfrac{k_a}{\mu_a}\left(\nabla p_a + \beta \rho_a \boldsymbol{g}(T - T_o)\right) \\ \nabla \boldsymbol{v} = 0 \end{cases} \tag{3.31}$$

where

$p_a\ (P_a)$ air pressure

$\boldsymbol{g}\ (m/s^2)$ gravity acceleration

$k_a\ (kg/msPa)$ air permeability

$\mu_a\ \ (kg/ms)$ dynamic viscosity of air

As a summary, the transport mechanisms and corresponding equations applied by HAM-BE to calculate the coupled heat, air and moisture transport in building materials are listed in Table 3.2.

Table 3.2 Heat, air and moisture transfer mechanisms of HAM-BE

Phenomena	Mechanism	Driving Potential	Equations
Heat	Conduction	Temperature gradient	$q_{cond} = -\lambda(w,T)\nabla T$
	Convection	Air pressure difference	$q_{conv} = v\ \rho_a c_{p,a} T$
	Enthalpy flows	Moisture movement and phase change	$q_{en} = g_v \cdot (L_v + c_{p,v} T) + g_l c_{p,l} T$
Moisture	Vapor diffusion	Vapor pressure gradient	$g_{v,d} = -\delta_p(w,T)\ \nabla P_v$
	Capillary suction	Capillary pressure gradient	$g_l = K_l \nabla P_c$
Air	Natural or forced convection	Air pressure difference due to thermal gradient or wind	$v = -\frac{k_a}{\mu_a}\left(\nabla p_a + \beta \rho_a g (T - T_o)\right)$

3-5 Material propeties for hygrothermal modeling

As described in the above sections, the material properties used in HAM-BE include dry density, specific thermal capacity, thermal conductivity, moisture storage capacity, vapor permeability, liquid permeability, and air permeability. Their input formats are summarized here.

Constant:

Dry material density	ρ	(kg/m^3)
Specific heat capacity of material	c_p	(J/kgK)
Air permeability	k_a	$(kg/msPa)$

Functions of moisture state variables:

Thermal conductivity

$$\lambda(w) = \lambda_w + (\lambda_d - \lambda_w)\frac{w_{sat} - w}{w_{sat}} \qquad (W/m\,K)$$

Moisture storage curve (Equation 3.10) with a uni-modal equation

$$w(P_c;\alpha,n,m) = w_{sat}\left[1+(\alpha P_c)^n\right]^{-m}$$

Moisture storage capacity

$$\xi = \left|\frac{\partial w}{\partial P_c}\right|$$

Vapor permeability (Equation 3.17)

$$\delta_{p,pure} = \frac{M_w}{RT} \frac{26.1 \cdot 10^{-6}}{\mu_{dry}} \cdot \frac{1 - \frac{w}{w_{sat}}}{(1-p) \cdot (1 - \frac{w}{w_{sat}})^2 + p} \qquad (s)$$

Liquid permeability

$K_l = f(P_c)$ Interpolation or fitting function of data series

The required material properties for HAM-BE are summarized in Table 3.3 below. The definition of the term, measurement instrument and test method are provided briefly in columns 2 and 3 respectively.

Table 3.3 Material properties and corresponding measurement methods

Material property	Definition	Measurement method and procedure
Thermal conductivity	Thermal conductivity is defined as the heat flux per unit temperature gradient in the direction perpendicular to an isothermal surface, under steady-state conditions.	Guarded hot plate apparatus (ASTM C177-04) or heat flow meter apparatus (ASTM C518)
	A sorption isotherm establishes the relation	Chamber with constant RH and T (such as glass urns with salt

Sorption Isotherm	between moisture ratio or moisture content in a porous material with respect to relative humidity (RH) and temperature. The routes from RH 0 to 100% traced from dry to wet or from wet to dry, were called absorption and desorption, respectively. The difference between absorption and desorption is referred to as hygroscopic hysteresis.	solutions and small environmental chamber) Under a given temperature, the dry material specimen is exposed to a set RH, until equilibrium reached, the weight is recorded, the RH is then increased, and hence and so forth until sorption plot can be drawn (ASTM C1498-01).
Capillary suction curve	At high RH level, sorption is replaced by the equilibrium between moisture ratio and capillary pressure, and the result is called the water retention or suction curve. (Bomberg et al 2002)	Pressure plate apparatus Under certain air pressures, test specimens saturated with water under vacuum keep perfect hygric contact with plates, water is extracted out of the pore structure until an equilibrium

		state is established. The equilibrium values for moisture contents in the specimens and the corresponding pressures are recorded.
Moisture content	Moisture content is defined as mass of moisture per unit volume of the dry material (or per unit mass of the dry material).	The sample is weighed, dried then weighed. (ASTM D4442-92)
Water vapor permeability/ permeance	Definition: $\delta_p = \frac{g_v L}{A \Delta p_v}$ $(kg/msPa)$ g_v (kg/s) Water vapor flow rate across an area L (m) Thickness of the specimen A (m^2) Area of the specimen Δp_v (Pa) Vapor pressure difference across the specimen surface	Dry cup (0/50% RH) or wet cup (50/100% RH) measurement. Also any pairs of RH conditions Under isothermal conditions, a test specimen separates two environments that differ in relative humidity. Then the rate of vapor flow across the specimen is gravimetrically determined. From these data the

		water vapor permeability of the material is calculated. (ASTM E96)
Water Absorption Coefficient	The water absorption coefficient is the slope of the line of mass increase against the square root of time divided by the area of the surface in contact with water.	One surface of the specimen is placed in contact with liquid water. The increase in mass as a result of moisture absorption is recorded as a function of time. (CEN Standard 89 N 370 E)
Moisture Diffusivity	Definition $g_l = -D_w \frac{\partial w}{\partial x}$ $g_l\,(kg/sm^2)$ Water flow rate $D_w\,(m^2/s)$ Moisture diffusivity $w\,(kg/m^3)$ Moisture content	One surface of the specimen contacted with water is allowed to diffuse vapor into the specimen. The distribution of moisture within the specimen is determined as a function of time at various intervals until the moving moisture front advances to half of the specimen. The data are analyzed to derive the moisture diffusivity as a function

		of moisture content. (Alvarez 1998, Drchalova et al 2002)
Air Permeability/ Permeance	Definition $k_a = \frac{g_a L}{A \Delta p}$ k_a $(kg/msPa)$ Air Permeability g_a (kg/s) Air flow rate L (m) Thickness of the specimen Δp (Pa) Air pressure difference across the specimen surfaces	An air pressure difference applied on test specimens, keep the air pressure and the airflow rate at a steady state and the pressure differential across the specimen are recorded. (ASTM C522-03)

3-6 Boundary conditions of hygrothermal modeling

The outdoor/indoor loading on the building envelope's boundary include transient heat and vapor exchange between the air and the surface of the building materials, long-wave radiation, solar radiation and rain absorption. As summarized by Kunzel (1995), the heat and moisture exchange between building envelope's surface and the interior and exterior surrounding can be classified into three kinds of boundary conditions:

1. Surface conditions are the same as the ambient conditions when the building component is in contact with water or the earth. In the scope of building physics, this

boundary condition applies when the component surface is completely wetted from rain or ground water.

2. A constant heat or mass flow occurs on the building surface. This boundary condition characterizes the influence of solar radiation on heat transport and the uptake of rain water when the surface is not completely wetted. Symmetry conditions and adiabatic or water and vapor-tight conditions are covered by zero flows at the component boundaries.
3. Heat and moisture transfer through a transitional resistance between the building surface and its surroundings. It constitutes the most common kind of heat and moisture exchange.

In the development of hygrothermal models for building envelope study, the first kind boundary is rarely applicable. The second and third kind of boundary conditions were integrated in the numerical formats of the HAM-BE's boundary conditions.

3-6-1 Moisture flow through exterior surface

The moisture flow through the exterior surface of the building envelope includes vapor absorption/desorption between the building's surface and the outdoor air and water absorption from rain:

$$g_{n,e} = \beta_{p,e}(p_{v,e} - p_{surf,e}) + g_{rain} \qquad (3.32)$$

where

$g_{n,e}\,(kg/m^2 \cdot s)$ moisture flow through the exterior surface of a building

$\beta_{p,e}\,(kg/m^2sPa)$ vapor transfer coefficient of the exterior surface

$p_{v,e}\,(Pa)$ water vapor pressure of outdoor air

$p_{surf,e}\,(Pa)$ water vapor pressure on exterior surface

$g_{rain}\,(kg/m^2s)$ moisture source from rain absorption

The moisture content at the exterior surface is limited to the saturation point and no runoff water is considered in the calculation.

3-6-2 Heat flow through exterior surface

The heat flow through the exterior surface of the building includes latent heat of vapor absorption/desorption, sensible heat of rain absorption, solar radiation and long-wave radiation between the building surface and surrounding environment.

a) Latent heat of vapor absorption/desorption

The assumption accepted in hygrothermal modeling is that when vapor is absorbed by the building surface, it releases the latent heat (and slightly warm up the material surface and vicinity); when vapor leaves the building surface, it carries away the latent heat from the material. Thus, the latent heat of vapor can be obtained as:

$$q_v = L_v \beta_{p,e}(p_{v,e} - p_{surf,e}) \tag{3.33}$$

b) Heat flow with rain absorption

When rain water is absorbed by the building surface, the sensible heat carried to the building surface is calculated as:

$$q_{rain} = g_{rain} c_{p,l} T_a \qquad (3.34)$$

where

q_{rain} (W/m^2) sensible heat of rain water

T_a (K) temperature of outdoor air, assuming the temperature of rain is equal to that of outdoor air.

c) Solar radiation

The solar radiation reaching the surface of a building is partially absorbed by the material. According to Hagentoft (Hagentoft 2001), the net heat flow due to solar radiation (q_{sol}) absorbed at a building envelope's surface is:

$$q_{sol} = \alpha_{sol} I_{sol}^0 \cos(\theta) = \alpha_{sol} I_{sol} \qquad (3.35)$$

where

α_{sol} (-) absorptivity for solar radiation

I_{sol}^0 (W/m^2) solar radiation energy flow transmitted through an imaginary surface with a surface normal to the solar rays

θ (-) angle between the normal of the building envelope surface and the solar rays

I_{sol} (W/m^2) normal component (to the building surface) of the incident solar radiation

d) Long wave radiation

The building surface can transmit heat to the building's surroundings in the form of long wave radiation. Assuming the surroundings is black body and has the temperature equal to the sky temperature, the long-wave radiation between the building's surface and the surroundings can be calculated through:

$$q_{lw} = \alpha_r (T^r - T_{surf}) \tag{3.36}$$

where

q_{lw} (W/m^2) long-wave radiation between the building surface and the surroundings T_{surf} (K) temperature of the building surface

T^r (K) sky temperature, assuming the temperature of the building's surroundings is equal to the sky temperature

α_r (W/m^2K) long-wave radiation surface heat transfer coefficient, determined by the temperature of the building surface, the temperature of the surroundings (assuming equal to sky temperature) and the emissivity of the building surface

The sky temperature is determined by the cloudiness, the air temperature, and the inclination of the building surface, expressed as an empirical equation (Hagentoft 2001):

$T^r = 1.2\ T_a - 14$ Horizontal surface, clear sky, (K) (3.37)

$T^r = 1.1\ T_a - 5$ Vertical surface, clear sky (K)

$T^r = T_a$ Cloudy sky

and the long-wave radiation surface heat transfer coefficient is calculated by:

$$\alpha_r = 4\varepsilon\sigma\overline{T}^3 \tag{3.38}$$

Here, ε is the emissivity of the building surface, $\overline{T}$ is the average temperature of building surface and the building's surroundings, expressed as: $\overline{T} = \frac{T^r + T_{surf}}{2}$

To define an equivalent exterior temperature T^{eq}, the solar radiation, long-wave radiation, and convection at the exterior building surface can be lumped together:

$$\begin{cases} T^{eq} = T_a + \frac{1}{\alpha_e}\left(q_{sol} + \alpha_r(T^r - T_a)\right) \\ q_{sol} = \alpha_{sol}\ I_{sol} \end{cases} \tag{3.39}$$

Here, α_e (W/m^2K) is the effective heat transfer coefficient at the exterior surface:

$$\alpha_e = \alpha_c + \alpha_r \tag{3.40}$$

The long-wave radiation heat transfer coefficient has been described in Equation 3.38, and the convective heat transfer coefficient is determined by air temperature and air velocity on the building surface and an empirical expression (Hagentoft 2001) is given as:

Windward side: $\alpha_c = 5 + 4.5v - 0.14v^2 \qquad (v \le 10\ m/s)$ (3.41)

Leeward side: $\alpha_c = 5 + 1.5v \qquad (v \le 8\ m/s)$

Therefore, the heat flow across the exterior surface, $q_{n,e}$ (W/m^2), including the effect of conduction, convection, long-wave and solar radiation, latent heat flow due to vapor transfer and sensible heat flow due to rain absorption, is expressed as:

$$q_{n,e} = \alpha_e (T^{eq} - T_{surf,e}) + L_v \beta_{p,e} (p_{v,e} - p_{surf,e}) + g_{rain} c_{p,l} T_a \quad (3.42)$$

3-6-3 Moisture flow through interior surface

No solar radiation or rainfall is allowed for indoor surfaces; therefore, the data required to define the interior boundary has only two parameters: temperature and relative humidity. The moisture flow across the interior wall, $g_{n,i}\,(kg/m^2 \cdot s)$, is expressed as:

$$g_{n,i} = \beta_{p,i} (p_{v,i} - p_{surf,i}) \quad (3.43)$$

where

$\beta_{p,i}\,(kg/m^2 sPa)$ vapor transfer coefficient of the interior surface

$p_{v,i}\,(Pa)$ water vapor pressure of the indoor air

$p_{surf,i}\,(Pa)$ water vapor pressure on interior surface

3-6-4 Heat flow through interior surface

Heat transfer across the interior surface of the building envelope, $q_{n,i}\,(W/m^2)$, is given in:

$$q_{n,i} = \alpha_i (T_i - T_{surf,i}) + L_v \beta_{p,i} (p_{v,i} - p_{surf,i}) \quad (3.44)$$

where

$\alpha_i\,(W/m^2 K)$ heat transfer coefficient at the interior surface

$T_i\,(K)$ temperature of indoor air

$T_{surf,i}\,(K)$ temperature of the interior surface

Since the surface heat transfer coefficient is highly influenced by localized factors: the

building shape and the locations of surrounding constructions, the wind flow field and the climate data. In case the information is not sufficient to determine the surface heat transfer coefficient, approximate values were used in hygrothermal modeling work (Kunzel 1995, Burch 1997). The exterior heat transfer coefficient is in the range between 20 - 30 $W/m^2 \cdot K$, and the interior heat transfer coefficient is about 5-10 $W/m^2 \cdot K$.

Compared to the surface heat transfer coefficient, the surface moisture transfer coefficient is more difficult to determine, since there is no reliable and accurate model to calculate it. As common practice, the moisture transfer coefficient can be analogized from the heat transfer coefficient through 'Lewis analogy' (Hagentoft 2004, Janssen et al. 2006), shown as Equation 3.45.

$$\beta_p = 7.7\ 10^{-9}\ \alpha \qquad (3.45)$$

From the above boundary equations, the required meteorological parameters for hygrothermal modeling are exterior/interior temperature, relative humidity, outdoor/indoor relative humidity or vapor pressure, rainfall, solar radiation, cloud factor, wind speed and direction. Data from locations of interest can be input as interpolation files in the hygrothermal tool. The necessary factors to represent weather load are the weather database for European and North American climate and are available for moisture study purposes (Tenwolde & Colliver 2001). It is worthy to note that to apply hourly average value of climate data can underestimate the harsh weather load, like wind driven rain. It is expected that optimized weather data be developed for hygrothermal

analysis. In the IEA Annex 24 Project, a "Moisture Design Reference Years" was developed to reflect the extreme weather condition loading on the building envelope (Rode 2001).

3-7 Conservation equations of combined heat and moisture transport

From Sections 3.2 to 3.5, the conservation equations of combined heat and moisture transport are summarized below:

Moisture conservation equation (Equation 3.22)

$$\frac{\partial w}{\partial t} = \nabla(\delta_p P'_{sat} \nabla T + \delta_p P_{sat} \nabla \phi - \nu \rho_v - K_l \nabla P_c)$$

Energy conservation equation (Equation 3.29)

$$(c_p \rho + c_{p,l} w)\frac{\partial T}{\partial t} = \nabla(\lambda \nabla T + L_v \delta_p \nabla P_v - \nu L_v \rho_v - \nu \rho_a c_{p,a} T)$$

The moisture state in a porous material can be identified by three independent state variables: the total air pressure, one state variable for heat transfer, and one moisture state variable (Claesson 1993). If in porous material, the air pressure is assumed to be constant; only two independent state variables are required. The only state variable for heat transfer calculation is temperature, but various moisture state variables appear in the conservation equations (Equations 3.22 & 3.29), including relative humidity ϕ, vapor

density ρ_v, vapor pressure P_v, capillary pressure P_c, and moisture content w. To solve the conservation equations, it is necessary to select one moisture state variable and convert all other moisture state variables to this one.

HAM-BE applies "phase-divided method" to separate moisture flow as vapor flow driven by vapor pressure gradient and liquid flow driven by capillary pressure; the moisture storage curve and liquid permeability were defined as the functions of capillary pressure. Even though the capillary pressure cannot be measured directly and can only be obtained from the Kelvin equation; it is convenient to use the capillary pressure as the moisture state variable in the conservation equations. The other moisture state variables are converted to the capillary pressure through analytical equations. The advantage to use capillary pressure can be explained as follows: capillary pressure is the thermodynamics potential of liquid flow in porous materials; the moisture retention curve, as a function of capillary pressure, has an accurate expression in both hygroscopic and over-hygroscopic regions; capillary pressure is continuous at the interface of different materials; capillary pressure is the physical potential for water liquid transfer and liquid flow is much larger than vapor transfer and has more important influence in the analysis of building envelopes' hygrothermal behavior; and the relative humidity and water vapor pressure have exclusive relations to the capillary pressure.

At the local equilibrium condition, moisture state variables: vapor density $\rho_v (kg/m^3)$, water vapor pressure P_v (Pa), relative humidity ϕ, capillary pressure P_c (Pa), and

moisture content mass by volume w (kg/m^3), can be converted between each other through analytical equations. The state variables ϕ, ρ_v, and P_v are related to each other by Equation 3.1.

$$\phi = \frac{p_v}{p_{sat}} = \frac{\rho_v}{\rho_{v,sat}}$$

The general gas law relates the vapor density to the partial vapor pressure:

$$p_v = R_v \; T \; \rho_v \tag{3.46}$$

At the equilibrium condition, the water vapor pressure p_v and the capillary pressure P_c satisfy Kelvin's relation as shown in Equation 3.7, $\ln\phi = -\frac{P_c}{\rho_l R_v T}$. Therefore,

$$\frac{\partial \phi}{\partial P_c} = -\frac{\phi}{\rho_l R_v T} \tag{3.47}$$

The moisture content w is related to the capillary pressure P_c by the moisture retention curve (moisture content versus capillary pressure).

To define the slope of moisture the storage curve as moisture storage capacity:

$$\xi = \left|\frac{\partial w}{\partial P_c}\right| \tag{3.48}$$

since $\frac{\partial w}{\partial P_c} = -\left|\frac{\partial w}{\partial P_c}\right|$; then, $\frac{\partial w}{\partial t} = -\left|\frac{\partial w}{\partial p_c}\right|\frac{\partial P_c}{\partial t}$. To add the moisture source term (Q_m) to represent any possible moisture source/sink in the materials, the moisture conservation equation (Equation 3.22) can be rewritten as:

$$\frac{\partial w}{\partial t} = \nabla(\delta_p p_{sat}^{'} \nabla T) + \nabla(\delta_p P_{sat} \nabla \phi) - \nabla(K_l \nabla P_c) - \boldsymbol{v} \cdot \nabla \rho_v + Q_m$$

Then,

$$\xi \frac{\partial P_c}{\partial t} = \nabla\left((-\delta_p \phi P_{sat}^{'})\nabla T\right) + \nabla\left((K_l - \delta_p P_{sat} \frac{\partial \phi}{\partial P_c})\nabla P_c\right) + \boldsymbol{v} \frac{\partial \rho_v}{\partial T} \cdot \nabla T + \boldsymbol{v} \frac{\partial \rho_v}{\partial P_c} \cdot \nabla P_c + Q_m \quad (3.49)$$

To use capillary pressure as the independent moisture state variable in the conservation equation, the heat conservation equation (Equation 3.29) can be rewritten as:

$$(c_p \rho + c_{p,l} w)\frac{\partial T}{\partial t} = \nabla(\lambda \nabla T) + \nabla(L_v \delta_p \nabla P_v) - \boldsymbol{v}\, \rho_a c_{p,a} \cdot \nabla T - \boldsymbol{v} L_v \cdot \nabla \rho_v$$

To define $C = c_p \rho + c_{p,l} w$, the above equation can be written as:

$$C \frac{\partial T}{\partial t} = \nabla(\lambda \nabla T) + \nabla(L_v \delta_p \nabla P_v) - \boldsymbol{v}\, \rho_a c_{p,a} \cdot \nabla T - \boldsymbol{v} L_v \cdot \nabla \rho_v$$

Since $P_v = P_{sat}\ \phi$, the above equation can be written as:

$$C \frac{\partial T}{\partial t} = \nabla(\lambda \nabla T) + \nabla(L_v \delta_p P_{sat} \nabla \phi) + \nabla(L_v \delta_p \phi P_{sat}^{'} \nabla T) - \boldsymbol{v} \rho_a c_{p,a} \cdot \nabla T - \boldsymbol{v} L_v \cdot \nabla \rho_v \text{ then,}$$

$$C \frac{\partial T}{\partial t} = \nabla\left((\lambda + L_v \delta_p \phi P_{sat}^{'})\nabla T\right) + \nabla(L_v \delta_p P_{sat} \nabla \phi) - \boldsymbol{v} \rho_a c_{p,a} \cdot \nabla T - \boldsymbol{v} L_v \cdot \nabla \rho_v$$

To apply capillary pressure P_c as the independent moisture state variable, the above equation can be written as:

$$C\frac{\partial T}{\partial t}=\nabla\left(\lambda+L_v\delta_p\phi P_{sat}^{'})\nabla T\right)+\nabla(L_v\delta_p P_{sat}\frac{\partial\phi}{\partial p_c}\nabla P_c)-\nu\rho_a c_{p,a}\cdot\nabla T-$$

$$\nu L_v\cdot(\frac{\partial\rho_v}{\partial T}\nabla T+\frac{\partial\rho_v}{\partial P_c}\nabla P_c)$$

From Kelvin's law: $\frac{\partial\phi}{\partial P_c}=-\frac{\phi}{\rho_l R_v T}$ (Equation 3.47), the above equation can be written as:

$$C\frac{\partial T}{\partial t}=\nabla\left(\lambda+L_v\delta_p\phi P_{sat}^{'})\nabla T\right)-L_v\nabla(\frac{\delta_p P_{sat}\phi}{\rho_l R_v T}\nabla P_c)-\nu\rho_a c_{p,a}\cdot\nabla T$$

$$-\nu L_v\cdot(\frac{\partial\rho_v}{\partial T}\nabla T+\frac{\partial\rho_v}{\partial P_c}\nabla P_c)$$

To add a source term to represent possible heat source/sink (Q_h) in the materials, the energy conservation equation can be written as:

$$\begin{aligned}C\frac{\partial T}{\partial t}&=\nabla\left(\lambda+L_v\delta_p\phi P_{sat}^{'})\nabla T\right)-L_v\nabla(\frac{\delta_p P_{sat}\phi}{\rho_l R_v T}\nabla P_c)\\&-\nu(\rho_a c_{p,a}+L_v\frac{\partial\rho_v}{\partial T})\cdot\nabla T-\nu L_v(\frac{\partial\rho_v}{\partial P_c})\cdot\nabla P_c+Q_h\end{aligned}\qquad(3.50)$$

Therefore, the conservation equation of combined heat and moisture transport in building materials can be written as:

$$\begin{cases}\text{Energy conservation equation}\\C\frac{\partial T}{\partial t}=\nabla\left(\lambda+L_v\delta_p\phi P_{sat}^{'})\nabla T\right)-L_v\nabla(\frac{\delta_p P_{sat}\phi}{\rho_l R_v T}\nabla P_c)-\nu(\rho_a c_{p,a}+L_v\frac{\partial\rho_v}{\partial T})\cdot\nabla T-\nu L_v(\frac{\partial\rho_v}{\partial P_c})\cdot\nabla P_c+Q_h\\\text{Moisture conservation equaiton}\\\xi\frac{\partial P_c}{\partial t}=\nabla\left((-\delta_p\phi P_{sat}^{'})\nabla T\right)+\nabla\left((K_l-\delta_p P_{sat}\frac{\partial\phi}{\partial P_c})\nabla P_c\right)+\nu\frac{\partial\rho_v}{\partial T}\cdot\nabla T+\nu\frac{\partial\rho_v}{\partial P_c}\cdot\nabla P_c+Q_m\end{cases}\qquad(3.51)$$

The exterior boundary condition is described as:

$$\begin{cases} g_{n,e} = \beta_{p,e}(p_{v,e} - p_{surf,e}) + g_{rain} \\ q_{n,e} = \alpha_e(T^{eq} - T_{surf}) + L_v\beta_{p,e}(p_{v,e} - p_{surf,e}) + g_l c_l T_e \end{cases} \tag{3.52}$$

The interior boundary condition is described as:

$$\begin{cases} g_{n,i} = \beta_{p,i}(p_{v,i} - p_{surf,i}) \\ q_{n,i} = \alpha_i(T_i - T_{surf,i}) + L_v\beta_{p,i}(p_{v,i} - p_{surf,i}) \end{cases} \tag{3.53}$$

The air velocity is determined through the Darcy-Boussinesq equation (Equation 3.31).

$$\begin{cases} \boldsymbol{v} = -\dfrac{k_a}{\mu_a}\left(\nabla p_a + \beta\rho_a \boldsymbol{g}(T - T_o)\right) \\ \nabla \boldsymbol{v} = 0 \end{cases}$$

In the development of the advanced numerical models, certain assumptions are necessary and can be acknowledged as the limitations of the models (Karagiozis 2001). The assumptions adopted in HAM-BE are summarized here:

1. The material is macroscopically homogeneous;
2. The solid phase is a rigid matrix, and thermophysical properties are constant with space;
3. Enthalpy of each phase is a function of temperature and moisture;
4. Compressional work and viscous dissipation is negligible for each phase;

5. Local equilibrium exists among the phases of vapor and liquid;
6. Various transport mechanisms can be lumped;
7. Hysteresis of moisture retention curve was treated by applying average value of absorption and desorption curve;
8. The influence of temperature on the moisture retention curve and transport conductivities were neglected;
9. Gravity was not included as a force for liquid transport;
10. Vapor adsorption at the boundary surfaces releases the latent heat of vaporization and vice versa;
11. No runoff rain water at building surface was considered.

3-8 Implementation of HAM-BE in COMSOL environment

3-8-1 Coefficient form of governing equations of HAM-BE

The HAM-BE tool is hosted in the COMSOL environment, a commercial finite element solver for partial differential equations of linear/nonlinear, steady-state/time-dependent, eigenvalue/parametric types. When solving the PDEs, COMSOL uses the proven finite element method (FEM). The software runs the finite element analysis together with adaptive meshing and error control using a variety of direct or iterative numerical solvers for appropriate application. The direct solvers are UMFPACK and SPOOLES types and iterative solvers are GMRES and Conjugate Gradient types (COMSOL 2007). The

features of COMSOL are: providing equation-based models for common engineering/scientific phenomena that can be described by PDEs; fully coupled multi-physics process in 2D and 3D; predefined variables/functions for model description and post-processing; import of AutoCAD files and drawing tools to define objective domains/boundary; verified solving algorithms for optimized efficiency; connection with MATLAB/SIMULINK for extended modeling; user-friendly GUIs (graphic user interfaces) or script format for operation. The user avoids elaborate work in implementing and verifying the solution algorithm and input/output interfaces, and can focus on the physical model of the research. Moreover, hosted by the COMSOL, HAM-BE has the flexibility for the user to build/modify/extend models with changing research purposes; also, the modeling work can be transferred between different projects or research groups much easier than models implemented directly with programming languages.

Still, the essential knowledge of building physics and the finite element method is required to work effectively. The COMSOL has been used in modeling of building science phenomena, including air flow in indoor space and combined heat and moisture transfer in single material (Schijndel 2002). The previous development of HAM-BE in COMSOL was published in (Li et al. 2005, 2006).

The coefficient form of partial differential equation in COMSOL is presented in Equation 3.54.

$$\begin{cases} e_a \dfrac{\partial^2 u}{\partial T^2} + d_a \dfrac{\partial u}{\partial t} + \nabla \cdot \left(-c\nabla u - \alpha u + \gamma\right) + \beta \cdot \nabla u + au = f & in\ \Omega \\ \\ n \cdot \left(-c\nabla u - \alpha u + \gamma\right) + qu = g & on\ \partial\Omega \end{cases} \tag{3.54}$$

Ω is the computational domain—the union of all sub-domains. $\partial\Omega$ is the domain boundary and $\boldsymbol{n}$ is the outward unit normal vector on $\partial\Omega$. The first equation is the PDE, which must be satisfied in Ω. The second equation is the generalized Neumann type boundary condition, which must hold on $\partial\Omega$. u is the independent variable. All the coefficients in the equation are scalars except α, β, and γ, which are vectors with n components. The coefficient c can alternatively be an $n \times n$ matrix to model anisotropic materials, where n is the dimensions of Ω and equals to 2 for 2D models and 3 for 3D models.

The independent variables T and P_c in the conservation equations (Equation 3.53) can be written as a matrix form $u = (T, P_c)$, the above conservation equations can be rewritten to fit the coefficient form PDE:

$$\begin{bmatrix} C\dfrac{\partial T}{\partial t} \\ \xi\dfrac{\partial P_c}{\partial t} \end{bmatrix} = \begin{bmatrix} \nabla\left(\lambda + L_v\delta_p\phi P_{sat}^{'})\nabla T\right) - L_v\nabla(\dfrac{\delta_p P_{sat}\phi}{\rho_l R_v T}\nabla P_c) \\ \nabla\left((-\delta_p\phi P_{sat}^{'})\nabla T\right) + \nabla\left((K_l - \delta_p P_{sat}\dfrac{\partial\phi}{\partial P_c})\nabla P_c\right) \end{bmatrix} + \begin{bmatrix} -\nu(\rho_a c_{p,a} + L_v\dfrac{\partial\rho_v}{\partial T})\cdot\nabla T - \nu L_v(\dfrac{\partial\rho_v}{\partial P_c})\cdot\nabla P_c \\ \nu\dfrac{\partial\rho_v}{\partial T}\cdot\nabla T \qquad\qquad + \nu\dfrac{\partial\rho_v}{\partial P_c}\cdot\nabla P_c \end{bmatrix} + \begin{bmatrix} Q_h \\ Q_m \end{bmatrix},$$

then written as:

$$\begin{bmatrix} C \\ \xi \end{bmatrix}\begin{bmatrix} \frac{\partial T}{\partial t} \\ \frac{\partial P_c}{\partial t} \end{bmatrix} = \nabla\left(\begin{bmatrix} \lambda + L_v\delta_p\phi P_{sat}^{'} & -\frac{L_v\delta_p P_{sat}\phi}{\rho_l R_v T} \\ -\delta_p\phi P_{sat}^{'} & K_l + \frac{\delta_p P_{sat}\phi}{\rho_l R_v T} \end{bmatrix}\begin{bmatrix} \nabla T \\ \nabla P_c \end{bmatrix}\right) + \begin{bmatrix} -\nu(\rho_a c_{p,a} + L_v\frac{\partial \rho_v}{\partial T}) & -\nu L_v(\frac{\partial \rho_v}{\partial P_c}) \\ \nu\frac{\partial \rho_v}{\partial T} & \nu\frac{\partial \rho_v}{\partial P_c} \end{bmatrix}\cdot\begin{bmatrix} \nabla T \\ \nabla P_c \end{bmatrix} + \begin{bmatrix} Q_h \\ Q_m \end{bmatrix},$$

further written as:

$$\begin{bmatrix} C \\ \xi \end{bmatrix}\begin{bmatrix} \frac{\partial T}{\partial t} \\ \frac{\partial P_c}{\partial t} \end{bmatrix} = \nabla\left(\begin{bmatrix} \lambda + L_v\delta_p\phi P_{sat}^{'} & -\frac{L_v\delta_p P_{sat}\phi}{\rho_l R_v T} \\ -\delta_p\phi P_{sat}^{'} & K_l + \frac{\delta_p P_{sat}\phi}{\rho_l R_v T} \end{bmatrix}\nabla\begin{bmatrix} T \\ P_c \end{bmatrix}\right) + \begin{bmatrix} -\nu(\rho_a c_{p,a} + L_v\frac{\partial \rho_v}{\partial T}) & -\nu L_v(\frac{\partial \rho_v}{\partial P_c}) \\ \nu\frac{\partial \rho_v}{\partial T} & \nu\frac{\partial \rho_v}{\partial P_c} \end{bmatrix}\cdot\nabla\begin{bmatrix} T \\ P_c \end{bmatrix} + \begin{bmatrix} Q_h \\ Q_m \end{bmatrix}.$$

To apply d_a, c and β to replace the matrix coefficients in the above equation, the matrix form of the conservation equation can be obtained:

$$d_a\begin{bmatrix} \frac{\partial T}{\partial t} \\ \frac{\partial P_{suc}}{\partial t} \end{bmatrix} = \nabla\left(c\nabla\begin{bmatrix} T \\ P_{suc} \end{bmatrix}\right) + \beta\cdot\nabla\begin{bmatrix} T \\ P_{suc} \end{bmatrix} + \begin{bmatrix} Q_h \\ Q_m \end{bmatrix} \qquad in\ \Omega \qquad (3.55)$$

d_a is the damping coefficient and written as:

$$d_a = \begin{bmatrix} c_p\rho + c_l w & 0 \\ 0 & \xi \end{bmatrix};$$

c is the diffusive coefficient and written as:

$$c = \begin{bmatrix} \lambda + L_v\delta_p\phi P_{sat}^{'} & -\frac{L_v\delta_p P_{sat}\phi}{\rho_l R_v T} \\ -\delta_p\phi P_{sat}^{'} & K_l + \frac{\delta_p P_{sat}\phi}{\rho_l R_v T} \end{bmatrix};$$

β is the convective coefficient and written as:

$$\beta = \nu\begin{bmatrix} -(\rho_a c_{p,a} + L_v\frac{\partial \rho_v}{\partial T}) & \frac{L_v\phi}{\rho_l R_v T}\frac{\partial \rho_v}{\partial \phi} \\ \frac{\partial \rho_v}{\partial T} & -(\frac{\phi}{\rho_l R_v T}\frac{\partial \rho_v}{\partial \phi}) \end{bmatrix}$$

where $\boldsymbol{v}$ (m/s) air velocity

The Neumann type equation of exterior boundary condition is represented as:

$$\begin{cases} \boldsymbol{n}\cdot\left(-c\nabla u-\alpha u+\gamma\right)+qu=g \\ q=0 \\ g=\begin{bmatrix} \alpha_e(T^{eq}-T_{surf,e})+L_v\beta_{p,e}(p_{v,e}-p_{surf,e})+g_{rain}c_{p,l}T_a \\ \beta_{p,e}(p_{v,e}-p_{surf,e})+g_{rain} \end{bmatrix} \end{cases} \tag{3.56}$$

The Neumann type equation of interior boundary condition is represented as:

$$\begin{cases} \boldsymbol{n}\cdot\left(-c\nabla u-\alpha u+\gamma\right)+qu=g \\ q=0 \\ g=\begin{bmatrix} \alpha_i(T_i-T_{surf,i})+L_v\beta_{p,i}(p_{v,i}-p_{surf,i}) \\ \beta_{p,i}(p_{v,i}-p_{surf,i}) \end{bmatrix} \end{cases} \tag{3.57}$$

3-8-2 Procedure of HAM-BE modeling

The procedure to run HAM-BE modeling in COMSOL was described in this part. The words in Italic style are the command names in the COMSOL's menu:

1. To determine the dimension of simulation (*Model Navigator* → *Space dimension* → *1D, 2D* or *3D*); to define the coupled conservation equations of heat and moisture transport as the coefficient PDEs (*Multiphysics* → *Model Navigator* → *Application modes* → *COMSOL Multiphysics* → *PDE modes* → *PDE, coefficient form*); then, to define the *dependent variable* as *T* (temperature) and *Pc* (capillary pressure); in the

case air convection is considered, to select the applicable fluid dynamic mode (*Multiphysics → Model Navigator → Application modes → Fluid Dynamics → Impressible Navier Stokes or Darcy-Boussinesq*);

2. To define the geometry of subdomains by two ways: a) import an existing CAD file (*File → Import → CAD Data From File*); b) to draw the subdomains through CAD tool provided in the *Draw* menu;
3. To input the material properties and boundary conditions as constants (*Options → Constants*), expressions (*Options → Expressions → Global / Scalar / Subdomain / Boundary Expressions*) and functions (*Options → Functions → Analytical /Interpolation functions*); outputs for post-processing analysis can be also defined as expressions and integration variables over subdomains and boundaries for quantities such as heat/moisture flux and average values (*Options → Integration Coupling Variables → Subdomain / Boundary / Point Variables*);
4. For each subdomain, to select appropriate governing equations by switching the dotted equations in *Model Navigator*, then input the coefficients of the governing equations (*Physics → Subdomain settings*), initial condition (*Physics → Subdomain settings*) and boundary conditions (*Physics → Boundary settings*); for the subdomain with multiple governing equations, the operation of each equations can be switched at *Model Navigator*;
5. The mesh mode can be defined in the *Mesh* menu by various methods: the *Initialize Mesh* creates a relative rough mesh distribution; the *Refine Mesh* can create smaller

meshes; and in the *Free Mesh Parameters* the mesh number and size can be specified at the subdomain, boundary and point levels. The predefined mesh elements in COMSOL are triangular type and in *Mapped Mesh Parameters* quadrilateral mesh elements can be selected;

6. To set solving algorithm by first selecting the *Solver* type: *Stationary*, *Time dependent*, *Eigenvalue* or *Parametric*; then setting *Time stepping* and type of *Linear system solver*: *direct* or *indirect*;
7. To run simulation (*Solve* → *Solve Problem*), then achieve the simulation results through *Postprocessing* menu or export predefined variables as data file (*File* → *Export*).

The procedure listed here is the basic steps to run HAM-BE in COMSOL. For specific modeling task for various research interests, the references can be the COMSOL Modeling Guide (COMSOL 2007) and relevant publications from researchers engaging in modeling practice with COMSOL software.

The modern simulation software, such as COMSOL provides easy operation interfaces; users can do their modeling work after short time training. However, the essential knowledge of building physics and numerical simulation technique is still critical for the user to setup the model correctly and capable to explain the results. One challenge in numerical modeling is to achieve accurate results within acceptable time consumption. To reach optimized efficiency in model development, several aspects should be

considered:

1. To build the physical model with proper simplification. The physical model of the systems studied is a simplified and abstracted numerical expression of the real process. To build the physical model from the real situation, profound knowledge is required to apply appropriate assumptions: to retain the dominant process and neglect the non-important ones; to use 1D simulation instead of 2D simulation, if the 2D simulation does not provide important information that cannot be obtained from 1D simulation; and to apply analytical equations instead of interpolation in the description of material properties.
2. To use less degree of freedom (DOF). In discretized finite element model, degree of freedom is a critical measurement of the amount of calculation and defined as the product of the number of dependent variables and the number of mesh nodes. In case the governing equation is chosen (the dependent variables are set), the system with less mesh nodes will have smaller DOF.
3. To choose proper mesh size and time step. Sensitivity analysis demonstrates that the mesh size and time step can have significant or rather smaller inference to the convergence, depending on the studied phenomena. Generally speaking, the cases with fast mass (moisture) transport through the simulated object or at the boundary, like rain absorption, requires fine meshess and smaller time steps to generate correct convergence.
4. To create efficient geometry. Several tips should be considered to create the geometry

of the domains with good quality mesh and result in reasonable solution times for the finite element analysis. They include the use of symmetry to reduce the size of a finite element model; removing unnecessary interior boundaries of several geometry objects with same physical properties, since the extra points, lines, and surfaces added can cause the mesh generator to create extra mesh elements and even mesh failure; avoiding excessively small details, holes, and gaps, since small details and holes can lead to large meshes and finite element models or even failure during mesh generation; avoiding singularities (sharp corner or angle that can create problems during meshing and analysis) and rounding sharp corners by a fillet to create a radius in the corner; and treat thin building components as boundary resistance.

4 EVALUATION OF HAM-BE

Since the transient heat and moisture transport process has strong nonlinear features, usually there is no analytical solution except for limited stationary situations. The validation work is critical to verify the new model through inter-model comparison or comparison to experimental results. Two tasks are carried out to validate HAM-BE: inter-model comparison with the benchmarks of the HAMSTAD project and comparison with measured results of a laboratory experiment of full-size wall panels. The purpose of validation is to verify the numerical model, including governing equations, material data, boundary setting and their integration; and also to test the accuracy and efficiency of HAM-BE as a numerical tool for building envelope study.

4-1 Inter-model comparison against HAMSTEAD benchmarks

In 2001, the European Commission initiated the HAMSTAD project (Heat Air and Moisture Standards Development) to propose a standardized HAM modeling procedure to replace the less accurate Glaser method. The development included the methodology to determine and describe the moisture storage function, the moisture conductivities and the numerical model of non-isothermal moisture flow (vapor and liquid phases) in

building materials. As one important contribution of the HAMSTAD project, five benchmarking cases were developed to validate the existing and future hygrothermal tools. All the benchmarking cases are one dimensional and each covers at least two moisture transfer mechanisms. Moreover, the cases have been selected in order to cover various combinations of climatic loads and material combinations. The detail description of the benchmarks and simulation results were given by Hagentoft (2002a, b). An "open methodology" was proposed to stimulate competition and commercialization of numerical codes. The European partners of the project included TNO Building and Construction Research, the Netherlands; University of Leuven, Laboratory for Building Physics, Belgium; Chalmers University of Technology, Department of Building Physics, Sweden; University of Technology Dresden, Institute of Building Climatology, Germany; University of Edinburgh, Centre for Material Science and Engineering, UK; Technion – Institute of Technology, Israel; Czech Technical University, Department of Structural, Czech; and Eindhoven University of Technology, Department of Applied Physics, The Netherlands. The Institute for Research in Construction of Canada (IRC/NRC) participated on a voluntary basis in the project.

To undertake inter-model comparison in HAM-BE, given data of the HAMSTAD benchmarks: material properties, initial condition and boundary conditions, are input through corresponding interface of COMSOL as constants, analytical expressions or interpolation functions; geometric information of the studied building envelope is drawn through the CAD interface of COMSOL; coefficients of the conservation equation and

boundary equations (Equations 3.55 to 3.57) are adopted to serve each benchmarking case; the mesh mode is generated with consideration of the physical phenomena and efficient time consumption; the solver type and solving parameters are selected and simulation starts. After running of simulation, the required outputs, e.g. temperature, moisture content and relative humidity at certain locations and time, are exported in the forms of graphic plots and ASCII data files.

To validate the HAM-BE tool, four of the five benchmarks are undertaken in HAM-BE. The profile of each benchmark is interpreted here and the details of the benchmarks' material data, boundary settings, geometry of objects, required outputs were well documented in Hagentoft (2002a, b). The simulation results of HAM-BE are compared to published results of HAMSTAD project and satisfactory agreement is observed.

4-1-1 Case of "Insulated Roof"

This benchmark deals with interstitial condensation occurring at the contact surface between two materials. The construction, from external side to interior side, is built up as follows; vapor-tight seal, 100mm load bearing material and 50mm thermal insulation, shown in Figure 4.1. The materials have different thermal and moisture properties – the load bearing material is capillary active, while the insulation is hygroscopic but capillary non-active (infinite resistance to liquid flow), and thermal conductivities differ by a factor 50 (at dry conditions). The structure is perfectly airtight. The simulation covers five years. The required outputs are moisture contents of each material through the simulation and

the heat flow into the structure from the interior side.

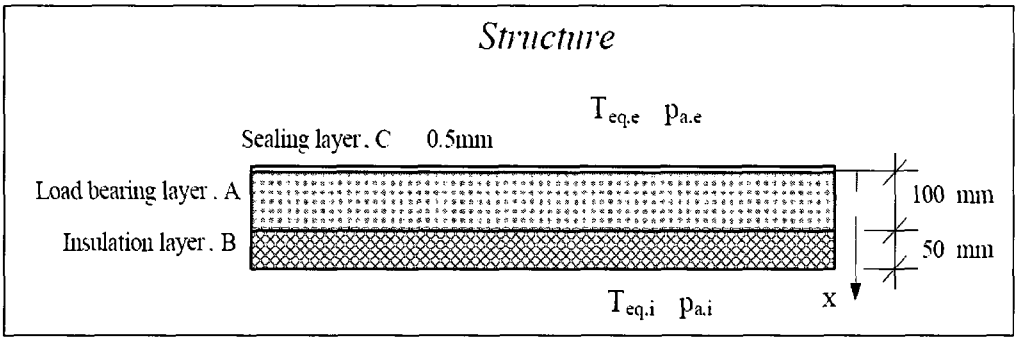

Figure 4.1 Construction detail of benchmarking case "insulated roof"

The simulation results of HAM-BE are compared with the published data of the HAMSTAD project and presented in Figures 4.2 to 4.6. The results of HAM-BE shows accurate agreement with the benchmarking data.

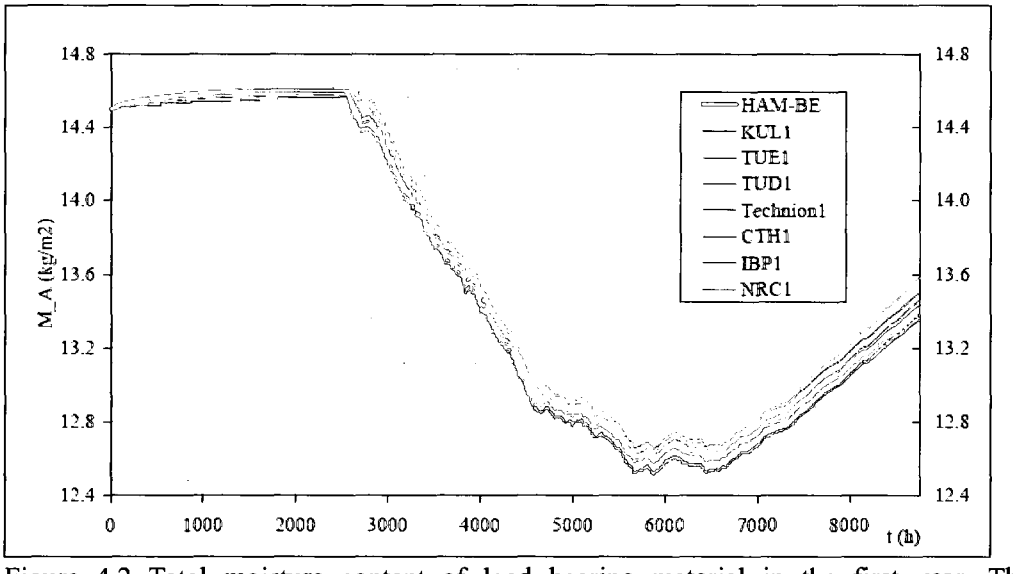

Figure 4.2 Total moisture content of load bearing material in the first year. The

benchmarking data were provided by the HAMSTAD's partners: Catholic University of Leuven, Belgium (KUL); Eindhoven University of Technology, the Netherlands (TUE); National Research Council, Canada (NRC); University of Technology Dresden, Germany (TUD); Technion-Institute of Technology, Israel (Technion); Chalmers University of Technology, Sweden (CTH); and Institute of Building Physics, Germany (IBP).

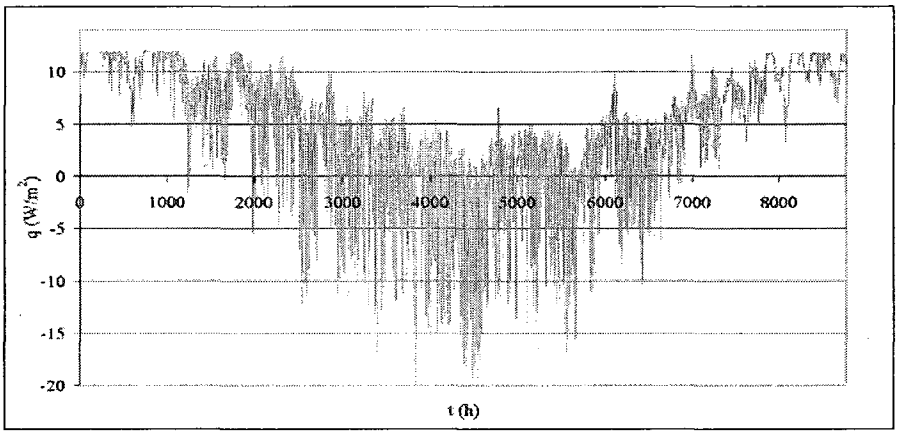

a)

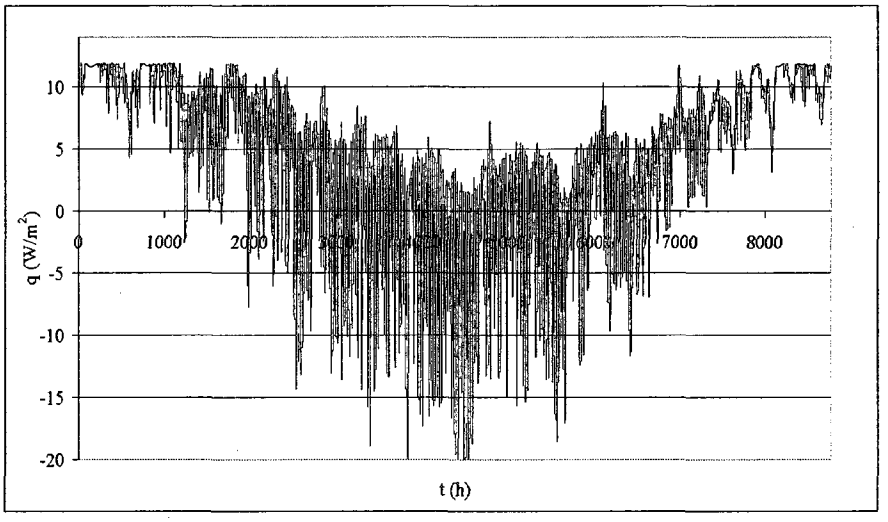

b)

Figure 4.3 Heat flow from interior to roof in the first year: a) result from average value of seven hygrothermal models; b) result of HAM-BE

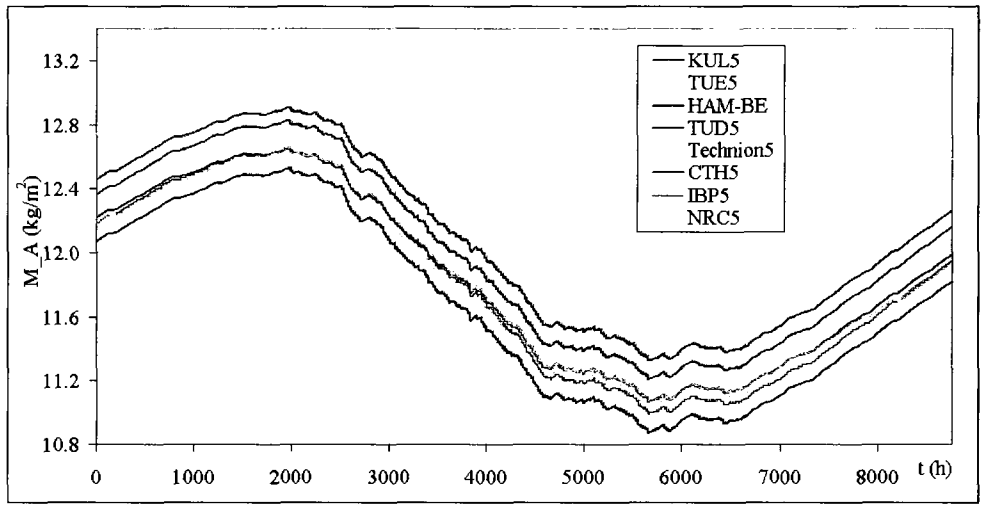

Figure 4.4 Total moisture content in load bearing material of the 5th year

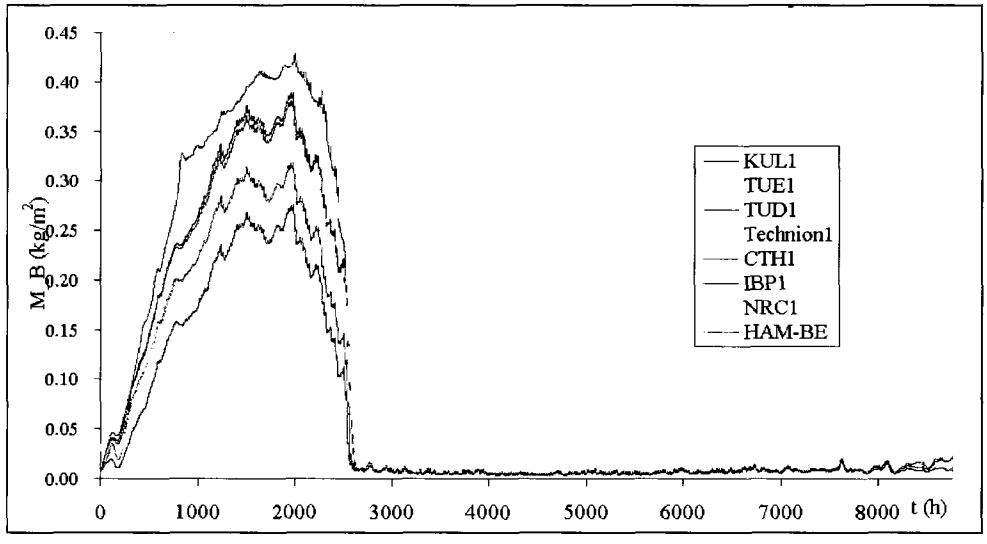

Figure 4.5 Total moisture content in insulation material of the first year

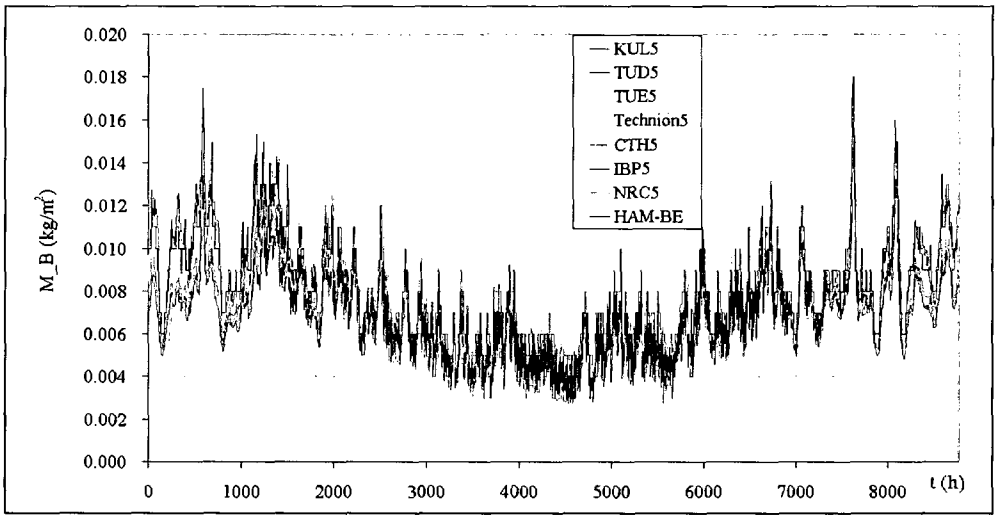

Figure 4.6 Total moisture content in insulation material of the 5th year

4-1-2 Case of "Analytical Solution"

This benchmark deals with the moisture redistribution in a homogeneous layer under isothermal conditions (Figure 4.7). Since the temperature difference through the interior and exterior is eliminated, an analytical solution can be calculated. The thickness of the layer is 200 mm. The layer is initially in moisture equilibrium with the ambient air, which has a constant relative humidity. Moisture movement is caused by a sudden but different change in relative humidity in the surroundings. The structure is perfectly airtight. The simulation covers 1000 hours. The required outputs are the moisture content distribution cross the material at 100, 300 and 1000 hours of simulation. HAM-BE and other tools show very good and uniform agreement to the analytical solution (Figures 4.8 to 4.13).

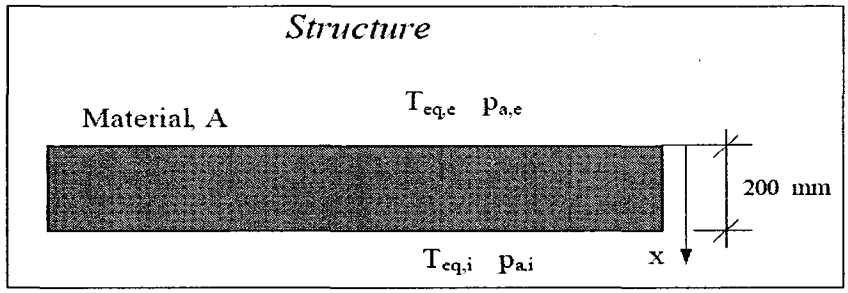

Figure 4.7 Construction detail of benchmarking case "analytical case"

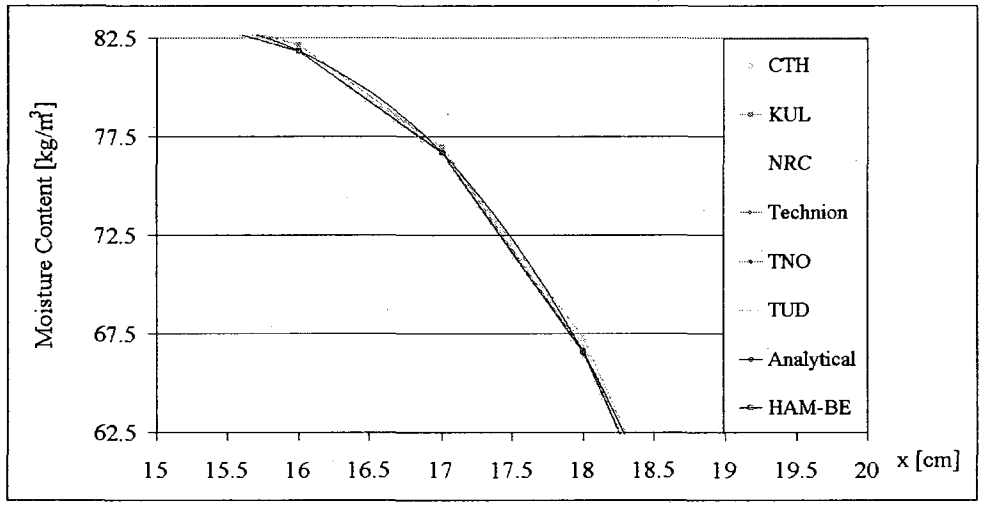

Figure 4.8 Moisture content across the sample (15.5cm to 18.5cm) after 100 hours

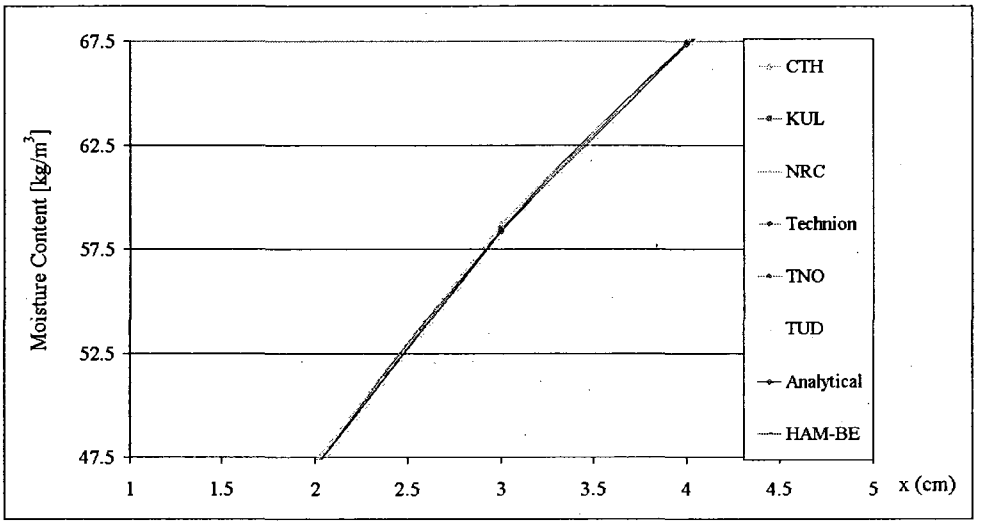

Figure 4.9 Moisture content cross the sample (2cm to 4cm) after 300 hours

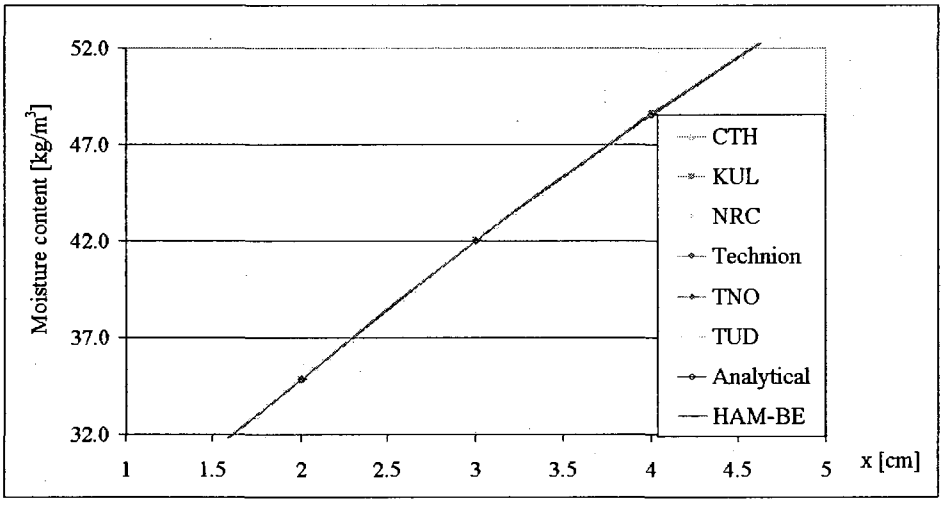

Figure 4.10 Moisture contents cross sample (1.5cm to 4.5cm) after 1000 hours

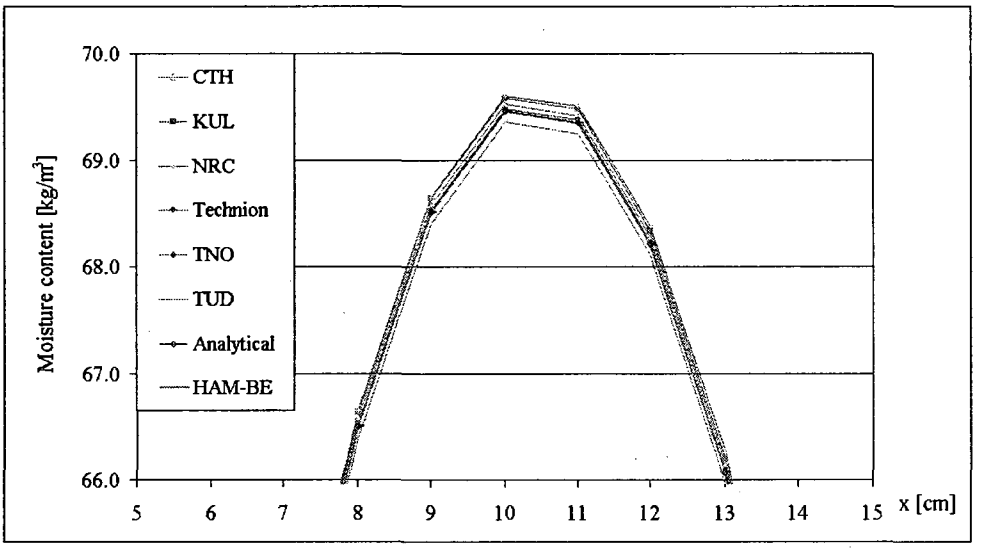

Figure 4.11 Moisture content cross the sample (7.5cm to 13cm) after 1000 hours

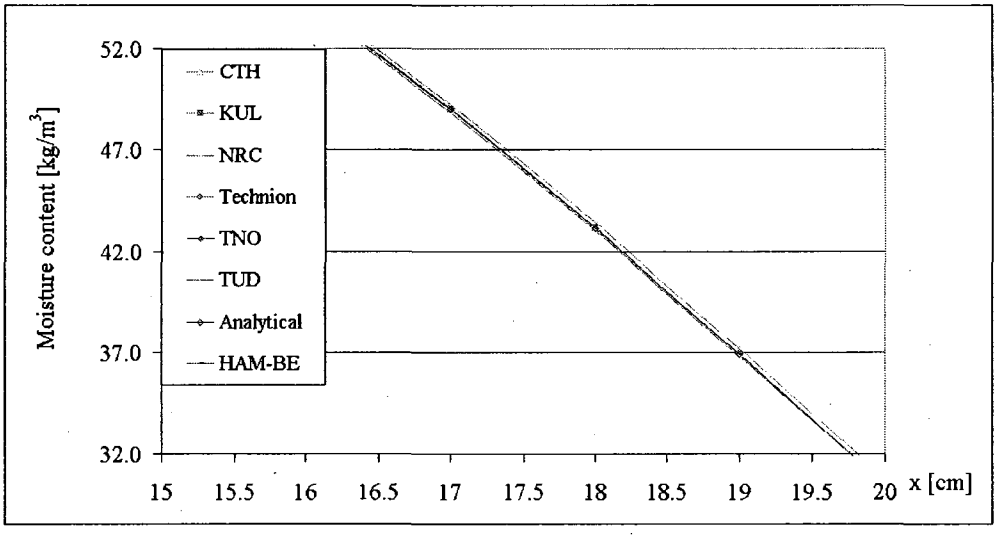

Figure 4.12 Moisture content cross the sample (16cm to 20cm) after 1000 hours

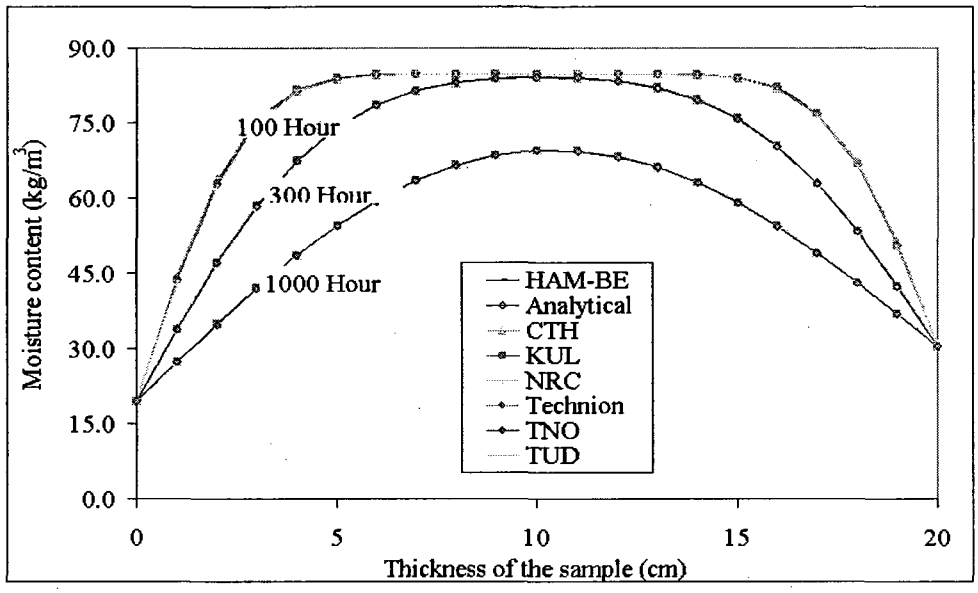

Figure 4.13 Moisture content across the sample after 100, 300 and 1,000 hours

4-1-3 Case of "Response Analysis"

This benchmark case deals with moisture movement inside a wall with a hygroscopic finish (Figure 4.14). The exterior part is 100-mm thick and the finish is 20 mm thick. The climatic load of the case is rather severe, generating several extreme heat and moisture phenomena like moisture condensation induced by cooling, alternating drying and wetting, moisture redistribution across the contact surface between two capillary active materials, etc, as shown in Figures 4.15 and 4.16. The selected materials further complicate the case, with the first layer having an extremely fast liquid transfer. The structure is perfectly airtight and simulation time is 4 days. The required outputs are the hourly values of temperature and moisture content at the outer and inner surfaces; and the temperature and moisture profiles cross the wall at 6 hour interval. Partial of the required

outputs were presented in Figures 4.17 to 4.23. Both temperature and moisture content profiles are in very good agreement.

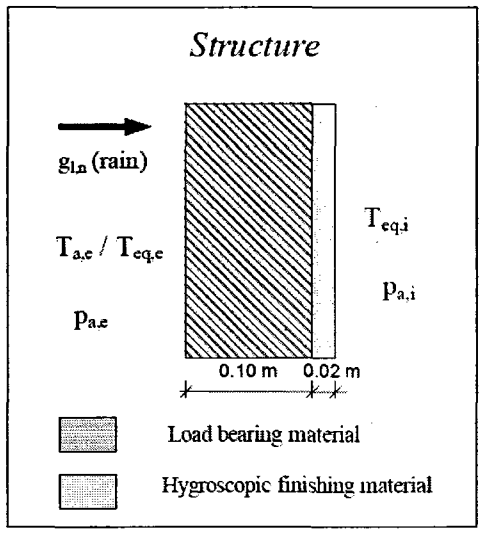

Figure 4.14 Construction detail of benchmarking case "response analysis"

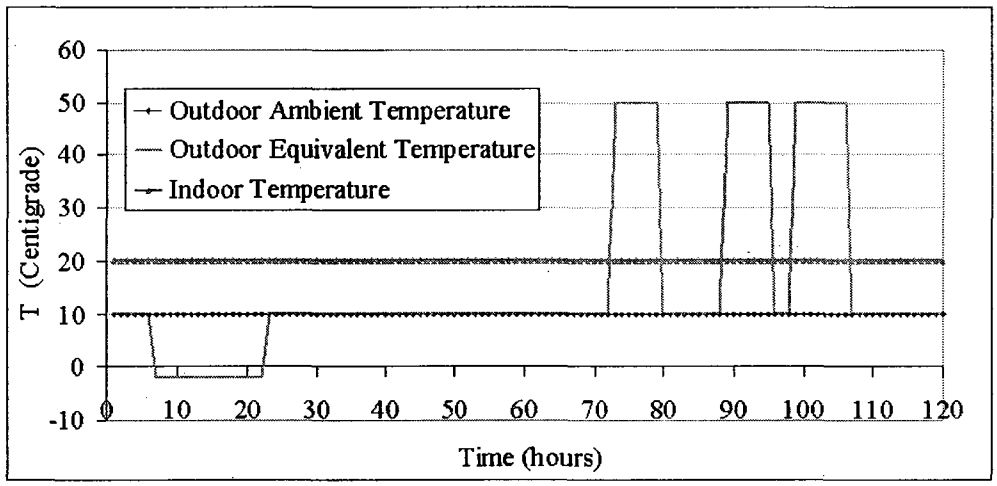

Figure 4.15 Boundary loads of Benchmark case "response analysis": Outdoor and indoor temperatures

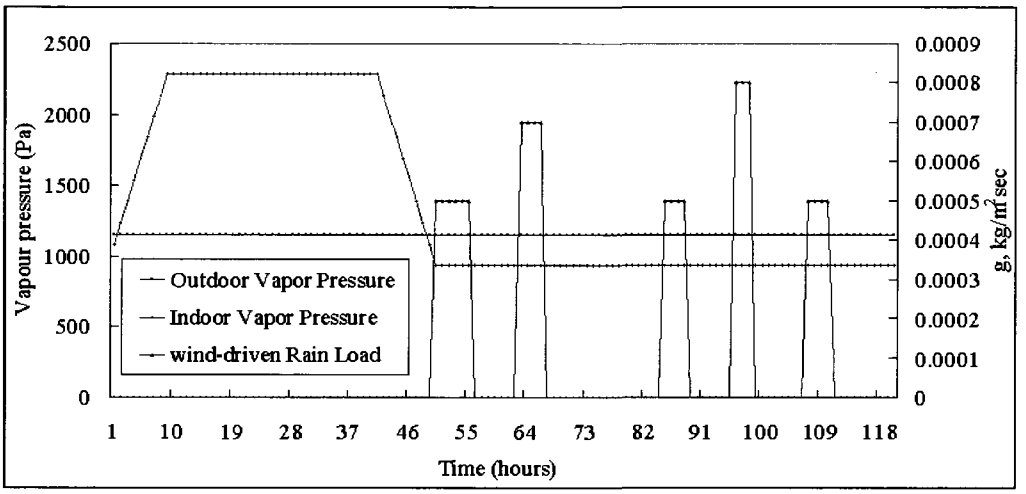

Figure 4.16 Boundary loads of Benchmark case "response analysis": vapor pressure and Wind-driven rain

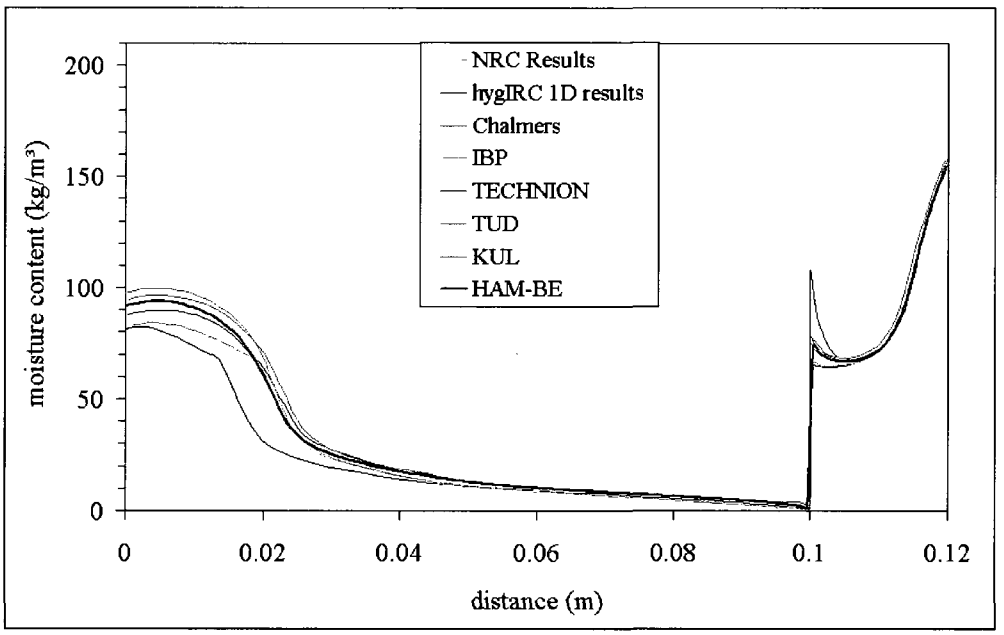

Figure 4.17 Moisture profile cross the two-layer wall after 24 hours of simulation

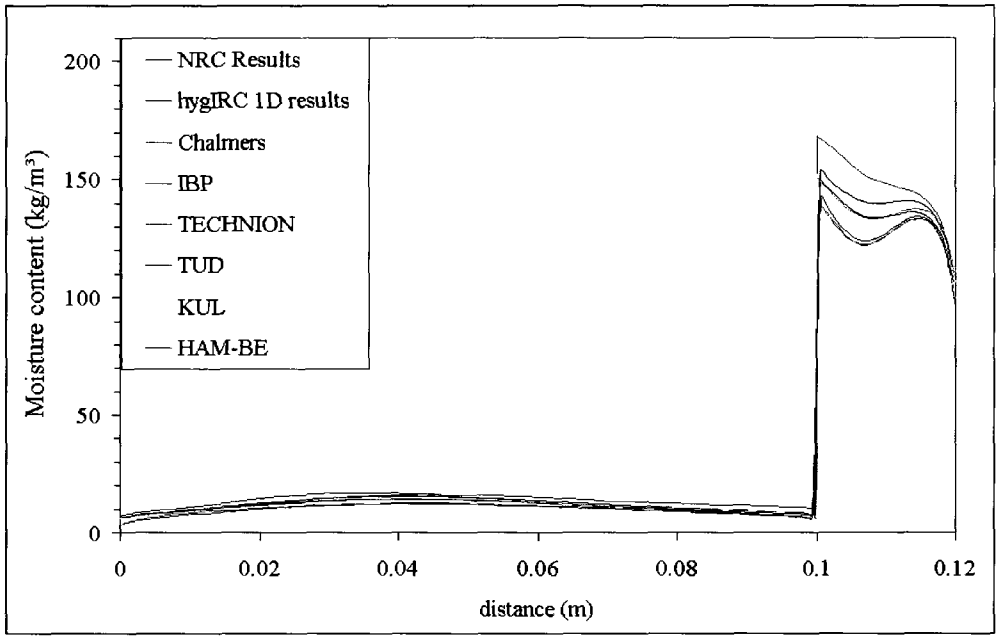

Figure 4.18 Moisture profile cross the two layer wall after 48 hours of simulation

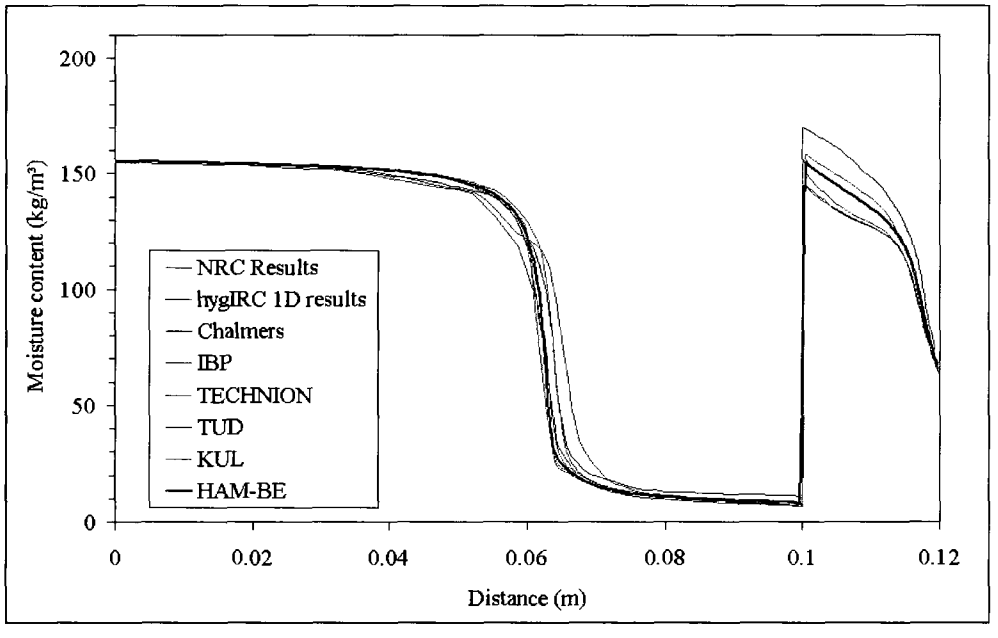

Figure 4.19 Moisture profile cross the two layer wall after 54 hours of simulation

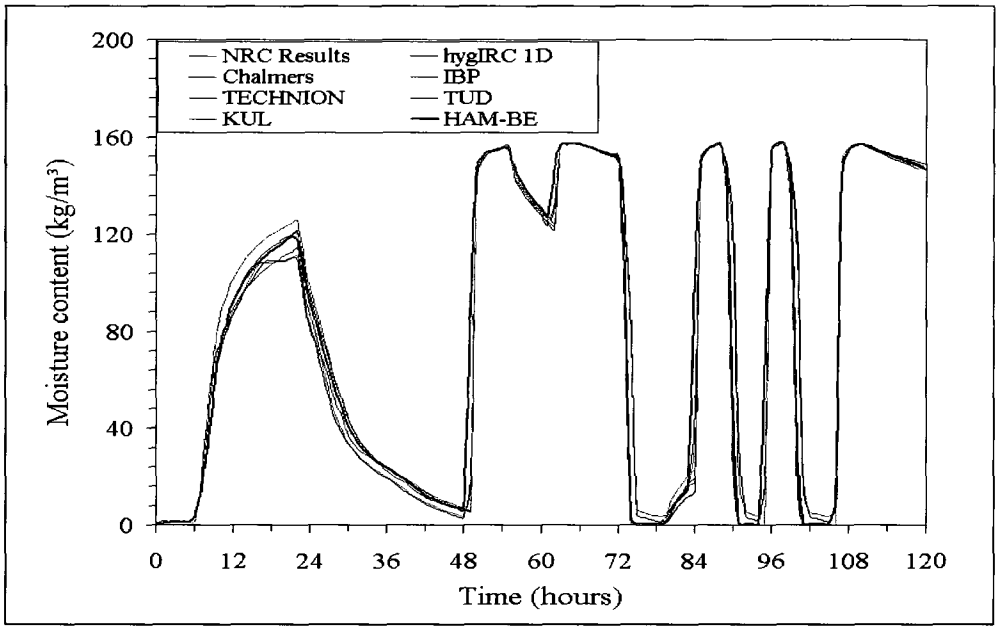

Figure 4.20 Moisture content on outer surface during the simulation period

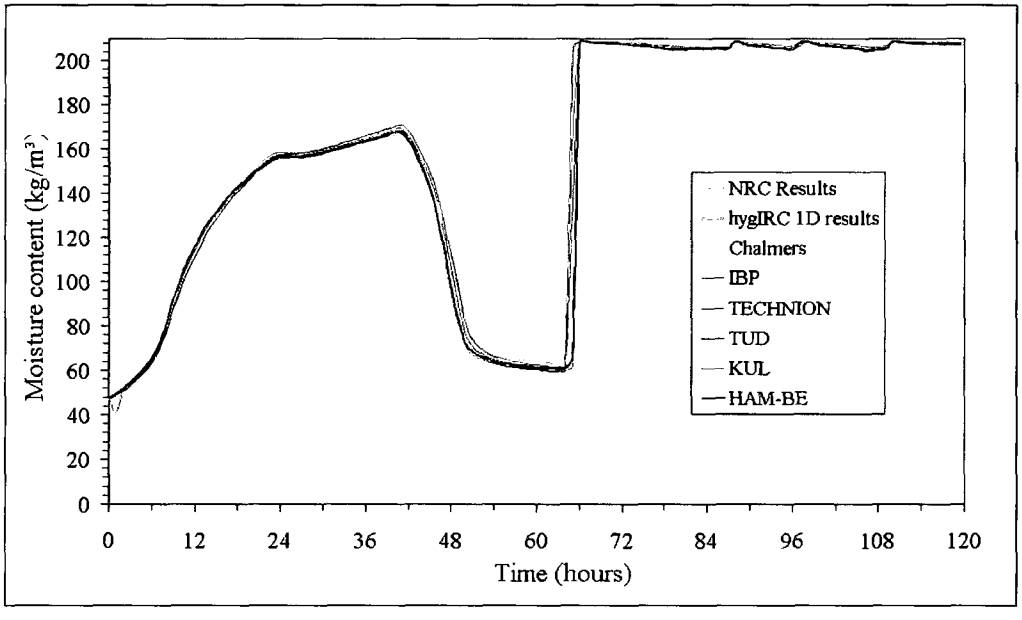

Figure 4.21 Moisture content on inner surface during the simulation period

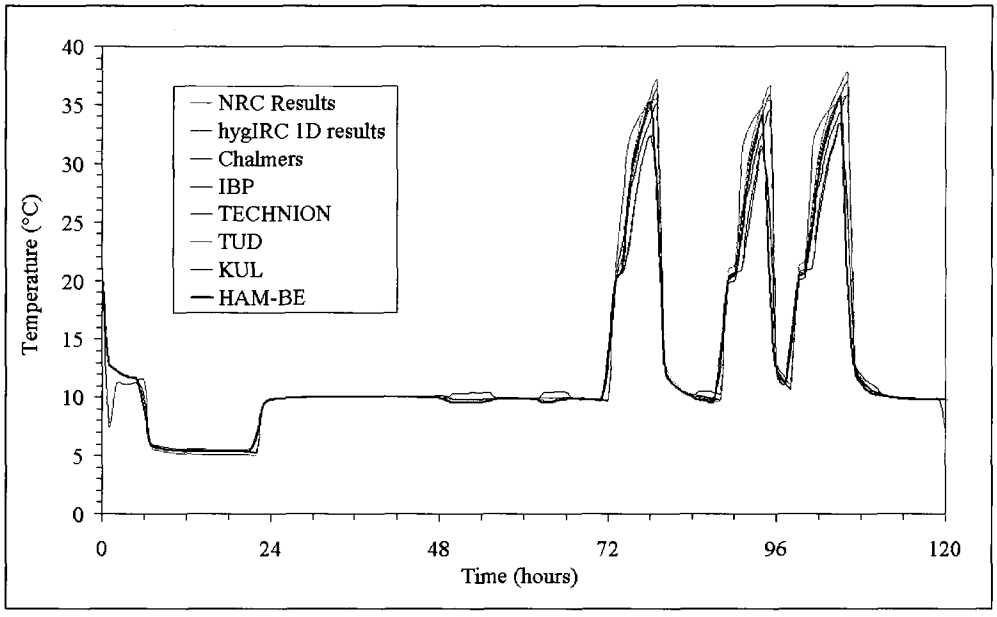

Figure 4.22 Temperature on outer surface during the simulation period

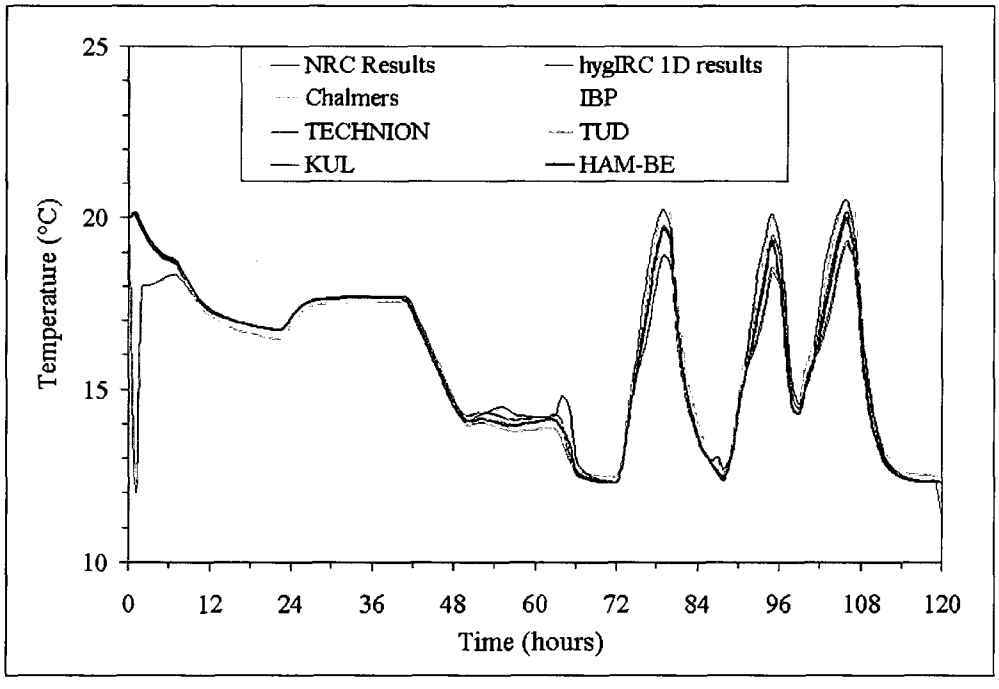

Figure 4.23 Temperature on inter surface during the simulation period

4-1-4 Case of "Capillary-active Insulation"

The benchmark deals with a wall with a layer of inside insulation (Figure 4.24). The inside insulation's performance is investigated with capillary-active feature and without it. The required outputs of this benchmarking case are the relative humidity and water content profiles at the end of the 60 days simulation time. The results of HAM-BE and data of HAMSTAD project are compared and shown in Figure 4.25 to 4.27.

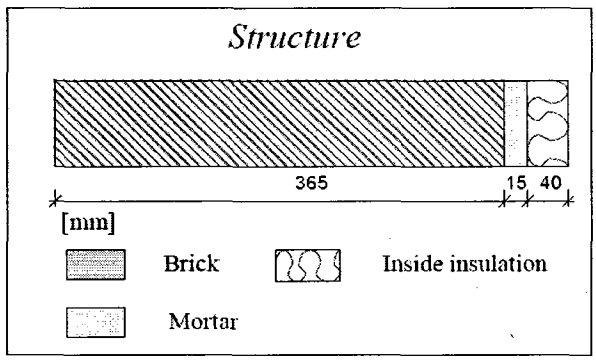

Figure 4.24 Construction detail of benchmarking case "Capillary active inside insulation material"

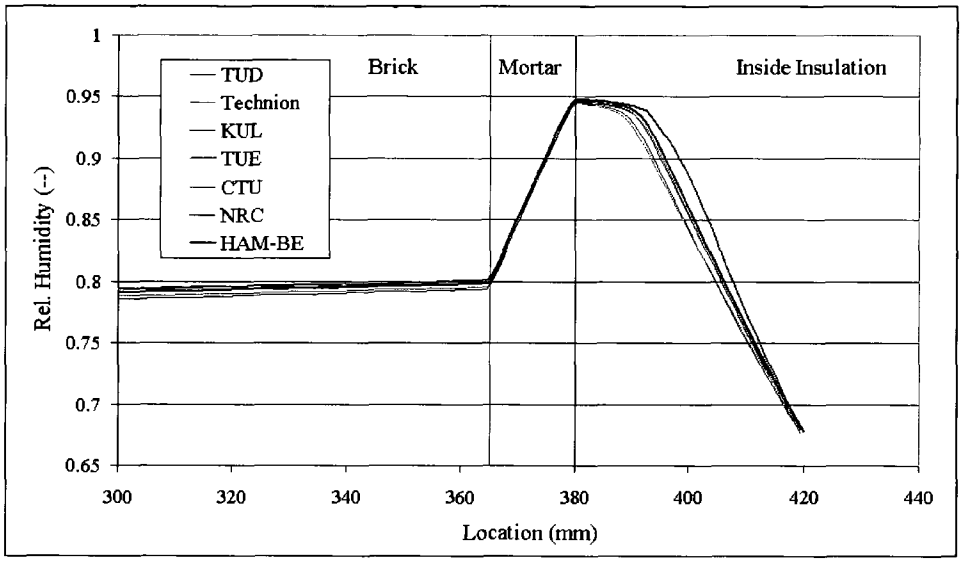

Figure 4.25 Relative humidity profiles across brick/mortar/insulation wall at the end of simulation

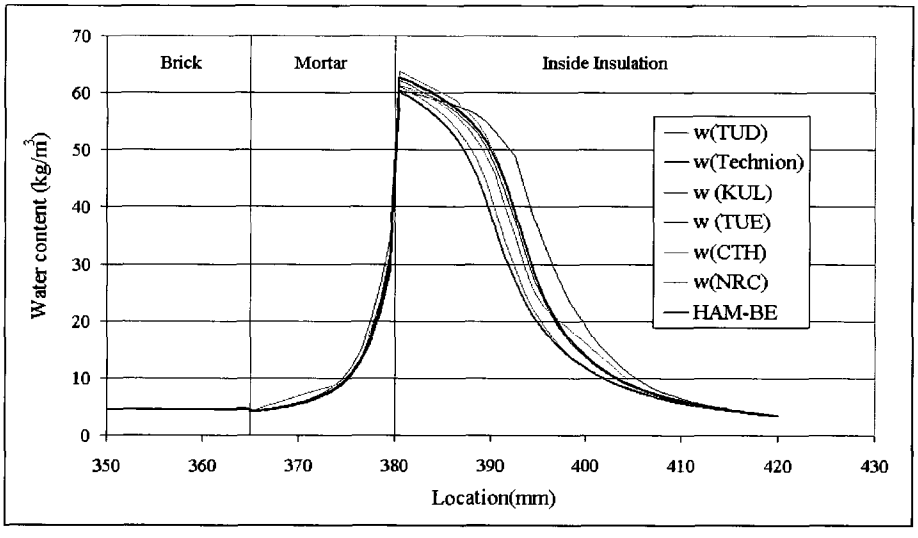

Figure 4.26 Moisture content profiles across brick/mortar/insulation wall at the end of simulation

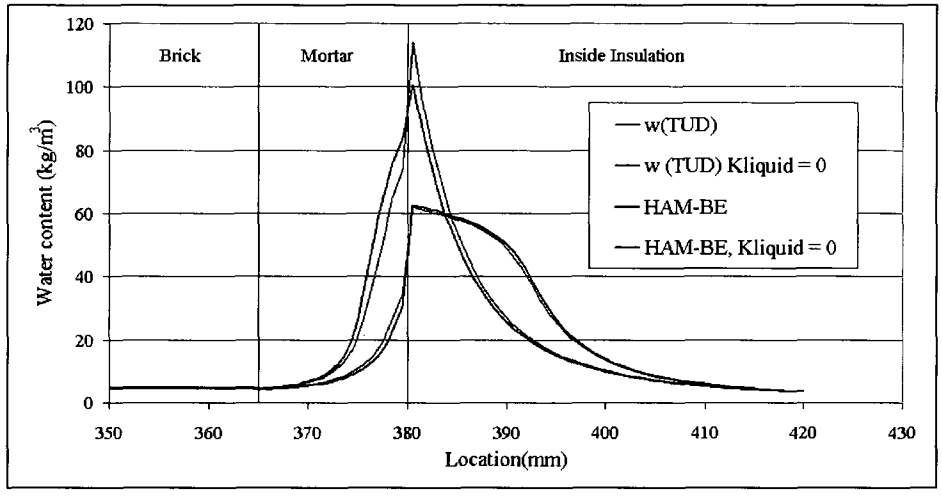

Figure 4.27 Moisture profiles with and without capillary conductivity

In the four inter-model comparisons, the results produced by HAM-BE have close agreement with the benchmarking data. In the benchmarking case with analytical solution, HAM-BE presents accurate agreement, as other hygrothermal tools. In other benchmarking cases, more complicated hygrothermal phenomena are handled and deviations can be observed among the simulation results from different hygrothermal tools. Since the nonlinear character of these benchmark cases, the "definite solution" is not available. Still, the curves of HAM-BE in all the comparison seated in the middle of all curves, which suggests excellent accuracy and reliability of the tool.

4-2 Validation with experimental data of full-scale walls

4-2-1 Introduction of the full-scale wall experiment

Extensive data from a laboratory experiment program of full-size wall panels, named as

Collaborative Research & Development (abbreviated as CRD), are used to further validate HAM-BE. The experiment aimed at verifying a new testing method to evaluate the relative drying performance of different wood-frame building envelope systems and employed 31 wall panels with various design configurations as the enclosure of a two-story test hut built within a large environmental chamber (Fazio et al. 2006a; 2007). The design plan of the test hut is shown in Figures 4.28 and 4.29 (Alturkistani et al. 2008). Configurations of the wall panels represented the construction practice in residential houses in Canada. Each wall panel is 2.44 m (8') high by 0.76 m (30") wide; it included a full 0.406 m (16") stud cavity with 2x6 wood studs in the middle and two smaller, insulated cavities (0.14m or 5.5" wide) at two sides of the central cavity to serve as thermal guard zones (Figure 4.30). The stud cavities were insulated with fiberglass batt, and finished by painted interior gypsum boards. Each wall panel was encased on top, bottom, and on two vertical sides with plywood boards, painted with two layers of latex vapor barrier primer-sealer, as a vapor separator of the specimen with the environment except for exterior and interior wall surfaces. Joints with the separator by sheathing and drywall were caulked to prevent air or vapor leakage.

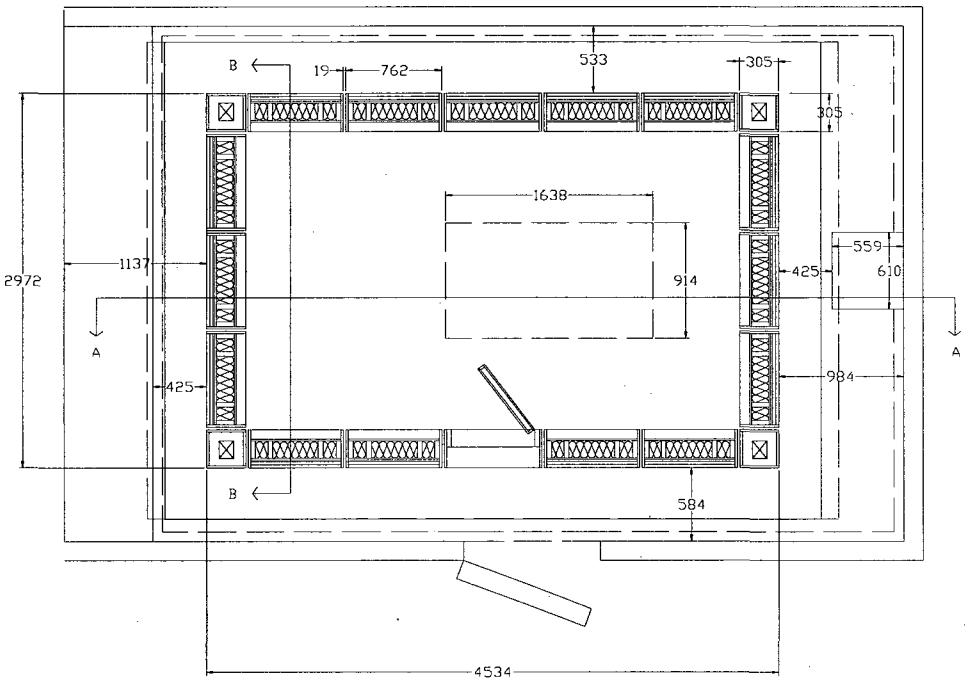

Figure 4.28 Plan of first floor of the test hut, the second floor has the same plan but with a wall panel replaced the service door (Alturkistani et al. 2008)

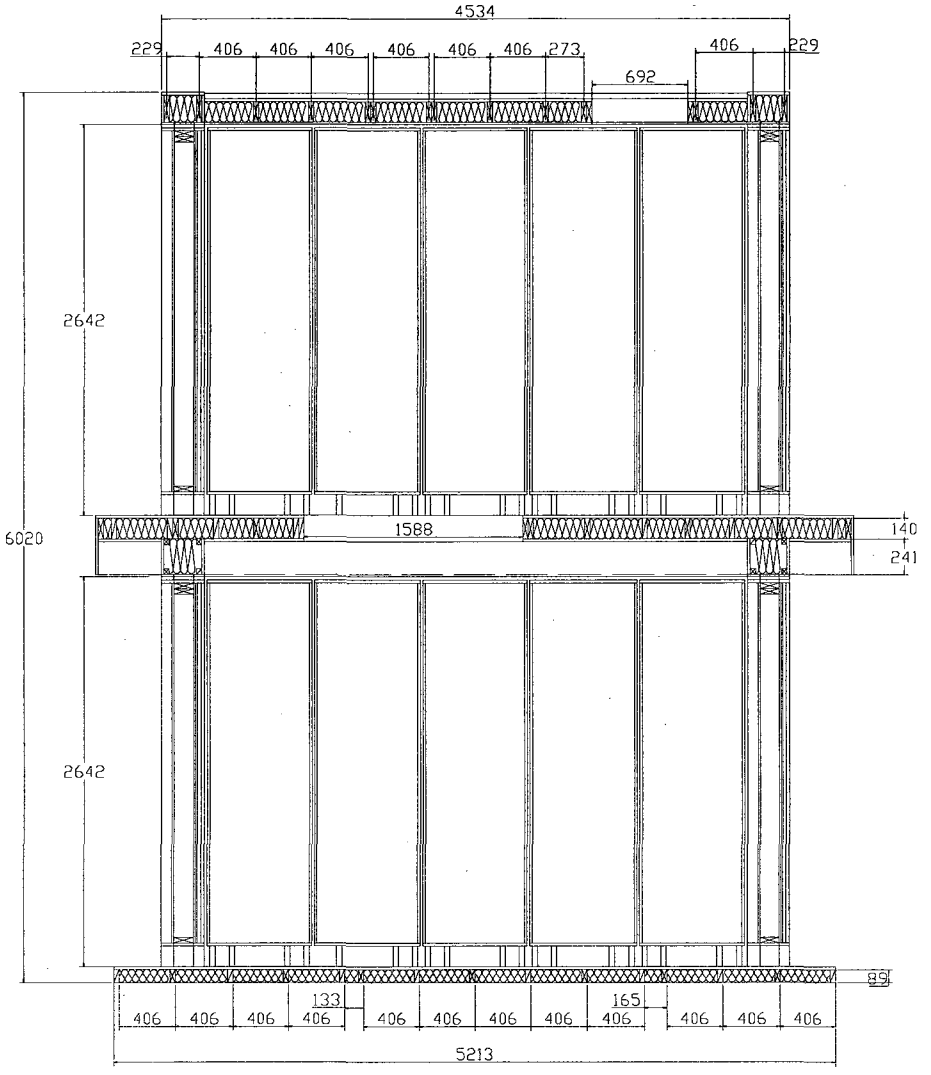

Figure 4.29 Vertical section of the test hut (Alturkistani et al. 2008)

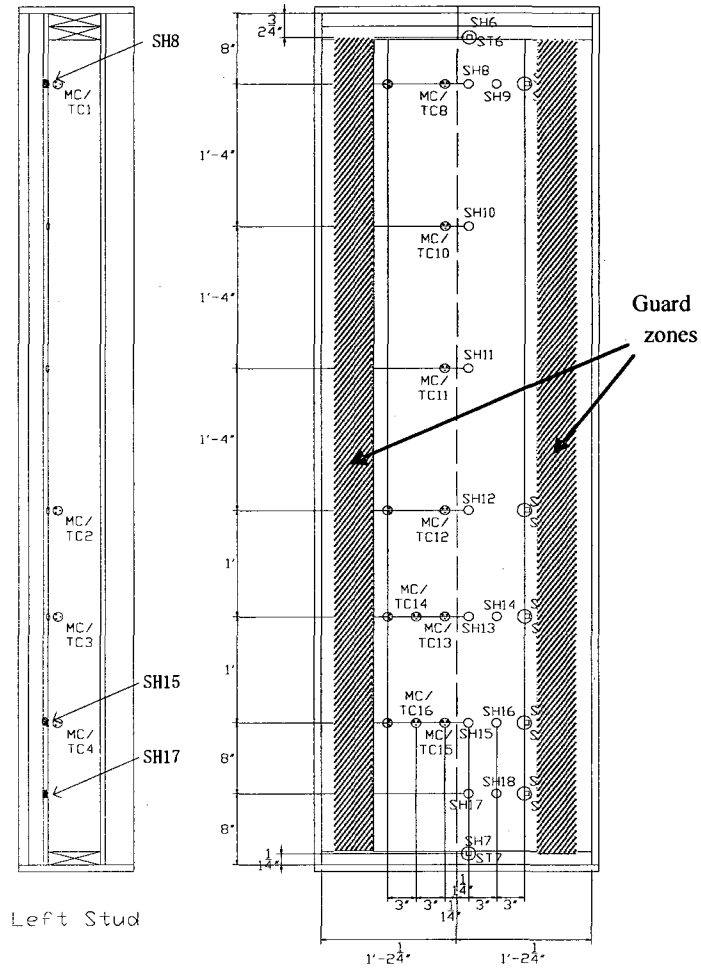

Figure 4.30 Locations of gravimetric samples (SH), moisture content pins (MC) and thermocouples (TC) on the wall panels (Fazio et al. 2006a)

To investigate various design configurations, 24 of the total 31 wall panels were made in 12 duplicate pairs with each pair having the same design configurations and placed at the same locations on the first and second floors of the test hut. The parameters investigated

in the experiment included two types of claddings: wood siding on furring and spun bonded polyolefin membrane with crinkled surface as weather barrier (Tyvek) or three-coat cement stucco on metallic mesh over two layers of asphalt impregnated papers; the type of sheathing board: oriented strand board (OSB), plywood or fiberboard; and the presence and absence of vapor barrier. The section view of the wall panels in the experiment is presented in Figure 4.31. The investigated parameters of the duplicated wall panels are listed in Table 4.1.

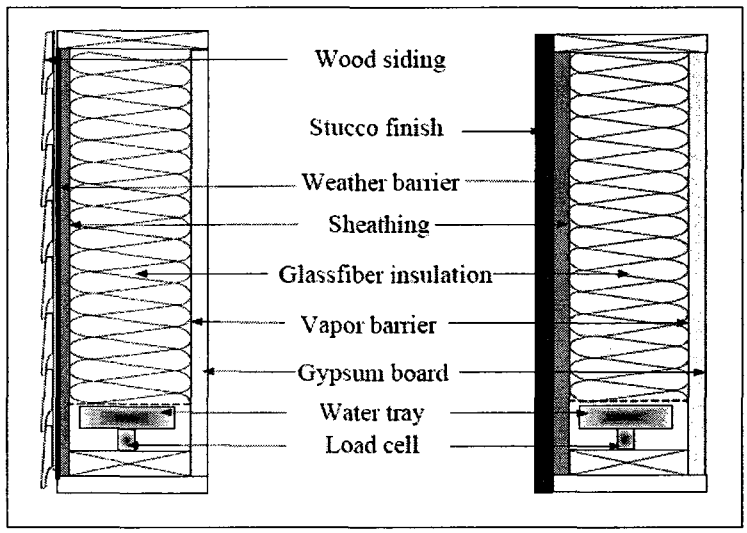

Figure 4.31 Configurations of tested wall panels. Water tray was put at top of the bottom plate in stud cavity (Fazio et al. 2007)

Table 4.1 Configurations of the wall panels in the experiment (Alturkistani et al. 2008)

Panel Number	Exterior cladding	Sheathing board	Polyethylene Vapor barrier	Figure # for MC profiles
5 & 17	Wood siding	OSB	Yes	4.35
6 & 18	STUCCO	OSB	Yes	4.36
7 & 19	Wood siding	Plywood board	Yes	4.37
8 & 20	STUCCO	Plywood board	Yes	4.38
9 & 21	Wood siding	Fiber board	Yes	4.39
10 & 22	Stucco	Fiber board	Yes	4.40
11 & 23	Wood siding	OSB	No	4.41
12 & 24	Stucco	OSB	No	4.42
13 & 25	Wood siding	Plywood board	No	4.43
14 & 26	STUCCO	Plywood board	No	4.44
15 & 27	Wood siding	fiberboard	No	4.45
16 & 28	STUCCO	fiberboard	No	4.46

In addition to the conventional boundary conditions at "indoor" and "outdoor", a new internal loading method was employed during the testing. A specially-designed water tray glued on a load cell was located on the top surface of the bottom plate of each specimen and served as the internal moisture source (Figure 4.32a). Moisture evaporating

from the trays would move into the space of the stud cavity, be absorbed in part by surrounding materials, and transport in part to the outside of the panel. To adjust intensity of moisture loading, the water trays consisted of three compartments which could be filled independently, thus providing three levels of loadings. The evaporation rate was scaled by the load cell underneath the tray (Figure 4.32b). The location of the water tray in the tested wall panel is presented in Figure 4.31 and 4.33. The moisture content of the sheathing boards and wood studs were monitored by resistive electronic moisture content transmitters and gravimetric samples. Thermocouples were installed on the sheathing boards and studs to measure surface temperatures. Relative humidity probes and temperature sensors were also hung between studs at two heights inside each stud cavity. The locations of the sensors and gravimetric samples on each specimen also were shown in Figure 4.30. More than 1,100 electric sensors and 465 gravimetric samples were installed in the wall assemblies to trace the moisture content changes. A data acquisition system was developed to collect the reading of the electric sensors; and the gravimetric samples were weighted manually at regular intervals (Fazio et al. 2006a).

a)

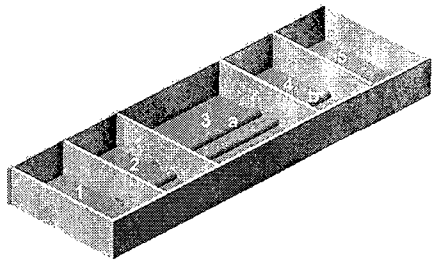

Figure 4.32 a) 3D view of the water tray, the dimension of tray is 343mm×114mm×38mm (Fazio et al. 2006a)

b)

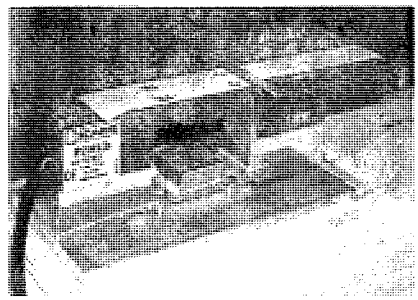

Figure 4.32 b) Load cell equipment (Fazio et al. 2006a)

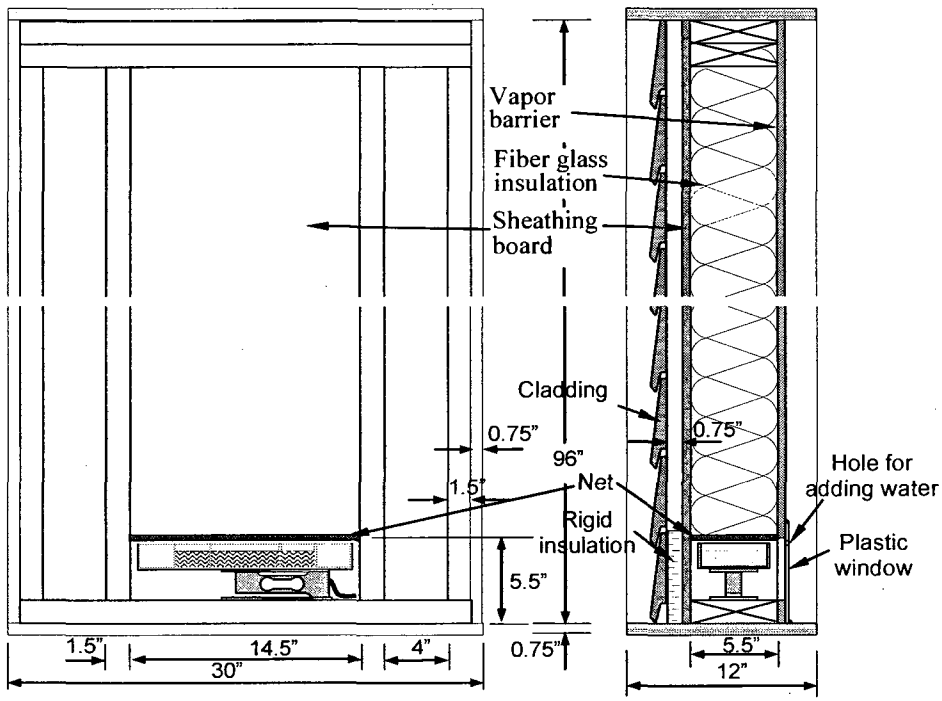

Figure 4.33 Location of water tray/load cell in the tested wall panels (Fazio el al. 2007)

The experiment was carried out in 5 periods of different loadings by varying interior/exterior temperatures, RH, and water surface areas, as listed in Table 4.2. Period 0 before the starting of testing was intended to condition wall panels to a constant initial condition. The temperature and RH inside the Environmental Chamber were set to monthly average values of Montreal (Candanedo et al. 2006), and inside the test hut to constant values of a residential dwelling.

Table 4.2 Boundary condiotns and moisture load of the CRD experiment

Period	Duration (day-day)	Interior condition		Exterior condition		Water tray
		T (°C)	RH (%)	T (°C)	RH (%)	
0	20 days	21	35	8	76	No water
1	1 – 86					1/3 filled
2	87 – 199					2/3 filled
3	200 – 227			5	75	
4	228 – 255			12	69	1/3 filled
5	256 – 284					No water

The material properties used in numerical simulation are calculated from measured data through laboratory experiment of the building materials used in the experiment. A sub-task of the experimental project was carried out through cooperation with the NRCC (National Resource Council of Canada) to determine the material properties of building

materials used in the experiment (Wu 2007, Wu et al. 2008). At the end of the experiment, samples for each type materials were cut from the wall panels, sealed and sent to the laboratory of the NRCC. Complying with the protocols of ASTM (American Society for Testing and Materials) and CEN (European Committee of Standardization), measurements were carried out to determine the required materials properties by HAM-BE: thermal conductivity, heat capacity, moisture capacity, vapor permeability, liquid diffusivity and air permeability. For each material, e.g. fiberglass insulation, OSB, plywood board, various manufacturers and products can be found in market and recorded material properties in literature are from different resources and noticeable variations exist. To use the materials properties obtained from measurement of the same materials used in the experiment contributes to control the variations of material properties and improve the accuracy of comparison between measurement and numerical simulation. In Table 4.3, the numerical expressions of material properties used in the modeling work are given.

Table 4.3 Material properties used in numerical simulation, data from Wu (2007)

Materials	Hygrothermal Properties
OSB board	Thickness: 11.64 mm Dry density: $\rho = 664 \quad (kg/m^3)$ Thermal conductivity: $\lambda = 0.09 + 0.16\frac{w}{664} \qquad W/(m \cdot K)$

	Moisture storage curve: $w = 1040 \cdot \left(\frac{1}{1+(4.75e\text{-}6 \cdot Pc)^{1.5451}} \right)^{(0.3528)}$ (kg/m^3) Vapor permeability: $\delta_p = 4.05e\text{-}13$ (s) Liquid water permeability: $K = \exp(-1.221e\text{-}14 \cdot w^6 + 2.502e\text{-}11 \cdot w^5 - 2.053e\text{-}8 \cdot w^4$ $+8.685e\text{-}6 \cdot w^3 - 0.002038 \cdot w^2 + 0.2676 \cdot w - 48.6)$ (s)
Plywood board	Thickness: 12.57 (mm) Dry density: $\rho = 456$ (kg/m^3) Thermal conductivity: $\lambda = 0.084 + (0.25 - 0.084)\frac{w}{976}$ $W/(m \cdot K)$ Moisture storage: $w = 799 \cdot \left(\frac{1}{1+(9.841e\text{-}6 \cdot Pc)^{1.468}} \right)^{(0.3188)}$ (kg/m^3) Vapor permeability: $\delta_p = 1.8e\text{-}13$ (s) Liquid water permeability: $K = \exp(4.423e\text{-}18 \cdot w^7 - 1.758e\text{-}14 \cdot w^6 + 2.768e\text{-}11 \cdot w^5$ $-2.236e\text{-}8 \cdot w^4 + 9.98e\text{-}6 \cdot w^3 - 0.002473 \cdot w^2 + 0.3288 \cdot w - 49.6)$ (s)
Fiberboard	Thickness: 10.84 (mm) Dry density: $\rho = 279$ (kg/m^3) Thermal conductivity $\lambda = 0.05 + (0.25 - 0.05)\frac{w}{976}$ $(W/(m \cdot K))$ Moisture storage: $w = 976 \left(\frac{1}{1+(6.373e\text{-}005 \cdot Pc)^{1.436}} \right)^{(0.3036)}$ (kg/m^3) Vapor permeability: $\delta_p = 1.85e\text{-}11$ (s)
Gypsum board	Thickness: 12.60 (mm) Dry density: $\rho = 592$ (kg/m^3) Thermal conductivity:

	$\lambda = 0.16 + \frac{1.2}{600} w \quad (W/(m \cdot K))$ Moisture storage: $w = 706 \cdot \left(\frac{1}{1 + (1.045e\text{-}6 \cdot Pc)^{2.529}} \right)^{(0.6046)} \quad (kg/m^3)$ Vapor permeability: $\delta_p = 3.17e\text{-}11 \quad (s)$ Liquid water permeability: $K = \exp(-4.15e\text{-}19 \cdot w^8 + 1.242e\text{-}15 \cdot w^7 - 1.536e\text{-}12 \cdot w^6 + 1.012e\text{-}9 \cdot w^5 - 3.826e\text{-}7 \cdot w^4 + 8.333e\text{-}5 \cdot w^3 - 0.009976 \cdot w^2 + 0.601 \cdot w - 40.21) \quad (s)$
Stucco	Thickness: 19.56 mm Dry density: $\rho = 592 \quad (kg/m^3)$ Moisture storage: $w_s = 350 \cdot \left(\frac{1}{1 + (1.494e\text{-}6 \cdot Pc)^{1.362}} \right)^{(0.2658)} \quad (kg/m^3)$ Vapor permeability: $\delta_p = 1.37e\text{-}11 \quad (s)$ Liquid water permeability: $K = \exp(1.525e\text{-}011 \cdot w^5 - 3.203e\text{-}008 \cdot w^4 + 2.159e\text{-}005 \cdot w^3 - 0.006357 \cdot w^2 + 0.835 \cdot w - 70.64) \quad (s)$
Glass-fiber insulation	Dry density: $\rho = 11.51 \quad (kg/m^3)$ Thermal conductivity: $\lambda = 0.038 \quad (W/(m \cdot K))$ Vapor permeability: $\delta_p = 1.72e\text{-}10 \quad (s)$ Air permeability: 2.5 e-04 (*s*)
Polyethylene vapor barrier	Thickness: 0.153 (*mm*) vapor permanence: 3.0556e-012 (*s/m*)
Spun bonded polyolefin membrane	vapor permanence: 3.17E-09 $kg.m^{-2}.s.Pa$
Asphalt Impregnated Paper	Thickness: 0.64 (*mm*) vapor permanence: 6.413e-013*exp(7.096*rh) (*s/m*)

Notes: Material data are converted from the measurement taken by Wu (2007)

4-2-2 Comparisons between simulated and measured moisture profiles of sheathing board

In tailoring HAM-BE for the experiment, the 12 sets of duplicated wall panels are modeled by 2D vertical sections; the simulation employs the same settings of the experiment in geometry, materials, boundary conditions, initial condition and duration. The moisture loading of the internal water tray in a wall panel is modeled by a constant-moisture-flow boundary condition at the bottom of the stud cavity, while the flux value is taken as the measured water evaporation rate of the water tray.

The assumptions adopted in the simulation are noted:

1) The hygrothermal behavior is approximated by 2D HAM transport, the horizontal variation between studs is neglected;
2) The indoor/outdoor conditions are set to constant in HAM-BE for each test period, while in the experiment they had slight fluctuations;
3) The construction is airtight;
4) Top and bottom of the panel is perfectly isolated;
5) The building membranes (weather resistance barrier and polyethylene vapor barrier) have only vapor resistance but no thermal resistance.

A graphic profile of the numerical simulation results is shown in Figure 4.34. The

temperature gradient across the wall and the vapor pressure gradient along both the horizontal and vertical directions are observed. Also, it is observed that the moisture distribution of the sheathing boards was significantly uneven. Highest moisture accumulation is observed near the bottom of the sheathing board, due to vapor absorption from the nearby water trays. From the bottom and up along the sheathing board, moisture accumulation reduces gradually. The sheathing boards absorbed only slight amounts of moisture at the top during the whole experiment. Wall panels with various design parameters presented different level of moisture accumulation.

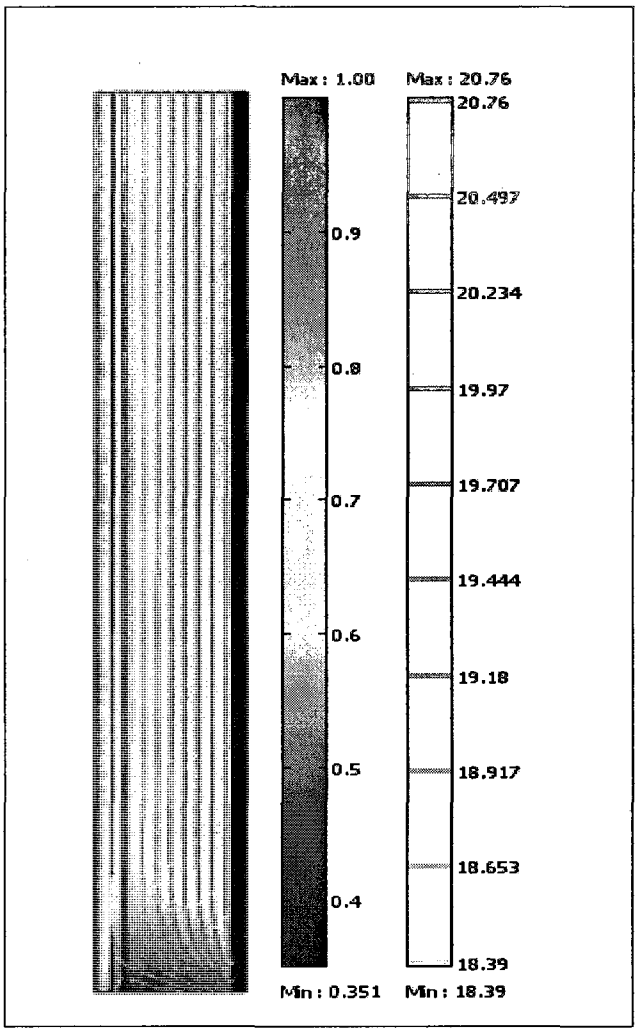

Figure 4.34 Graphic plot of temperature (contour lines) and relative humidity (colored surface) of full-height wall assemblies, result of HAM-BE (The cross section of the wall is expanded horizontally for a clearer view of the color map and color contour)

In the CRD experiment, the sheathing board was selected as the component in the wall assembly for which the absorbed moisture is monitored for the following reasons:

1. The sheathing board is located at the outer side of the wood studs; rain penetration cross the sheathing membrane (weather resistant barrier or building paper) will reach the

exterior and sometime interior side of sheathing board;

2. The sheathing board is located at the exterior side of the insulation; vapor condensation deriving from air leakage and vapor diffusion could occur at the sheathing board's surface in cases where the indoor space is heated and the air/vapor barrier may not be functional;

3. Most sheathing products are hygroscopic and can store moisture;

4. Moisture accumulated in other moisture storage components (wood frame, bottom plate and insulation) moves through the sheathing board in the outward drying process.

The comparisons between the experimental results and numerical modeling focus also on the temporal moisture content (MC) profiles at three heights of the sheathing. The predicted moisture contents are compared with moisture contents measured by gravimetric samples at locations close to the centerline of the sheathing. Sample 8 was located at the top of the sheathing, Sample 15 was located at 16 inches above the bottom plate, and the sample 17 was located at 8 inches above the bottom plate (Figure 4.30). The MCs of these gravimetric samples are considered to represent the moisture distribution in the sheathing boards along the height of the sheathing. For the 12 sets of duplicate panels, the average values of the two panels are used in comparison, which reduces the deviation caused by the individual variation of the gravimetric samples. The comparison between numerical modeling and measured data are presented in Figures 4.35 to 4.46, with the investigated parameters noted.

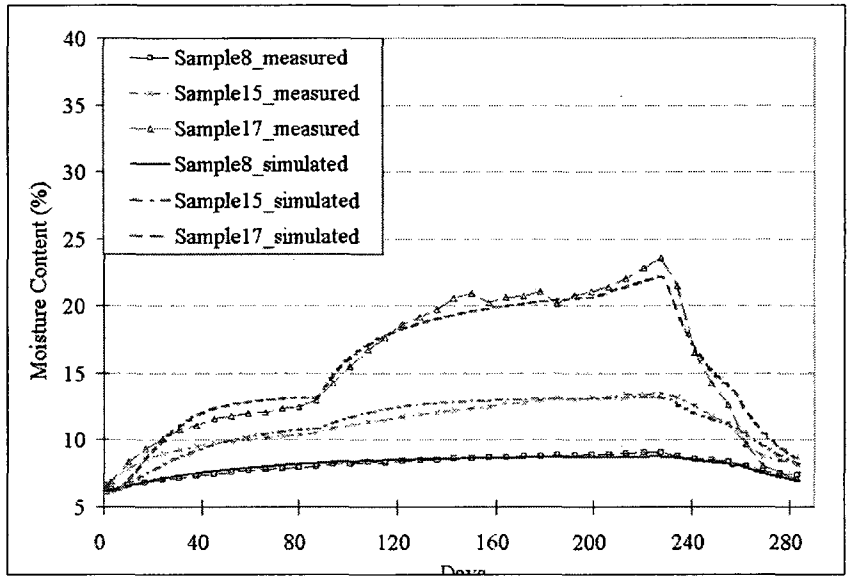

Figure 4.35 Measured and simulated moisture content at different heights of the sheathing board, design configurations of the wall (Panel No. 5&17): wood siding, OSB sheathing and polyethylene vapor barrier

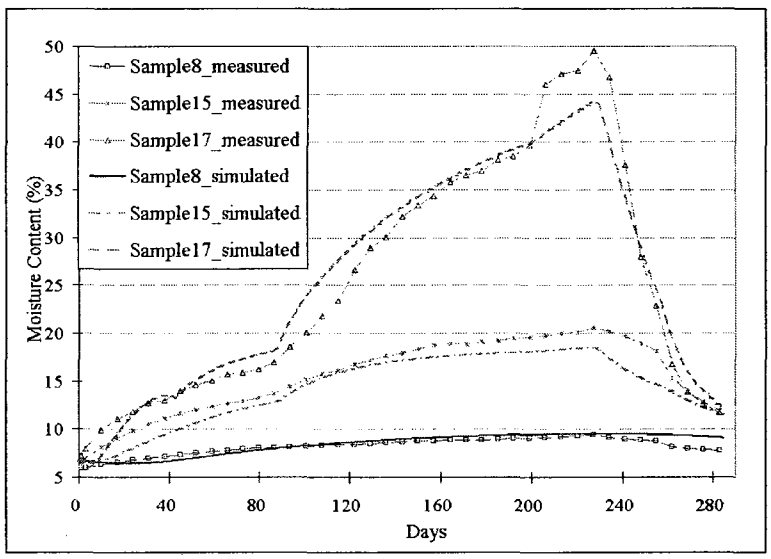

Figure 4.36 Measured and simulated moisture content at different heights of the sheathing board, design configurations of the wall (Panel No. 6&18): stucco finish, OSB sheathing and polyethylene vapor barrier

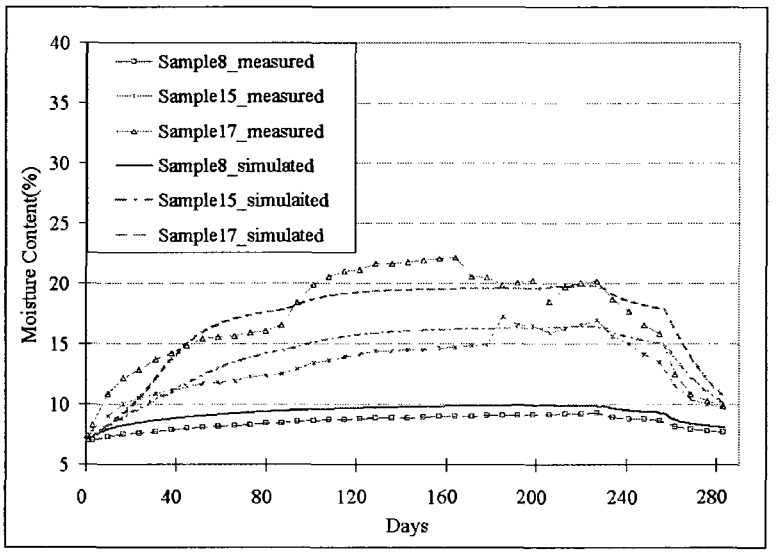

Figure 4.37 Measured and simulated moisture content at different heights of the sheathing board, design configurations of the wall (Panel No. 7&19): wood siding, plywood sheathing and polyethylene vapor barrier

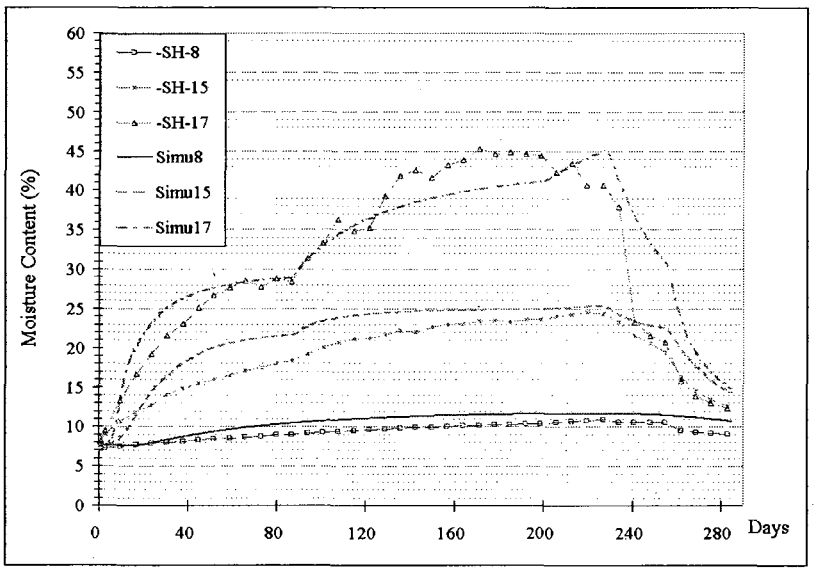

Figure 4.38 Measured and simulated moisture content at different heights of the sheathing board, design configurations of the wall (Panel No. 8&20): stucco, plywood sheathing and polyethylene vapor barrier

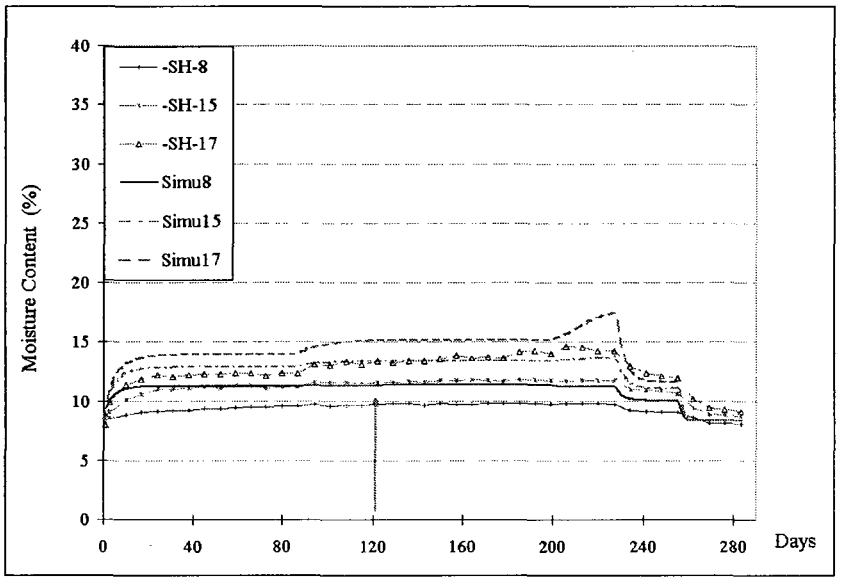

Figure 4.39 Measured and simulated moisture content at different heights of the sheathing board, design configurations of the wall (Panel No. 9&21): wood siding, fiberboard and vapor barrier

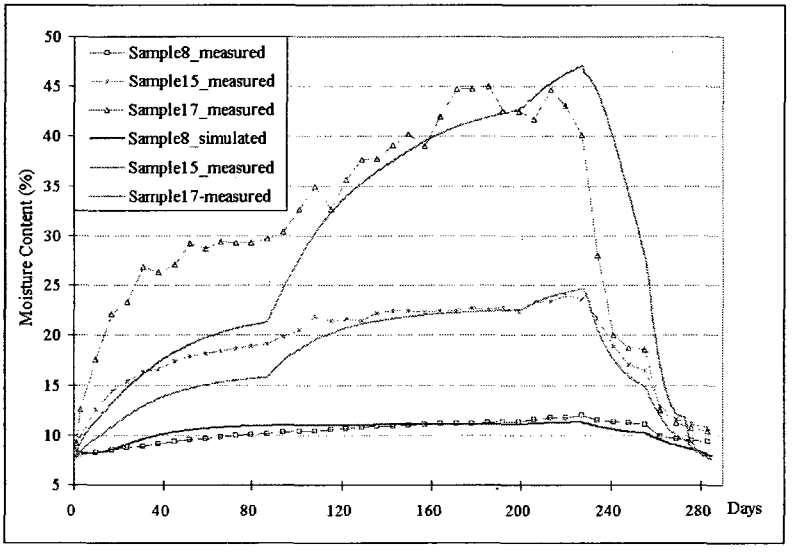

Figure 4.40 Measured and simulated moisture content at different heights of the sheathing board, design configurations of the wall panel (Panel No. 10&22): stucco, fiberboard sheathing and vapor barrier

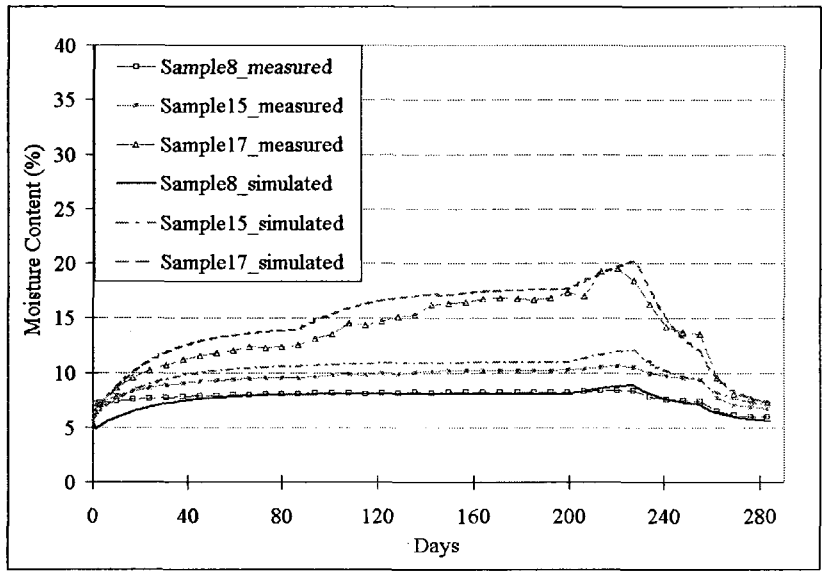

Figure 4.41 Measured and simulated moisture content at different heights of the sheathing board, design configurations of the wall (Panel No. 11 & 23): wood siding, OSB sheathing, and no vapor barrier

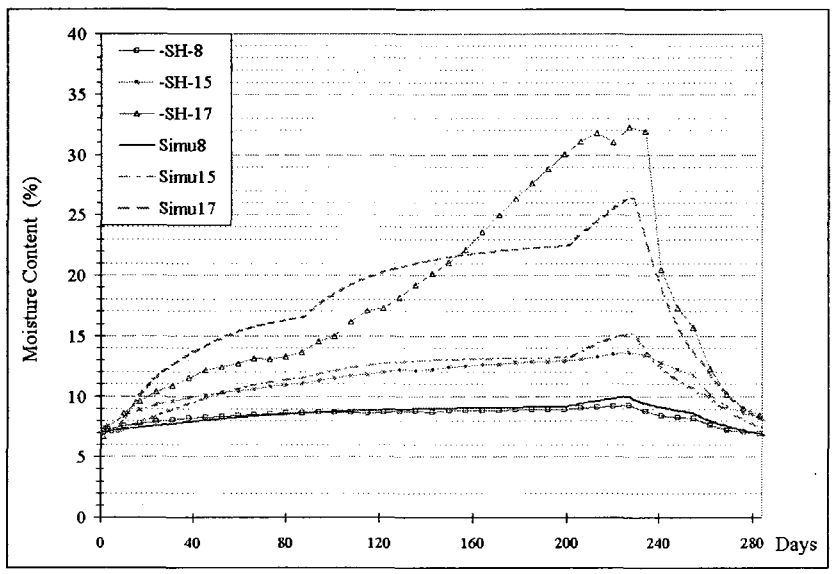

Figure 4.42 Measured and simulated moisture content at different heights of the sheathing board, design configurations of the wall (Panel No. 12 & 24): Stucco, OSB sheathing and no vapor barrier

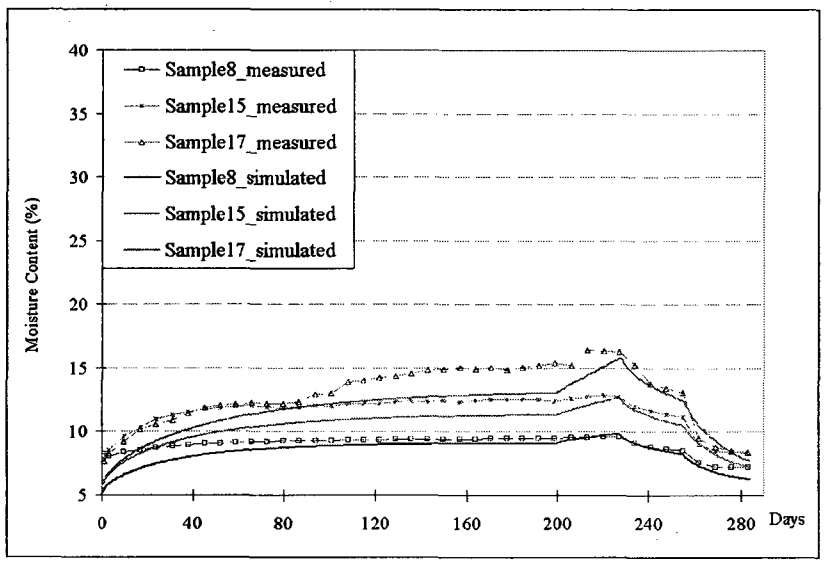

Figure 4.43 Measured and simulated moisture content at different heights of the sheathing board, design configurations of the wall (Panel No. 13&25): wood siding, plywood sheathing and no vapor barrier

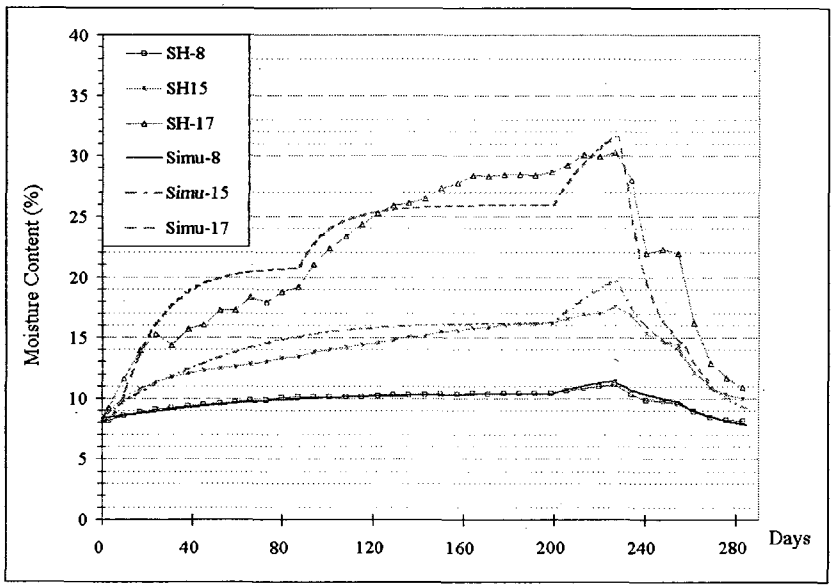

Figure 4.44 Measured and simulated moisture content at different heights of the sheathing board, design configurations of the wall (Panel No. 14&26): stucco, plywood sheathing and no vapor barrier

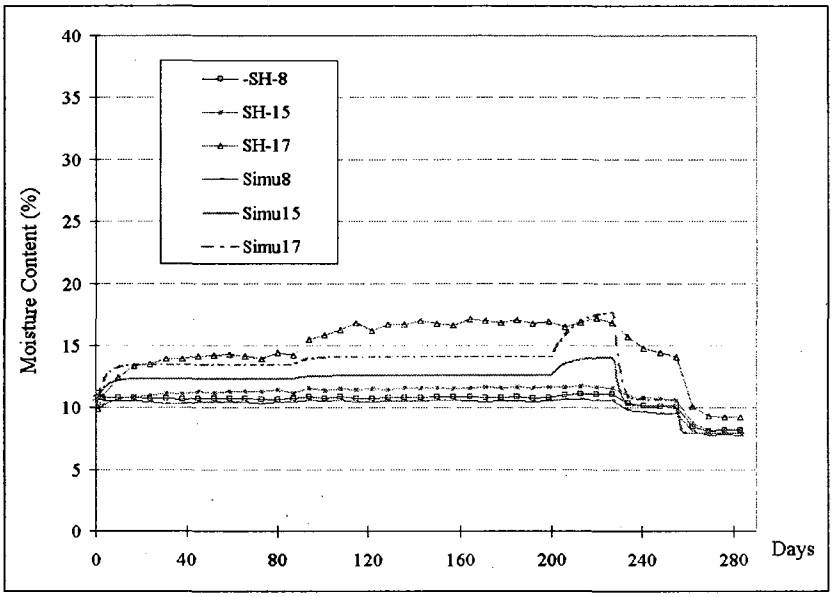

Figure 4.45 Measured and simulated moisture content at different heights of the sheathing board, design configurations of the wall (Panel No. 15&27): wood siding, fiberboard sheathing and no vapor barrier

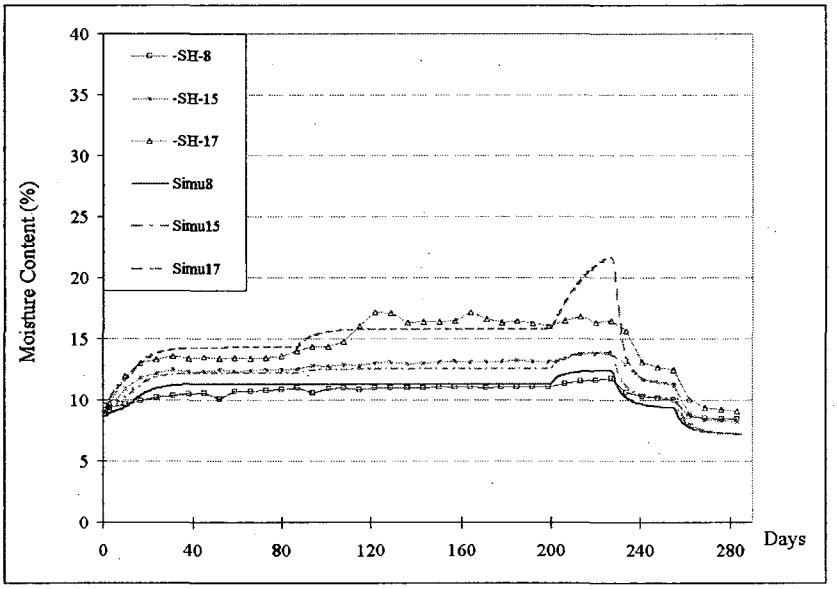

Figure 4.46 Measured and simulated moisture content at different heights of the sheathing board, design configurations of the wall (Panel No. 16&28): stucco, fiberboard sheathing and no vapor barrier

As the measured MC profiles shown in the above figures, in period 1, water was added in the tray and gravimetric samples started to absorb moisture. In period 2, with increased moisture load, the gravimetric samples' moisture content increased fast. In period 3, the lowered exterior temperature further augmented the moisture accumulation in sheathing boards. In period 4 and 5, the raised exterior temperature and reduced moisture loading resulted in quick drying process. Wall panels with different configurations (cladding, sheathing and vapor barrier) presented distinctive moisture profiles. The simulated MC profiles by HAM-BE generally follow closely those measured in the experiment.

Discrepancies between the numerical modeling and measurement are analyzed. With the assumptions listed above, the numerical modeling works under "idealized condition" and the moisture profiles are smooth and have clear and keen response to the settings of the boundary conditions, internal moisture loading, material properties and initial condition. The curves of numerical modeling can be explained in correspondence with theoretical analysis. Even thorough consideration was given to secure accuracy in the design and operation of the experiment; the measured moisture profiles from experiment can be affected by uncertain factors and presented discrepancies. The possible causes of deviation between experimental results and numerical modeling are listed in Table 4.4.

Table 4.4 Possible causes of deviation between experiment and numerical simulation

	Experiment	Numerical simulation
Material properties	Values are anisotropic, unevenly-distributed, moisture content and temperature dependent.	Values are generated from laboratory measurements and are only moisture content dependent.
Boundary condition	HVAC system was used to keep the temperature and relative humidity at the set values, but slight fluctuation existed during the experiment.	Set values applied in the experiment are used and kept constant in each period.
Initial value	The wall panels were put under constant condition for 20 days.	The initial moisture content is the average value of all the gravimetric samples.
Data collection	Gravimetric samples were taken out and weighted periodically by researchers.	Data are generated by numerical model with appropriate inputs.
Dimension	Hygrothermal transport in wall panels was 3-dimensional.	HAM-BE applies 2D simulation of the sectional view cross the wall panels.
Workmanship	The wall panels were well sealed and insulated.	No influence of workmanship is considered.

Through the validation, HAM-BE presents satisfactory capacity to predict the transient HAM transport in 2-deminsional building envelopes subjected to various levels of moisture loads in the building envelope and to changing boundary conditions. The simulation speed of HAM-BE is moderate, a simulation task on a personal computer (PC) can be completed in several hours or longer time, depending on the complication of the task. Some lessons for efficient model development are gained from the research presented. To realize the efficiency of modeling, one should: build the physical model with dominant transfer mechanisms and ignore less important ones; avoid details of geometry, for example, treat thin building sheets as boundary resistance; set reasonable fineness of mesh and time step; and apply analytical equations instead of interpolation in the description of material properties. Even though the hosting software, COMSOL, provides friendly interfaces for easy operation, the knowledge of building physics is critical for the user to build/simplify the physical model and to select the appropriate equations. Also, the knowledge and experience in the numerical method are valuable to adjust mesh modes, time step, solver, and solving parameters.

Based on the literature review carried out, HAM-BE represents the first successful 2D HAM model that is a fully developed to take advantages of dedicated commercial finite element software and is validated with full-scale experimental data. HAM-BE is capable to simulate transient and multi-dimensional heat, air and moisture transport in multi-layer building envelopes. State of the art knowledge of heat and moisture transport in building materials has been applied. Moisture-dependent material properties were applied.

Climatic loads can be applied from meteorological data (temperature, relative humidity, solar radiation, wind speed and precipitation) or from a set of experimental conditions. HAM-BE also has favorite flexibility for the user to build/modify/extend models; and it is convenient for the user to maintain and share his/her model with other researchers.

With validation, the numerical tool will be used as a "virtual laboratory" to extend cases studied experimentally, and also used to carry out parametric analyses of different types of building envelope configurations, which is of special interest to researchers in particular and to the industry in general. It should be noted, however, the numerical tool has shown to be reliable in the verified applications; further verification needs to be carried out by applying the tool to different cases and conditions.

5 INVESTIGATION OF WOOD-FRAME WALLS' DRYING PERFORMANCE

Chapter 4 describes the validation work of the HAM-BE tool through inter-model comparison, comparison of the results obtained form HAM-BE and measurements from the CRD project. The HAM-BE tool has been proven to be accurate and reliable in the range of conditions used in the validation. In this chapter, further work is done to investigate the wood-frame walls' hygrothermal performance.

The investigation is carried out in two stages. In Section 5-1, the influence of the selected design parameters on the drying performance of the CRD wall panels is investigated based on HAM-BE modeling described in Section 4.2. The modeling results are used to calculate the RHT Indices and to compare various wall panels' drying performance. The moisture sensitive component to be investigated to determine the RHT values is the lower part of the sheathing board. In Section 5-2, the hourly weather data of two targeted regions of the CRD project (Montreal and Vancouver) are set as the exterior boundary condition for the HAM-BE modeling. The lower part of the sheathing board is set at the high initial moisture content as the moisture loading. Extended numerical modeling is carried out by HAM-BE to investigate the influence of changed climates and design configurations to the drying of moisture accumulation in the wood-frame walls of

the CRD project. Based on HAM-BE modeling and literature, the guide to manage moisture penetration in wood-frame walls is summarized at the end of this chapter.

5-1 Analysis of wall panels' drying performance under CRD experimental conditions

The CRD experiment applied water trays inside the stud cavity as internal moisture loading in the drying test. The HAM-BE tool has been used to predict the moisture profiles of the sheathing board using measured values of the internal moisture loading and boundary conditions of the experiment. The comparison between experimental results and numerical simulation has been presented in Figures 4.35 to 4.46. In this part, the temperature and moisture content profiles produced by HAM-BE are used to calculate the RHT (relative humidity and temperature) index and the drying performance of the wall panels is analyzed.

5-1-1 Calculation of RHT index

Moisture accumulation in wood-frame building envelope may lead to the rot of material by decay fungi. The growth of fungi requires five essential conditions: source of fungal spores, suitable substrate (food), moisture, oxygen, and suitable temperature (Baker 1969). For wood-frame building envelopes, it is not practical to eliminate the airborne spores of fungi, oxygen and food (organic materials in building components). The temperature limits for growth of most fungi is between 0°*C* and 45°*C*. The optimum

temperatures for fungal growth lie between 20°*C* and 30°*C*. The temperature profile across the building envelope is managed by the design consideration of thermal comfort and energy consumption; usually it cannot be controlled to oppress fungi growth. Therefore, the solution to prevent fungi growth in wood-frame building envelope is to keep the moisture content in the materials under the safe level. While the average moisture content of wood is between 13-17 percent, it is generally accepted that the moisture content of wood must exceed the fiber saturation point (roughly >25-30% MC) for decay fungi grows. Optimal condition for wood decay is when wood moisture content is 40-60% MC, coupled with mild temperatures (Yang & Heinsohn 2007).

The empirical models to estimate the risk of fungi growth have been developed (Viitanen 1996, Ojanen 1998, Krus et al. 2001, Karagiozis 2002) to check suitable conditions of temperature, moisture content, exposure time, surface condition and materials. But those tools require sufficient input information and also lack accurate calibration. One alternative approaches to indicate the fungi growth potential is the RHT index developed at IRC (Institute for Research in Construction, National Research Council Canada) in the MEWS program (Moisture Management for Exterior Wall Systems) (Cornick & Dalgliesh 2003). The index links the damage potential for wooden materials in the building envelope to the occurrences when temperature and humidity are above certain critical threshold values.

The value of the RHT index is the sum of the non-zero products of the above-threshold-value temperature and the above-threshold-value relative humidity of a

selected location on an envelope component during a designated period such as one year. The equation to calculate the RHT index was shown in (Cornick & Dalgliesh 2003) as:

$$RHT\ Index = \sum_{t=1}^{n} (RH - RH_X) \times (T - T_X) \tag{5.1}$$

where RH (%) is the relative humidity of air, RH_X (%) the threshold relative humidity, T (^oC) the temperature of air, and T_x (^oC) the threshold temperature. In case RH is smaller than RH_x, the term of $(RH - RH_X)$ is considered as zero; and in case T is smaller than T_x, the term of $(T - T_X)$ is deemed to be zero. The index of the summation in Eq. 5.1, t, is the time step or interval that RH and T values are recorded. The larger the value of RHT index, the higher the risk of mold growth.

The threshold values of temperature and relative humidity can be set to reflect various damage processes. To reflect the moisture accumulation level in the wall assemblies, two sets of RHT indexes were used by Cornick & Dalgliesh (2003). The RHT80 index indicates the starting of mold growth and corrosion of metal accessories in the wall. The threshold temperature of the RHT80 is set to 0°C, and the threshold of relative humidity is set at 80%. The RHT95 index is used to indicate the occurrence of wood decay, and the threshold values are set at 95% RH and 5°C. It was noted that the value of a RHT index should be used only for relative comparison among simulation results, rather than to use the absolute values themselves (Beaulieu et al. 2002).

In the experiment of the CRD project (Fazio et al. 2006a, 2006b, 2007) and also the numerical simulation presented in this thesis, it has been observed that the lower part of

the sheathing boards had the highest moisture accumulation and the highest risk of fungi growth. Therefore, the analysis by RHT indices is focused on this region. A 40 cm height region from the bottom of the sheathing is defined as the "critical zone" in the investigation and the averaged temperature and RH of the critical zone is exported as hourly data from the numerical modeling. Then, the RHT index for the one-year period is calculated. An example of the wall panel's temperature and RH profiles is presented in Figure 5.1. The RHT index values of the 12 set of duplicate wall panels with various design configurations are listed in Table 5.1 in an ascending order of the RHT indices. In Figure 5.2, a graphic presentation of the RHT index is shown.

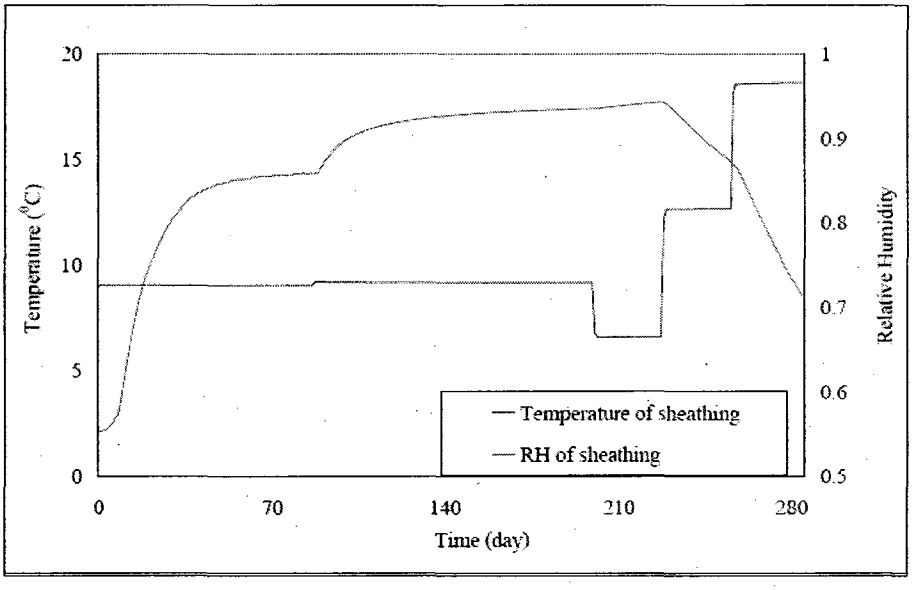

Figure 5.1 Averaged temperature and RH of the sheathing board,

to calculate the RHT index

Table 5.1 Values of RHT indices of wall panels from numerical simulation

Panel numbers	Cladding type	Sheathing type	Vapor barrier	RHT95 index	RHT80 index
13 & 25	Wood siding	Plywood	No	0	398
15 & 27	Wood siding	Fiberboard	No	0	560
11 & 23	Wood siding	OSB	No	0	1002
16 & 28	Stucco	Fiberboard	No	0	1140
9 & 21	Wood siding	Fiberboard	Yes	0	932
5 & 17	Wood siding	OSB	Yes	0	2494
7 & 19	Wood siding	Plywood	Yes	0	2996
12 & 24	Stucco	OSB	No	9	2822
14 & 26	Stucco	Plywood	No	118	3470
6 & 18	Stucco	OSB	Yes	360	4404
10 & 22	Stucco	Fiberboard	Yes	502	4898
8 & 20	Stucco	Plywood	Yes	668	5664

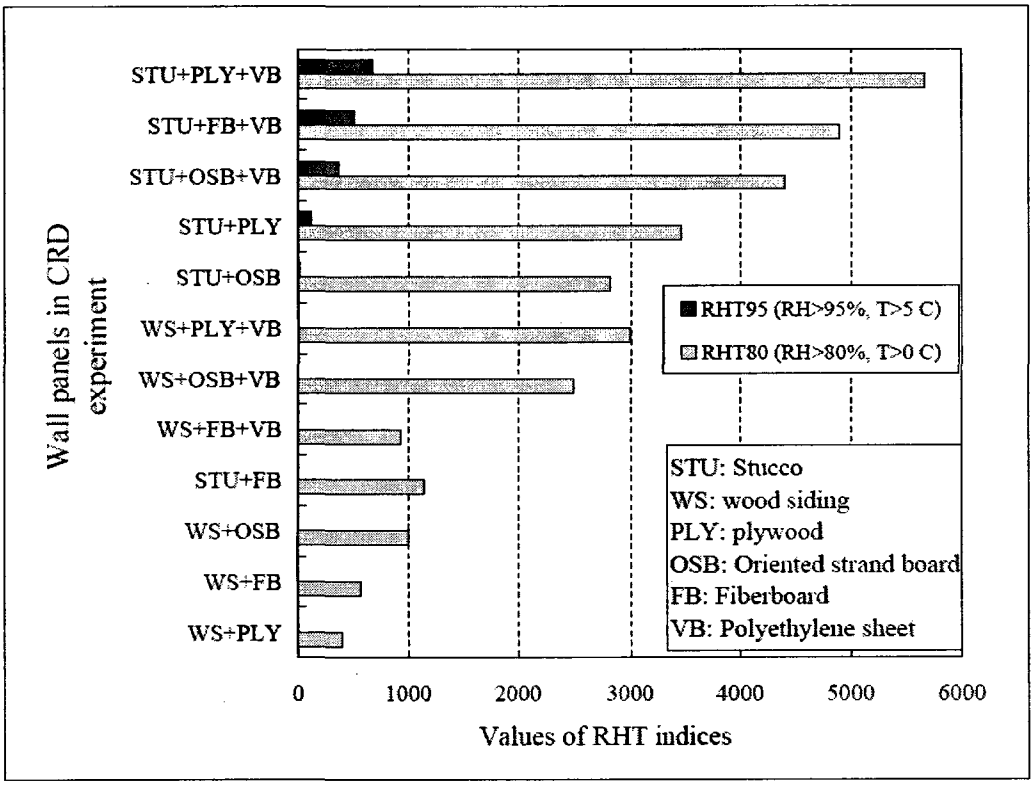

Figure 5.2 RHT indices of CRD wall assemblies

5-1-2 Analysis of wall assemblies' drying performance based on the RHT index

The influence of the parameters investigated (the type of cladding, the existence of vapor barrier, and the type of sheathing boards) is analyzed by using the 2 sets of calculated RHT indices. For the 12 set of design configurations, the wall assemblies with wood siding have significantly lower values of the RHT indices than the walls with stucco cladding. It indicates that the type of cladding has a noticeable influence to the drying process of moisture source inside the wall panels. The study reveals that the installation of polyethylene membrane as vapor barrier does not contribute the drying of moisture

inside the wall panels. The walls with polyethylene vapor barrier present higher RHT indices than the wall panels without the polyethylene vapor barrier. Through comparison of the RHT indices, the walls with fiberboard sheathing have lower values of the RHT indices than the walls with plywood and OSB as sheathing boards.

Type of cladding

The cladding has substantial influence to the walls' drying performance. The stucco cladding (20 mm stucco finish and 2 layers of asphalt impregnated papers) restrains the water evaporation from the stud cavities to the exterior and results in a high moisture accumulation in the sheathing board. In the 6 walls with stucco cladding, 5 walls have non-zero values of the RHT95 index and also highest RHT80 index (Figure 5.2), which indicates the potential for material decay. The wood siding walls have a much better drying performance, and the RHT95 index values of all the wood siding walls are zero, and the values of RHT80 also seat in the lower range (Figure 5.2).

Vapor barrier

Under the experimental conditions of the CRD project, the vapor barrier has negative influence on the drying process of moisture source inside the wall panel. As observed in Table 5.1 and Figure 5.2, the stucco walls with polyethylene vapor barrier have remarkably high values of RHT95, compared to the values of walls of other configurations since the stucco cladding (20 mm stucco and 2 layer of asphalt

impregnated building papers) on the outside and polyethylene membrane on the inside create a "moisture trap" restraining vapor flow to both the outward and inward directions. The high indices indicate that this design is susceptible to moisture-related damage. For wood siding walls, the installation of the vapor barrier also resulted in higher RHT80 values. For either stucco or wood siding as the cladding, the walls without a polyethylene vapor barrier have lower RHT index values than those with vapor barrier.

Type of sheathing boards

In the investigated parameters, the type of sheathing has a relatively smaller influence to the calculated RHT indices. From the moisture profiles and the values of the RHT indices, the walls with fiberboard have lower RHT indices than those with plywood or OSB boards, due to the higher vapor permanence of fiberboard. The plywood or OSB sheathing boards do not present significant difference and larger RHT indices as the result of high moisture accumulation in both types of sheathing boards are observed.

5-2 Investigation of wood-frame walls' drying performance exposed to climatic data of Montreal and Vancouver

In Section 5.1, the HAM-BE is applied to simulate the moisture profiles of the wall panels under the experimental conditions of the CRD project. The measured temperature

and relative humidity in the Environmental Chamber is used as the parameters to define the exterior boundary condition of the numerical modeling. The measured temperature and relative humidity in the test hut are used as the parameters to define the interior boundary conditions of the numerical modeling. The moisture loading is added at the bottom boundary of the stud cavity as a moisture source term set by the measured water evaporation rate during the CRD experiment.

In this section, to extend the data obtained from the CRD project, the HAM-BE tool is applied to examine the drying performance of the studied wall panels of the CRD project under the annual climate data of two targeted regions: Montreal and Vancouver. In the 2D numerical modeling, the bottom part of the sheathing board is set at initially high moisture content to work as the moisture load. The wall panels are exposed to hourly data of exterior/interior temperature and relative humidity of the one-year simulation period. The drying profiles of the wet sheathing parts are tracked to compare the drying performance of the wall panels.

The investigated parameters are the climate condition, claddings, sheathing materials, and the use or absence of polyethylene vapor barrier. In each parametric analysis, the investigated parameter is assigned to different values, and the rest of the modeling setting is unchanged. The drying curves of the sheathing boards are plotted and scientific analysis based on the observation is developed.

The investigation carried out by numerical simulation reinforces the findings of the CRD project. From the parametric analysis, it is demonstrated that the climate condition is the

most significant factor to affect the drying performance of the wall panels, subject to moisture accumulation inside the walls. The drying process occurs mainly in the summer season, when the outdoor temperature is relatively high and the relative humidity is low. In the investigated climates, the Montreal climate has larger value of Drying Index (defined in Equation 5.4) than the Vancouver climate, resulting in faster drying than the identical wall panels exposed to the Vancouver climate. The vapor permeance of the cladding and the sheathing board is the dominant factor for the outward drying process. The selection of both appropriate cladding and sheathing materials with higher vapor permeance contributes to faster drying and less moisture remaining in the wall. The vapor permeance of the inner side of the wall can be essentially changed by the installation of the polyethylene vapor barrier, and the inward drying is restricted. For an indoor space with a normal indoor humidity level, the polyethylene membrane is not beneficial under both the Montreal and Vancouver climate; rather, this application can restrain the drying process incase moisture accumulation in wall components occurs.

5-2-1 Modeling of wall panels' drying performance under hourly weather data

An approach to apply hourly weather data and initial moisture loading in HAM-BE is developed. The description and assumptions of the approach are given herewith. From field investigation, the path of rain penetration is that rainwater passes through the openings on the cladding (perimeters of windows or doors, unsealed joints or holes for mechanical/electrical routes) and the sheathing membrane, runs down along the

sheathing board, partially drains out and partially stays in moisture storage materials (sheathing board, wood frame and insulation). In HAM-BE modeling, the lower part of the sheathing board with the height of 40 cm is set at high moisture content by volume (200 kg/m^3) at the starting of the numerical simulation, to simulate the wetting result of rain penetration. The moisture content of this lower part of the sheathing is monitored to compare the relative drying performance of the wall panels. The wall panels in the simulation are composed of 2X6 studs for the Montreal cases and 2X4 studs for the Vancouver cases, to reflect local construction practices. The wall panels are well sealed and no air leakage cross the wall panel occurs. The configurations of the wall panels in HAM-BE modeling are illustrated in Figure 5.3.

The outdoor boundary conditions of numerical simulation are weather data of two targeted regions: Montreal and Vancouver. The weather data of the targeted regions are those provided by the WUFI-Pro software (IBP, German). The numerical simulation focuses on the influence of the surrounding air's temperature and humid ratio to the drying of the wet component in the wall; the wall is assumed to face north, solar gain is not taken into account, and the cladding materials do not absorb rainwater. Also, no air leakage across the wall panel is considered. Thus, the weather data of the outdoor boundary consist of hourly temperature and relative humidity or partial vapor pressure shown in Figures 5.4-5.7.

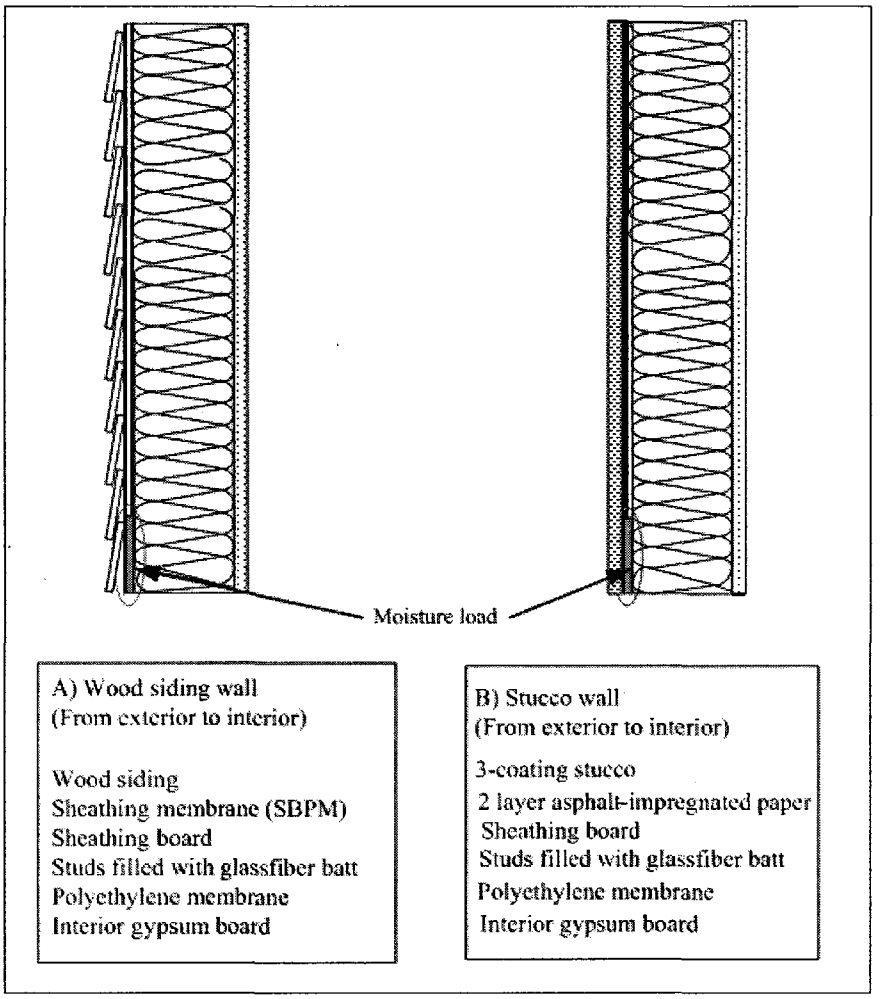

Figure 5.3 Wall assemblies with wet sheathing as moisture load

The indoor boundary conditions of the numerical simulation consist of hourly values of temperature and partial vapor pressure in the form of sinusoidal curves. The mean temperature is 21 °C and amplitude is 1 °C and the mean RH is 45% and amplitude is

10% (Figures 5.4-5.7). The starting point of simulation is November 1st and its duration is one year.

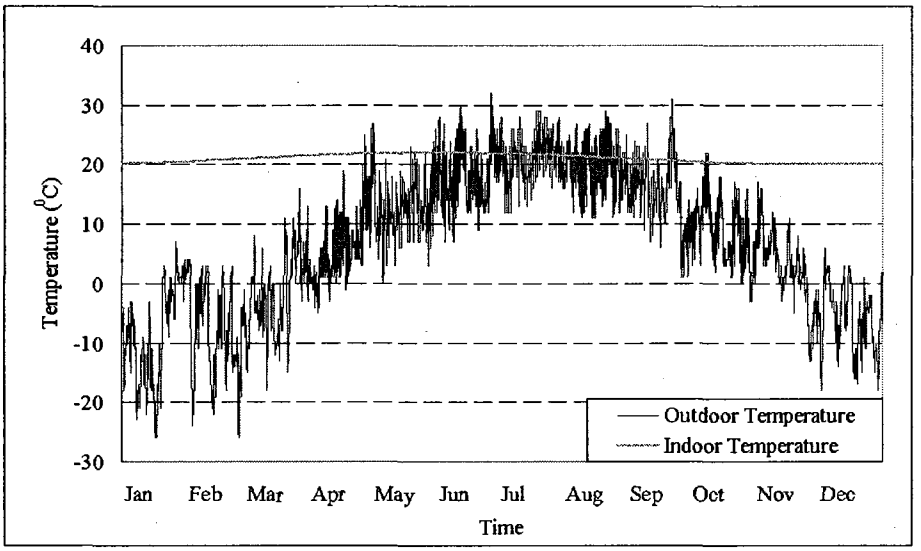

Figure 5.4 Outdoor and indoor temperatures for Montreal (Data from WUFI-Pro)

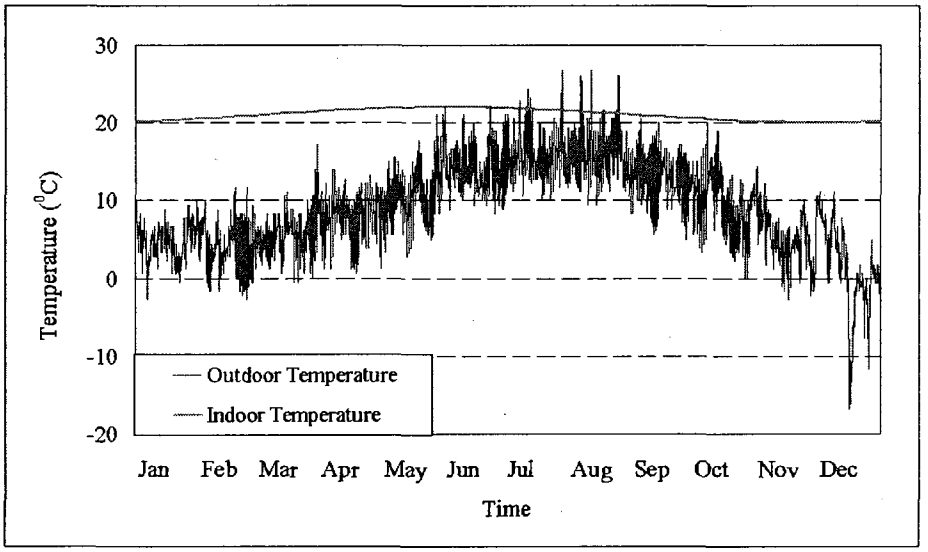

Figure 5.5 Outdoor and indoor temperatures for Vancouver (Data from WUFI-Pro)

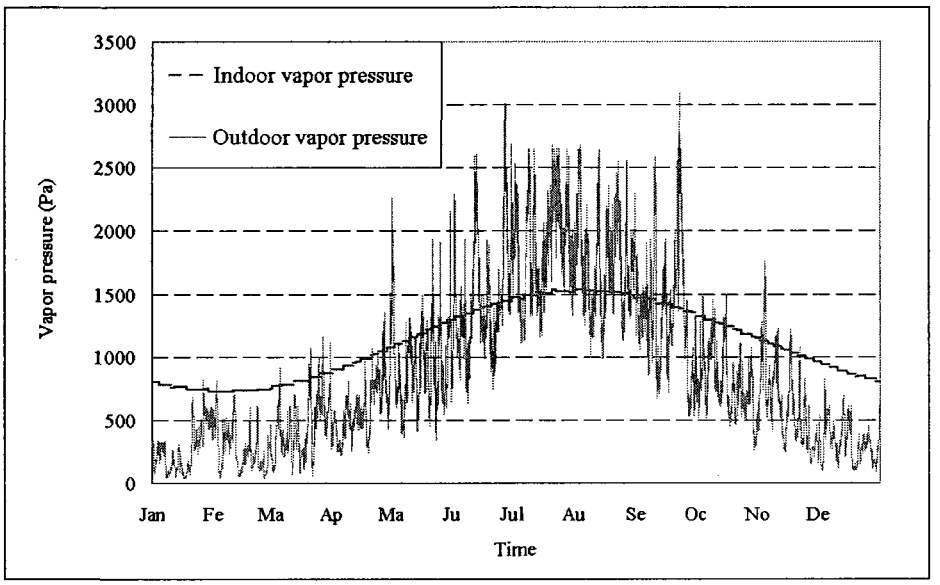

Figure 5.6 Outdoor/indoor vapor pressure for Montreal (Data from WUFI-Pro)

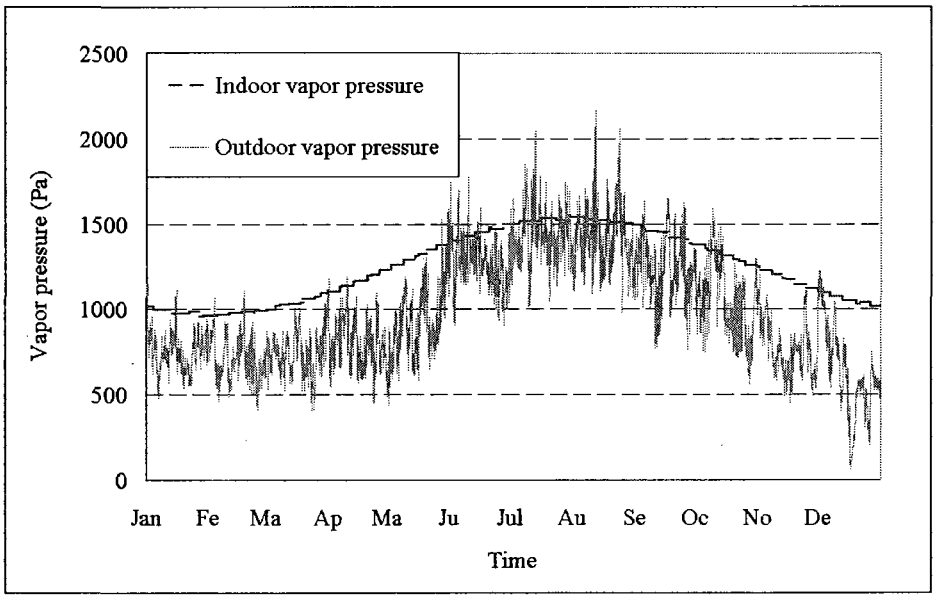

Figure 5.7 Outdoor and indoor vapor pressure for Vancouver (Data from WUFI-Pro)

5-2-2 Analysis based on numerical simulation

The investigated parameters by HAM-BE modeling are the climate data (Montreal and Vancouver), the type of claddings outside the sheathing board, the type of sheathing boards and the installation of polyethylene membrane at the warm side of stud cavity. The drying performance of the wall assemblies are evaluated based on the simulated moisture profiles of the monitored wet parts of the sheathing boards.

Influence of climatic conditions

Four simulation cases are carried out to investigate the influence of weather conditions on the drying of wood siding wall and stucco wall (Table 5.2). Because of the low vapor permeance of the polyethylene membrane (as vapor barrier), the inward drying is eliminated and the major drying direction is outward. The moisture profiles of the monitored wet components are shown in Figures 5.8 & 5.9.

Table 5.2 Simulation cases to investigate the influence of weather condition

Case 1	Panel: Wood siding cladding + OSB sheathing + vapor barrier Moisture loading: initial MC in the lower part of the sheathing (200kg/m^3) Indoor condition: sine-wave (21 ± 1°C, RH 45 ± 10%) Outdoor condition: Hourly weather data for Montreal
Case 2	Panel: Stucco cladding + OSB sheathing + vapor barrier. Moisture loading: initial MC in the lower part of sheathing (200kg/m^3) Indoor condition: sine-wave (21 ± 1°C, RH 45 ± 10%) Outdoor condition: Hourly weather data for Montreal
Case 3	Panel: Wood siding cladding + OSB sheathing + vapor barrier Moisture loading: initial MC in the lower part of the sheathing (200kg/m^3) Indoor condition: sine-wave (21 ± 1°C, RH 45 ± 10%) Outdoor condition: Hourly weather data for Vancouver
Case 4	Panel: Stucco cladding + OSB sheathing + vapor barrier. Moisture loading: initial MC in the lower part of the sheathing (200kg/m^3) Indoor condition: sine-wave (21 ± 1°C, RH 45 ± 10%) Outdoor condition: Hourly weather data for Vancouver

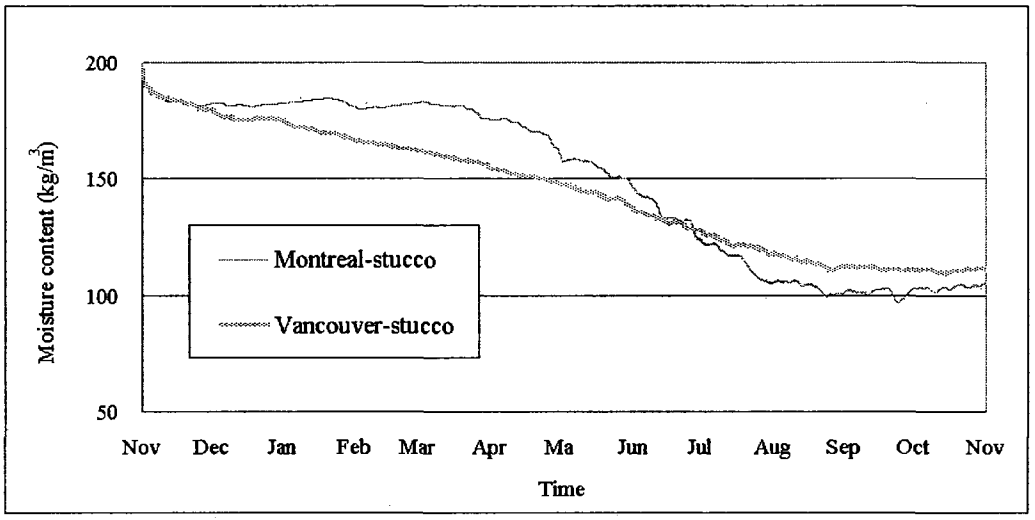

Figure 5.8 Drying of wet sheathing of stucco wall under Montreal and Vancouver climate data, simulated by HAM-BE

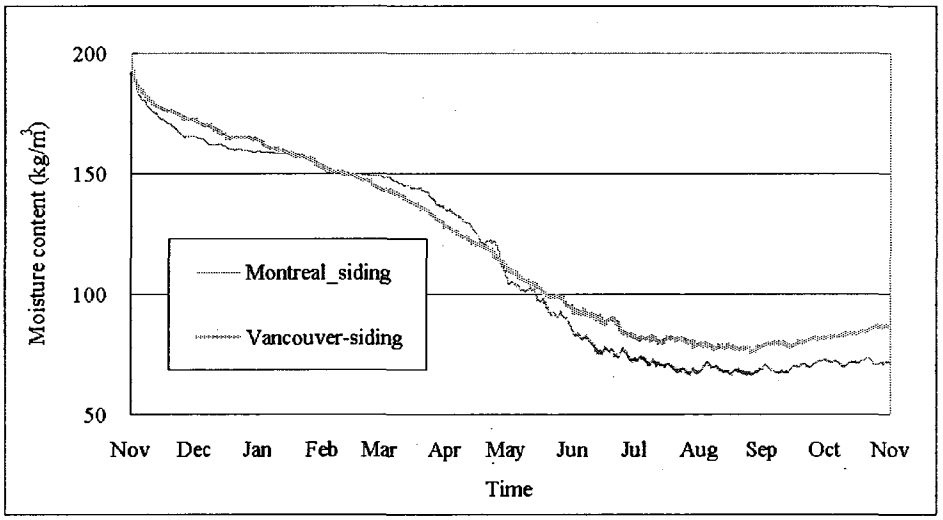

Figure 5.9 Drying of wet sheathing of wood siding walls under Montreal and Vancouver climate data, simulated by HAM-BE

In Figure 5.8, the drying profile of stucco wall under Montreal climate has the following observation. From the starting point of simulation (November 1st) till the end of March,

the wet sheathing board dries slowly and loses little moisture content. From April to September, a fast drying process is observed. From September to the end of simulation (November 1st of the following year), drying almost stops. The drying of stucco wall under the Vancouver climate presents rather a continuously constant drying process from the starting point (1st of November) to the September of the next year, then drying stops during from September to the end of the simulation (November 1st of the next year).

The drying profiles of the wood siding walls present similar tendencies: under the Montreal climate, the wall dries slowly in the period of November to April; the major drying process occurs in the period of May to August; and thorough September to the November, drying stops or there is even a slight increase in the sheathing's moisture content. Under the Vancouver climate, the drying process is continuous, without obvious fast and slow stages from November to September; the sheathing's moisture content increased slightly in the period of September to the end of simulation.

Other noticeable observations are that at the end of the simulation, the Montreal cases have lower moisture content than the Vancouver cases, for both stucco and wood siding walls; and the wood siding wall has less moisture accumulation under both Montreal and Vancouver climates.

To clarify the above observations, the climatic data of the two regions are analyzed. As shown in the climatic map (Figure 5.10), Montreal's climate is classified as humid continental with abundant precipitation. The winter is severely cold with average snowfall of 2.25 meters. The summer is the wettest season in the year statistically, but

also with plenty of sunshine. The average rainfall throughout the year is about 900 mm. Vancouver has a marine climate with lots of precipitation (average of 1,200 mm annually). Summer months are sunny with moderate temperatures. The winter is wet with precipitation in more than half of all days (data from Environment Canada).

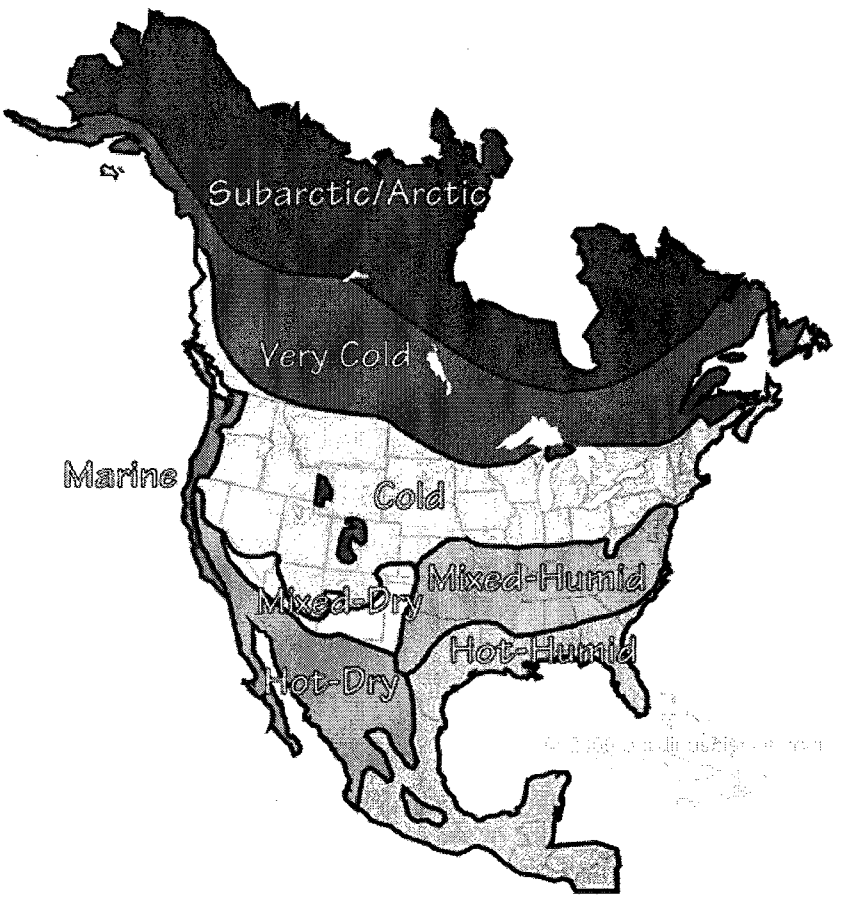

Figure 5.10 Climatic map of North America (BSC 2007)

Then, the concept of the Drying Index is used to calculate the maximum possible water

evaporation rate in the air of the climate region. Water evaporation can be affected by the air temperature, air movement, humid ratio and atmosphere pressure of the surroundings. One practical assumption is that water evaporation is proportional to the difference between saturation vapor pressure and the vapor pressure of ambient air (Dalton 1802), or the difference between saturated humid ratio and the actual humid ratio of the ambient air. The humid ratio of air is calculated by:

$$w_{air} = 0.622 * (P_v/(p - P_v)) \quad (5.2)$$

where

w_{air} (kg water/kg air) humidity ratio of air

P_v (kPa) partial vapor pressure

p (kPa) total pressure of air

Then, the difference of the humid ratio of the air and the saturated humid ratio of the air at time t is calculated by:

$$\Delta w_{air}(t) = w_{air,sat}(t) - w_{air}(t) \quad (5.3)$$

The summation of the (hourly) humid ratio differences to saturation for a period of time is defined as the drying index (Cornick et al. 2002) to represent the drying capacity provided by the climate condition and is denoted as DI. DI does not consider the building's characteristics. Its value for a specific climate can be calculated as:

$$DI = \sum_{i=1}^{k} \Delta w_{air,i}(t) \qquad (5.4)$$

where

DI (kg water/kg air of time period) drying index

k the number of hours in a particular period, eg. a month or a year

Based on the above equations, the monthly drying indices of Montreal and Vancouver are illustrated in Figure 5.11.

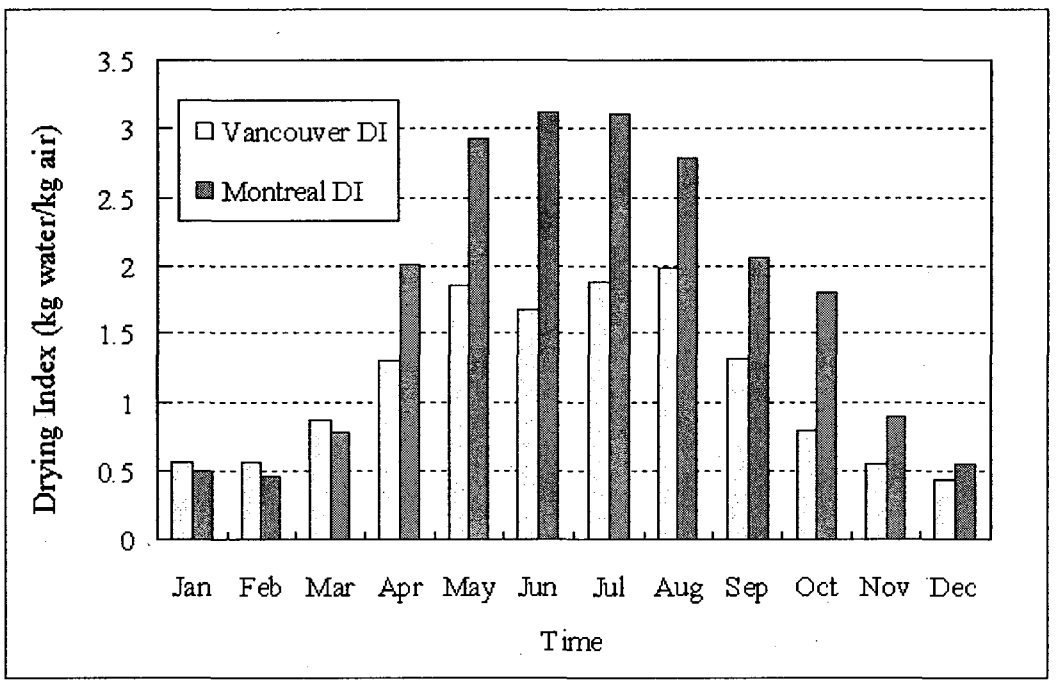

Figure 5.11 Monthly Drying Indices of Montreal and Vancouver

Since the polyethylene vapor barrier eliminates the inward drying, the dominant drying direction in the above simulation is outward and the drying rate relies on the saturation ratio of the outdoor air. The DI of Montreal has relatively higher values in the period of April to October; compared to the smaller values in the cold seasons (November to March). Therefore, the main drying process under the Montreal climate occurs in the period from April to October; in the rest of the months, the low drying index due to high humidity ratio in the air does not provide strong capacity for drying.

The Vancouver region features a moderate climate. The period with higher DI is from April to August, which is the major drying period. From September to March, the value of DI is relatively smaller and the drying process is restrained. The annual total of Montreal's DI is 25.33 kg water /kg air-year; Vancouver's annual DI is 16.59 kg water /kg air-year. The annually lumped DI of Montreal climate is much larger than that of Vancouver climate. Thus, wall systems with the same amount of moisture accumulation would dry faster under the Montreal climate than the Vancouver climate.

Cladding

The simulation cases in Table 5.2 are used to evaluate the drying performance of two types of cladding systems under the climate conditions of both Montreal and Vancouver: wood siding on furring with spun bonded polyolefin membrane with crinkled surface and 3 coating stucco over 2 layer asphalt impregnated papers. The configurations of the walls are: wood siding with OSB sheathing and vapor barrier; stucco with OSB sheathing and

vapor barrier. It is observed that wood siding has better drying performance than stucco walls, both in Montreal and in Vancouver climates (Figures 5.12 & 5.13).

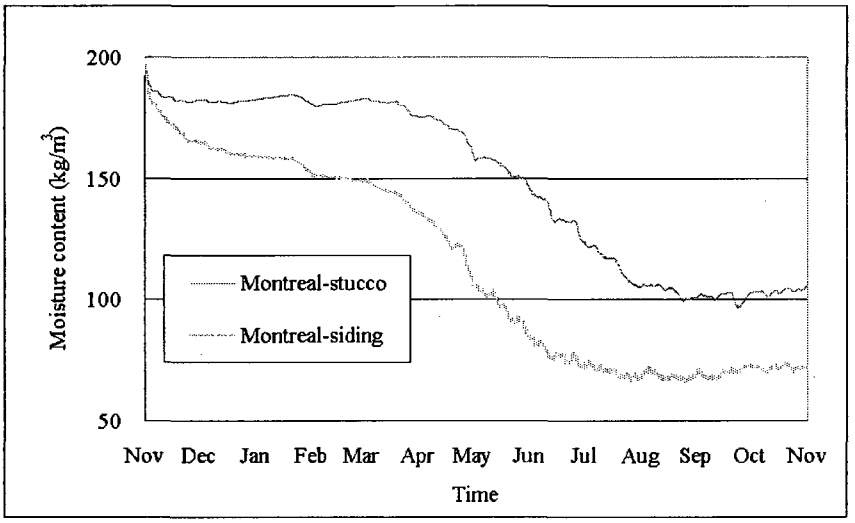

Figure 5.12 Drying of wet sheathing under Montreal climate, simulated by HAM-BE

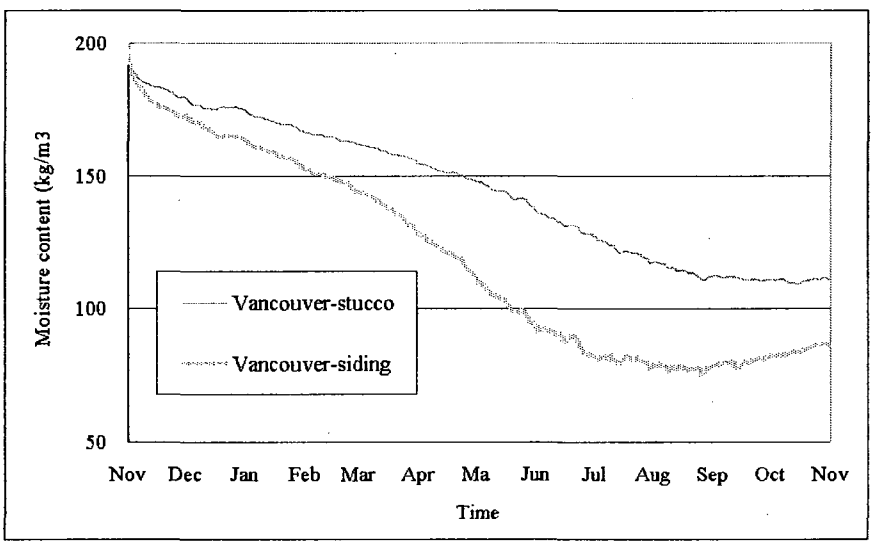

Figure 5.13 Drying of wet sheathing under Vancouver climate, simulated by HAM-BE

The vapor permeance of the cladding materials is a critical factor to affect the outward drying. According to the vapor permeance, building materials can be classified into four categories: vapor impermeable, vapor semi-impermeable, vapor semi-permeable and vapor permeable (BSC 2007). The categories and examples of the category are listed in Table 5.3. The units of the vapor permeance is ng/sm^2Pa and also perm (1 perm = 57.45 ng/sm^2Pa = 57.45E-12 kg/sm^2Pa). To interpret the drying performance of the investigated cladding systems, the vapor permeance of the wall systems' components are analyzed and presented in Table 5.4. Since the vapor permeance of most building materials is strongly moisture-dependent, two values (dry condition of 20% RH and wet condition of 90% RH) are presented. The vapor permeance of wood siding is based on empirical relations from tests (laboratory and test hut conditions) (BSC 2006). The value is independent of finishes or coatings on the wood, unless the treatment closes the width or reduces the length of the space between courses.

Table 5.3 Categories of building materials' vapor permeance

Category	Example
Vapor impermeable: 0.1 perm or less	Examples: Rubber membranes Polyethylene film Glass Aluminum foil Sheet metal Foil-faced insulating sheathing Foil-faced non-insulating sheathing
Vapor Semi-Impermeable: 1.0 perms or less and greater than 0.1 perm	Examples: Oil-based paints Most vinyl wall coverings Unfaced extruded polystyrene greater than 1-inch thick Traditional hard-coat stucco applied over building paper and OSB sheathing.
Vapor Semi-permeable: 10 perms or less and greater than 1.0 perms	Plywood Bitumen impregnated Kraft paper OSB Unfaced expanded polystyrene (EPS) Unfaced extruded polystyrene (XPS) 1-inch thick or less Fiber-faced isocyanurate Heavy asphalt impregnated building papers #30 pound Most latex based paints
Vapor Permeable: Greater than 10 perms	Unpainted gypsum board and plaster Unfaced fiberglass insulation Cellulose insulation Synthetic stucco Some latex-based paints Lightweight asphalt impregnated building papers (#15 building paper) Asphalt impregnated fiberboard sheathing Housewraps

Table 5.4 Vapor permeance of building materials in wood-frame walls

Cladding	3-coating stucco, 20mm 7.00E-10 kg/m^{2}sPa =12.18 perm (Dry) 1.26E-09 kg/m^{2}sPa = 21.93 perm (Wet) wood siding on furring 2.0108E-9 kg/m^{2}sPa = 35 perm
Sheathing membrane	two layers of asphalt impregnated papers 2.69E-12 kg/m^{2}sPa = 0.05 perm (Dry) 7.80E-10 kg/m^{2}sPa = 13.58 perm (Wet) spun bonded polyolefin membrane with crinkled surface 3.17E-9 kg/m^{2}sPa = 55.18 perm
Sheathing board	OSB 11.5mm: 3.52E-11 kg/m^{2}sPa = 0.61 perm (Dry) 4.65E-10 kg/m^{2}sPa = 8.09 perm (Wet) plywood 12.5mm: 1.43E-11 kg/m^{2}sPa = 0.25 perm (Dry) 1.80E-09 kg/m^{2}sPa = 31.33 perm (Wet) fiberboard 10.5mm: 1.71E-09 kg/m^{2}sPa = 29.77 perm (Dry) 1.74E-09 kg/m^{2}sPa = 30.29 perm (Wet)
Insulation	Glass fiber 140mm: 1.22857E-09 kg/m^{2}sPa = 21.39 perm
Vapor Barrier	Polyethylene membrane: 3e-12 kg/m^{2}sPa = 0.05 perm
Interior finish	Gypsum 12.5mm: 2.52E-09 kg/m^{2}sPa = 43.86 perm (Dry) 3.94E-09 kg/m^{2}sPa = 68.58 perm (Wet)

The vapor permeance of the wall components, expressed in the unit of perm, is illustrated in Figures 5.14 & 5.15. In all the components, the polyethylene vapor barrier is impermeable and has incomparable high vapor resistance. In case a polyethylene membrane is installed, the inward drying is almost eliminated and the drying direction can only be outward to outdoors. The drying of moisture in sheathing and wood-frame will rely mainly on the vapor resistance of the materials at the exterior side of the studs. The vapor permeance of the two claddings (materials from sheathing to outdoor space) is shown in Figure 5.16. The stucco cladding (20mm stucco finish and 2 layers of asphalt impregnated papers) has much larger vapor resistance than the wood siding wall (wood siding and SPBM). It is worth noting that the permeance of building materials in Figure 5.16 is equivalent to 90% RH; but the asphalt impregnated building papers can be impermeable to vapor diffusion when it is dry. As a result, the stucco cladding can be very vapor-resistant. It helps to explain the observed slower drying of wet materials behind the stucco cladding in Figures 5.12 & 5.13. Also, it indicates that in case moisture accumulates into the materials behind the stucco cladding, it will take relatively longer time to dry out and has higher risk to induce mold growth and other moisture-relative damage, comparing to wood siding wall.

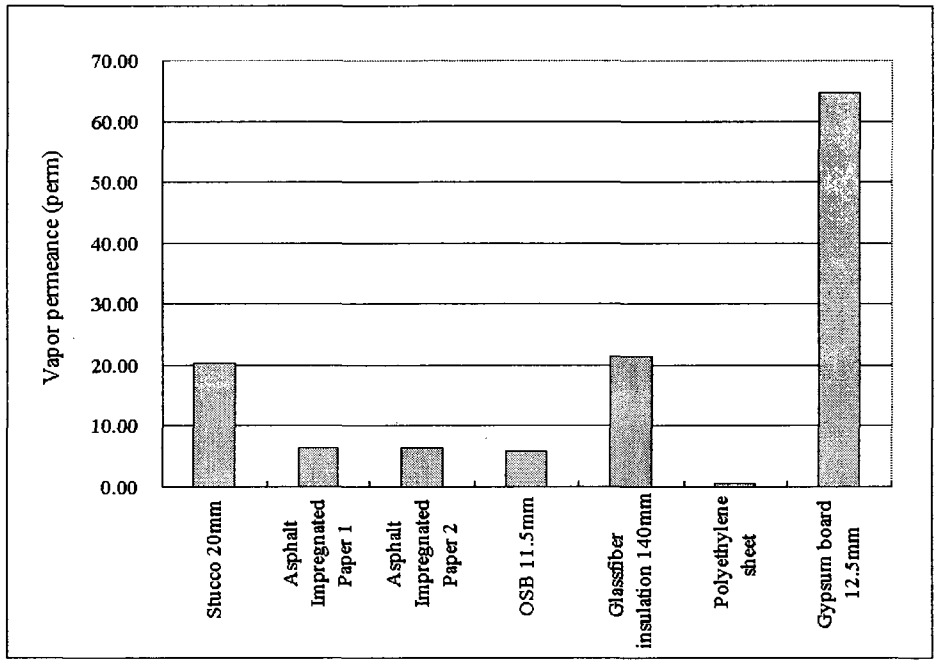

Figure 5.14 Vapor permeance of stucco wall's components

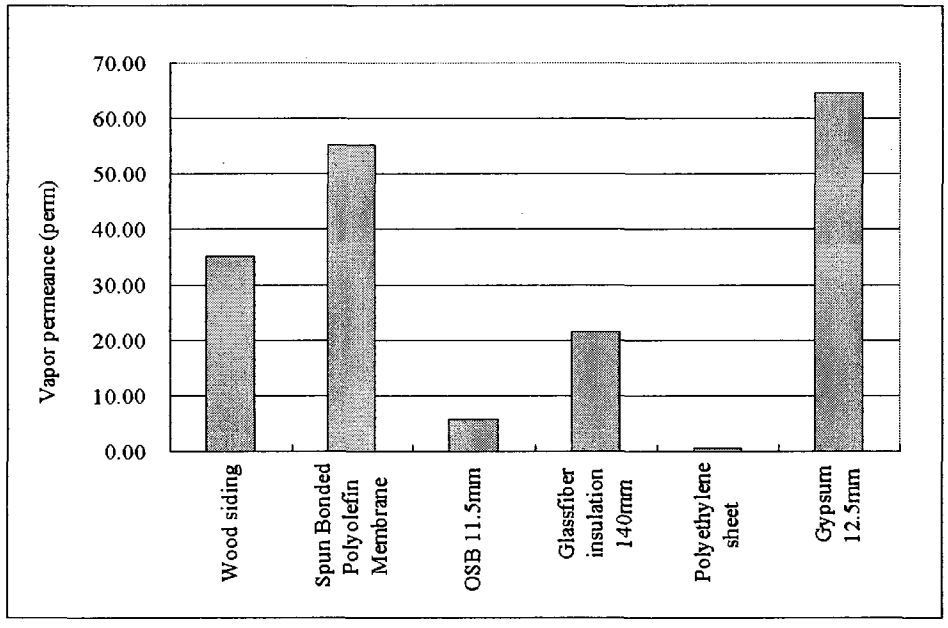

Figure 5.15 Vapor permeance of wood siding wall's components

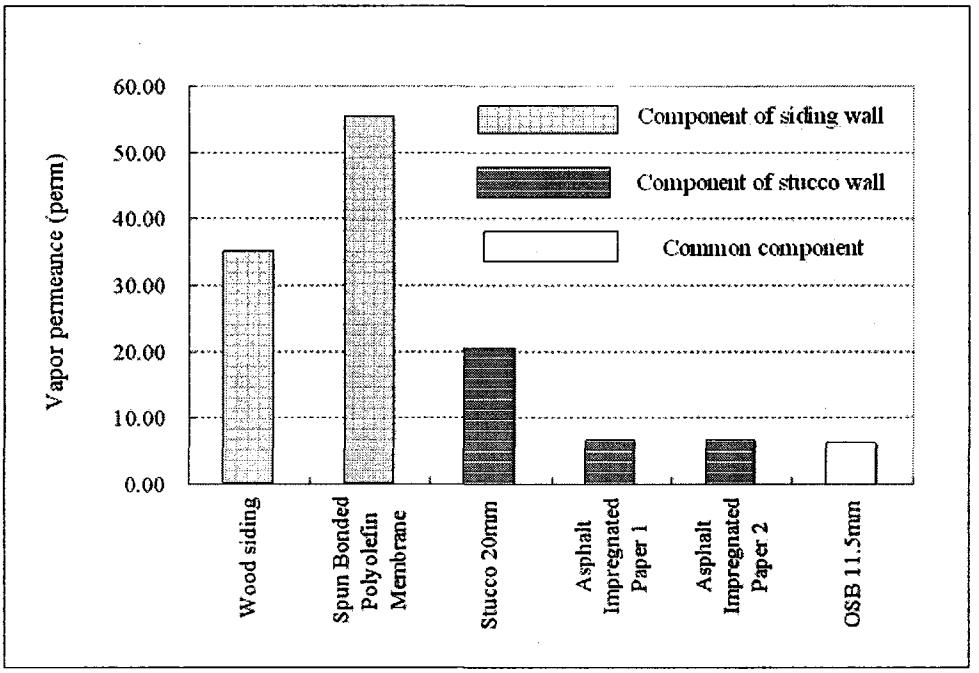

Figure 5.16 Comparison of building components' vapor permeance of two cladding types

To provide improved thermal comfort and structure protection, exterior insulation boards at the exterior side of the sheathing board, e.g. expanded polystyrene sheathing (EPS), are widely used in various wall systems, such as the exterior insulation finish system (EIFS). It is noticeable that due to the low vapor permeance of the exterior insulation sheathing (rated between semi-impermeable and semi-permeable), the outward drying will be significantly reduced. Simulation cases are carried out to investigate the drying performance of an exterior insulated wall. The description of the simulation cases is given in Table 5.5 and In Figure 5.17. After a 26 mm semi-right expanded polystyrene

foam sheathing is added above the OSB sheathing of a wood siding wall, the vapor resistance of the wall's components is illustrated. In Figure 5.18, the simulated drying profiles of the wet sheathing in the wall with and without the EPS are compared.

Table 5.5 Simulation settings to investigate the influence of exterior insulation board

Case 1	Panel: Wood siding cladding + OSB sheathing + vapor barrier Moisture loading: initial MC in the lower part of sheathing (200kg/m^3) Indoor condition: sine-wave (21 ± 1°C, RH 45 ± 10%) Outdoor condition: Hourly weather data of Montreal
Case 2	Panel: Wood siding cladding + EPS + OSB sheathing + vapor barrier Moisture loading: initial MC in lower part of sheathing (200kg/m^3) Indoor condition: sine-wave (21 ± 1°C, RH 45 ± 10%) Outdoor condition: Hourly weather data of Montreal

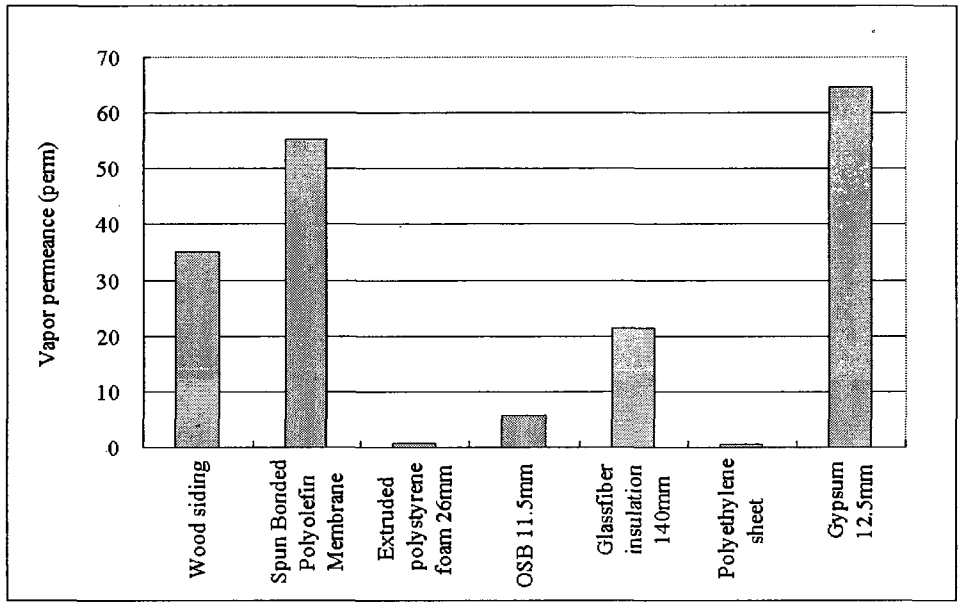

Figure 5.17 Vapor permeance of wood siding wall with exterior insulation sheathing

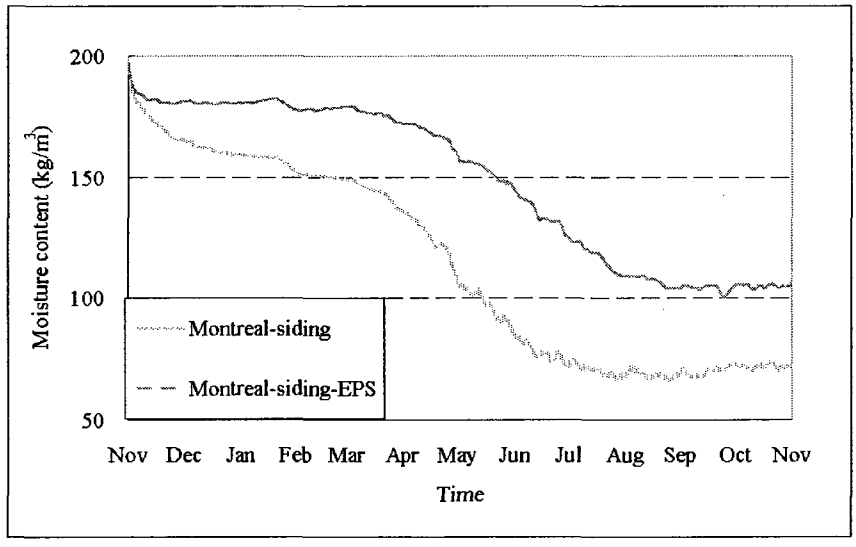

Figure 5.18 Drying of wet sheathing under Montreal climate, with or without EPS, simulated by HAM-BE

Polyethylene vapor barrier

The purpose of using polyethylene membrane (permeance less than 0.1 perm) as vapor barrier is to prevent condensation due to vapor diffusion from indoor space to the stud cavity. The assumption of this application is that vapor flow direction is from indoor space to outdoors. Unfortunately, this is only true for cold season with indoor heating; but not applicable in warm/hot season when the vapor flow direction can be from outdoor space to indoor space. In most areas of Canada, the climate includes both heating season and hot/warm season; and there is no single right position to install the polyethylene sheet. Various researches have revealed that the polyethylene sheet as vapor barrier is not necessary, even harmful to performance of the building envelope in mixed climates. It was stated by John Straube as "In many practical situations, a low permeance vapor barrier will not improve hygrothermal performance, and may in fact increase the likelihood of damaging condensation or trap moisture in the system. In some cases, a low-permeance vapor barrier may be called for, but in many practical high performance enclosures, none is needed, and eliminating them will actually improve performance by encouraging drying and avoiding solar-driven diffusion wetting. The preconceptions of many building codes, standards, and designers need to be modified to acknowledge the facts of low permeance vapor barriers" (Straube 2001). Also, the EEBA (Energy & Environmental Building Association) Builder's Guide for Cold Climates (Lstiburek 2006) stated: "Polyethylene on the inside of building assemblies in cold, mixed-humid, mixed-dry, hot-humid, and hot-dry climates is not generally a good idea." Instead, the

products with various vapor permeance, such as the Smart Vapor Barrier, is reported to have better moisture control of the condensation problem for mixed climate (Kunzel 1999).

The outdoor and indoor vapor pressure of Montreal and Vancouver climates has been shown in Figures 5.4 - 5.7. For both regions, outdoor vapor pressure can be higher than indoor vapor pressure in some period of the year. The vapor flow direction driven by vapor pressure gradient can be inward during the summer time and the inward drying should be considered to release the moisture accumulation in the wall assemblies. Eight simulation cases are carried out to investigate drying performance of the wall systems with or without the polyethylene sheet as vapor barrier. The description of the simulation cases are given in Table 5.6 and the simulation results are presented in Figures 5.19-5.22.

Table 5.6 Simulation settings to investigate the performance of vapor barrier under Montréal and Vancouver climates

Case 1	Panel: Stucco cladding + OSB sheathing + vapor barrier Moisture loading: initial MC in lower part of sheathing (200kg/m^3) Indoor condition: sine-wave (21 ± 1°C, RH 45 ± 10%) Outdoor condition: Hourly weather data of Montreal
Case 2	Panel: Stucco cladding + OSB sheathing Moisture loading: initial MC in lower part of sheathing (200kg/m^3) Indoor condition: sine-wave (21 ± 1°C, RH 45 ± 10%) Outdoor condition: Hourly weather data of Montreal
	Panel: Wood siding cladding + OSB sheathing + vapor barrier

Case 3	Moisture loading: initial MC in the lower part of sheathing (200kg/m^3) Indoor condition: sine-wave (21 ± 1°C, RH 45 ± 10%) Outdoor condition: Hourly weather data of Montreal
Case 4	Panel: Wood siding cladding + OSB sheathing Moisture loading: initial MC in the lower part of sheathing (200kg/m^3) Indoor condition: sine-wave (21 ± 1°C, RH 45 ± 10%) Outdoor condition: Hourly weather data of Montreal
Case 5	Panel: Stucco cladding + OSB sheathing + vapor barrier Moisture loading: initial MC in lower part of sheathing (200kg/m^3) Indoor condition: sine-wave (21 ± 1°C, RH 45 ± 10%) Outdoor condition: Hourly weather data of Vancouver
Case 6	Panel: Stucco cladding + OSB sheathing Moisture loading: initial MC in lower part of sheathing (200kg/m^3) Indoor condition: sine-wave (21 ± 1°C, RH 45 ± 10%) Outdoor condition: Hourly weather data of Vancouver
Case 7	Panel: Wood siding cladding + OSB sheathing + vapor barrier Moisture loading: initial MC in the lower part of sheathing (200kg/m^3) Indoor condition: sine-wave (21 ± 1°C, RH 45 ± 10%) Outdoor condition: Hourly weather data of Vancouver
Case 8	Panel: Wood siding cladding + OSB sheathing Moisture loading: initial MC in the lower part of sheathing (200kg/m^3) Indoor condition: sine-wave (21 ± 1°C, RH 45 ± 10%) Outdoor condition: Hourly weather data of Vancouver

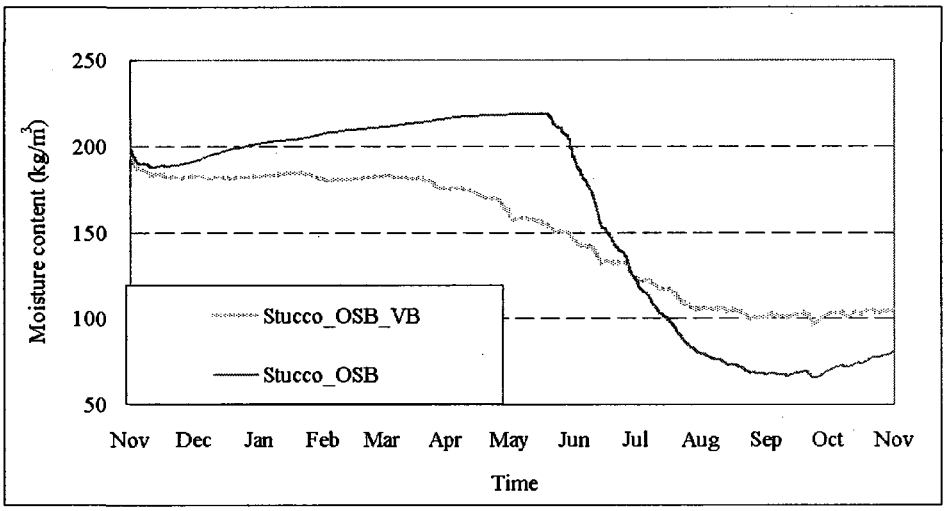

Figure 5.19 Drying of wet sheathing of stucco wall with and without polyethylene VB under Montreal climate, simulated by HAM-BE

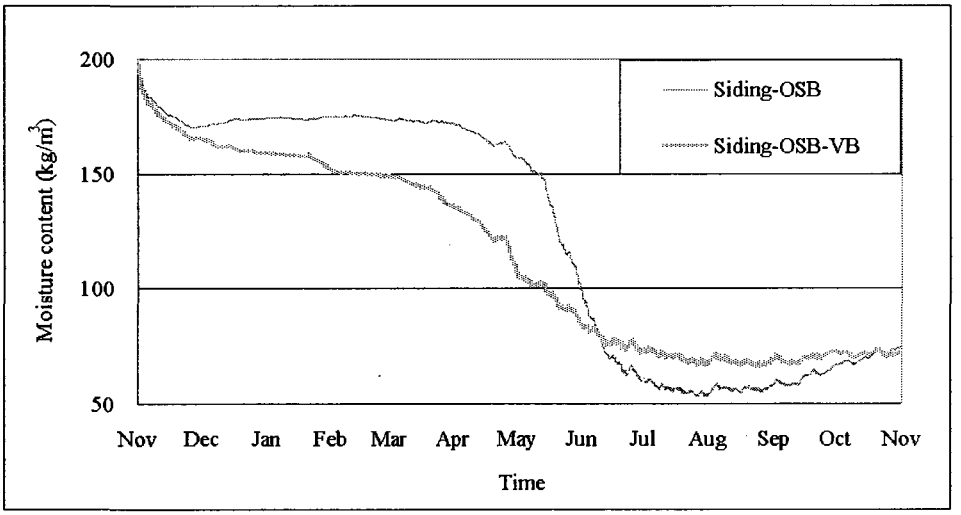

Figure 5.20 Drying of wet sheathing of wood siding wall with and without polyethylene VB under Montreal climate, simulated by HAM-BE

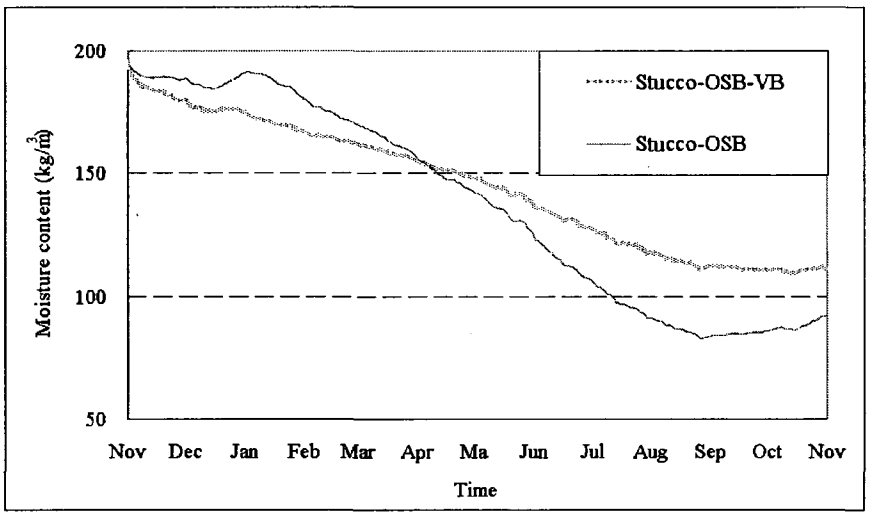

Figure 5.21 Drying of wet sheathing of stucco walls with and without polyethylene VB under Vancouver climate, simulated by HAM-BE

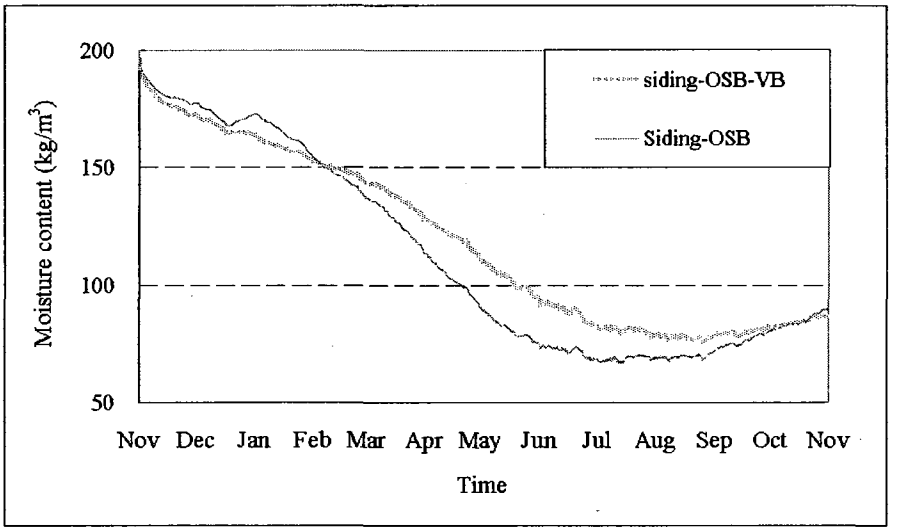

Figure 5.22 Drying of wood siding walls with and without polyethylene VB under Vancouver climate, simulated by HAM-BE

It is observed that the wall assemblies without polyethylene vapor barrier have higher moisture accumulation in the heating season (November to March), but dry faster in the

rest of the year (April to October). Stucco walls with the vapor barrier have more moisture accumulation than walls without polyethylene vapor barrier at the end of the simulation period, under both Montreal and Vancouver climates. Similarly, in walls with wood siding, the polyethylene vapor barrier does not foster the drying performance: the walls with and without polyethylene vapor barrier have the same close moisture contents at the end of simulation.

Basically, the critical factor to judge whether a polyethylene vapor barrier should be used is the outdoor and indoor humidity levels. A further simulation case is carried out to compare the drying performance of a wall panel (wood siding, OSB sheathing and no polyethylene vapor barrier), exposed to medium and high indoor humidity levels (Figure 5.23). The simulated drying profiles are presented in Figure 5.24. It is demonstrated that in the case where the indoor humidity level is kept at a high level, the polyethylene vapor barrier can protect the wall from significant moisture accumulation due to vapor diffusion.

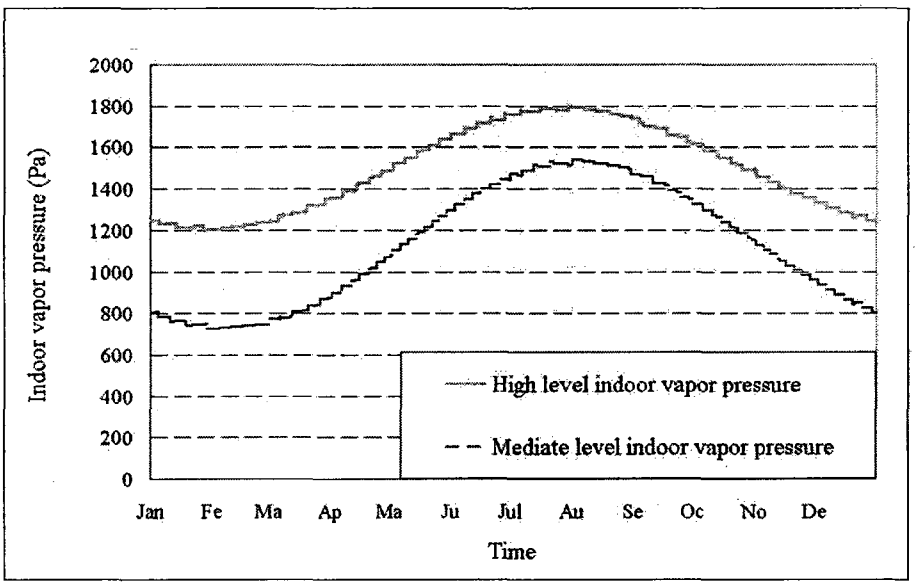

Figure 5.23 High and medium levels of indoor vapor pressure used in HAM-BE modeling

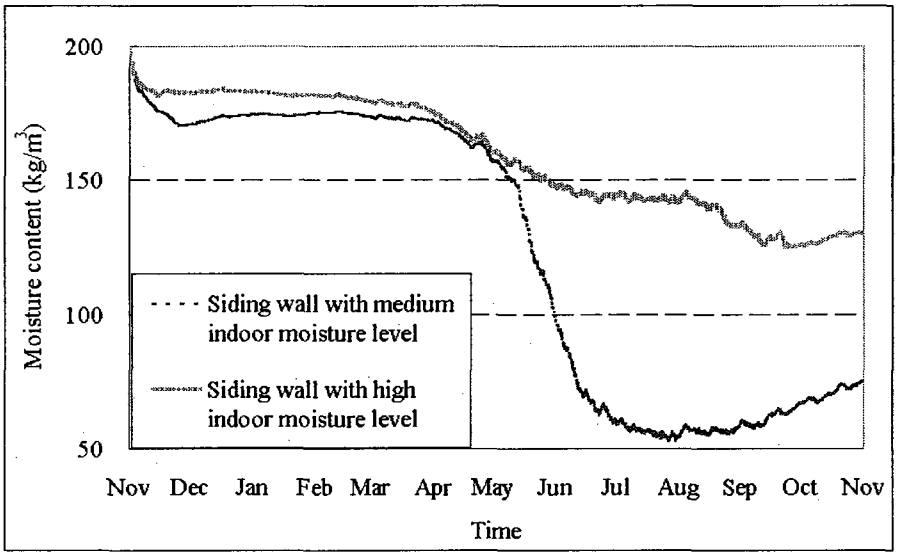

Figure 5.24 Drying of wet sheathing of wood siding wall affected by indoor humidity level, simulated by HAM-BE

Both Montreal and Vancouver climates have summer season and winter season, and the vapor diffusion could be inward or outward, depending on the vapor pressure gradient across the wall. Based on numerical simulation with described settings, the function of the polyethylene vapor barrier in the investigated wood-frame walls is summarized. The stucco cladding has relatively lower vapor permeance. The installation of polyethylene vapor barrier in a stucco wall prevents the vapor diffusion from indoor source in heating season and results in less moisture accumulation. Since the wall has low vapor permeance at both sides of the stud cavity, moisture intrusion from exterior and interior should be strictly avoided. Wood siding walls represent cladding systems of high outward vapor permeance. The installation of polyethylene vapor barrier is not beneficial to reduce moisture accumulation in the wall system, if indoor humidity level is low or moderate. For indoor space with high moisture generation, e.g. kitchen, bathroom and swimming pool, the polyethylene vapor barrier should be installed in any wall system composed of moisture sensitive materials.

Type of sheathing

The investigated sheathing materials were OSB, plywood, and fiberboard. The vapor permeance of the sheathing boards have been listed in Table 5.4. With the described boundary settings (Figures 5.2-5.5), the drying of the wet component with a high initial moisture content (200 kg/m^3) in the subject walls were simulated and the moisture

content profiles over time of the wet components were compared (Figures 5.25-5.28). For either Montreal or Vancouver climate, the wall with fiberboard presented fastest drying rate and lowest moisture accumulation by the end of the simulation period. The wall with plywood had slightly faster drying rate than that with OSB.

Through analysis of the hygroscopic properties of the three materials, all the three materials are hygroscopic and capillary-active. But the fiberboard has much larger vapor permeance than plywood and OSB. It should be mentioned that the presented simulation is solely based on the measured material properties in the CRD experiment, and does not cover the various engineering wood boards in the market. Still, it confirms that the choosing of sheathing material with higher vapor permeance can be beneficial for the wall's drying performance.

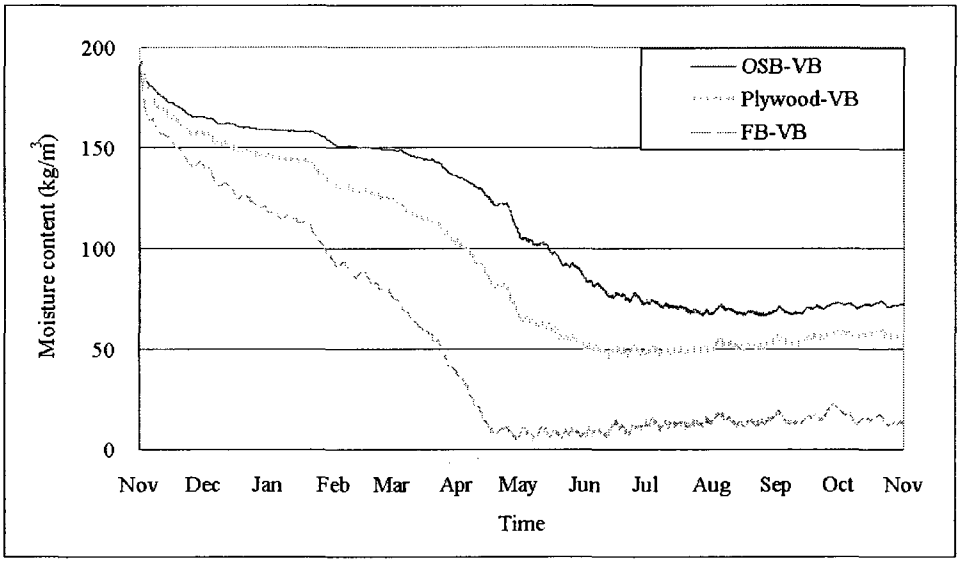

Figure 5.25 Drying of wet sheathing in wood siding walls under Montreal climate, comparison between OSB, plywood and FB, simulated by HAM-BE

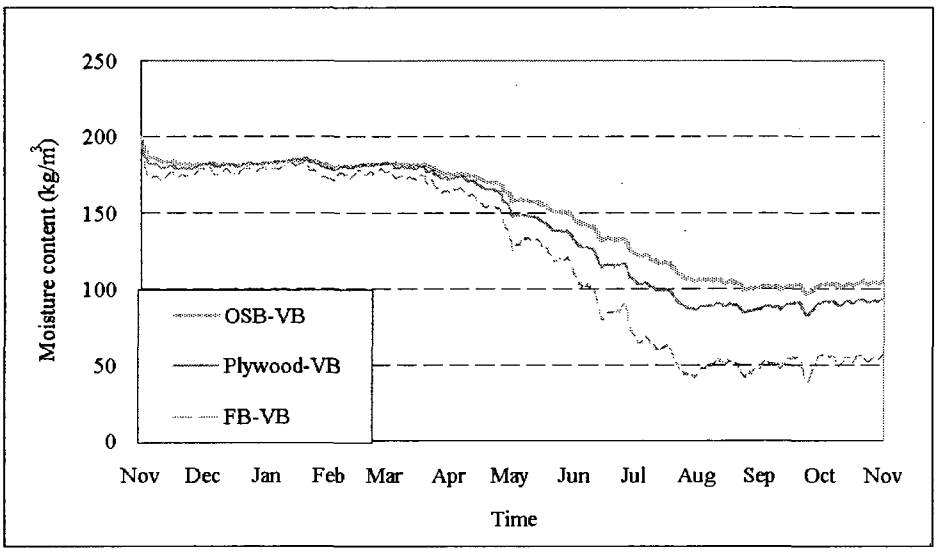

Figure 5.26 Drying of sheathing in stucco walls under Montreal climate, comparison between OSB, Plywood and FB, simulated by HAM-BE

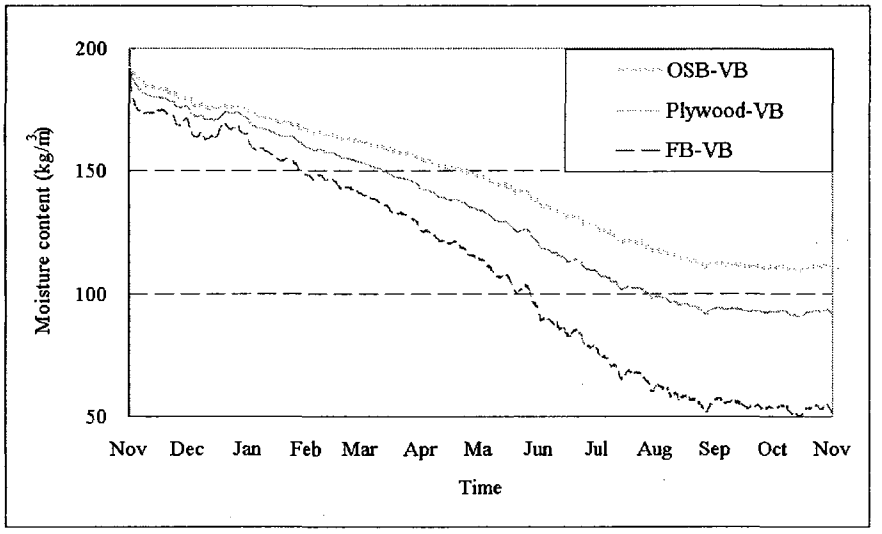

Figure 5.27 Drying of wet sheathing in stucco wall under Vancouver climate, comparison between OSB, Plywood and FB, simulated by HAM-BE

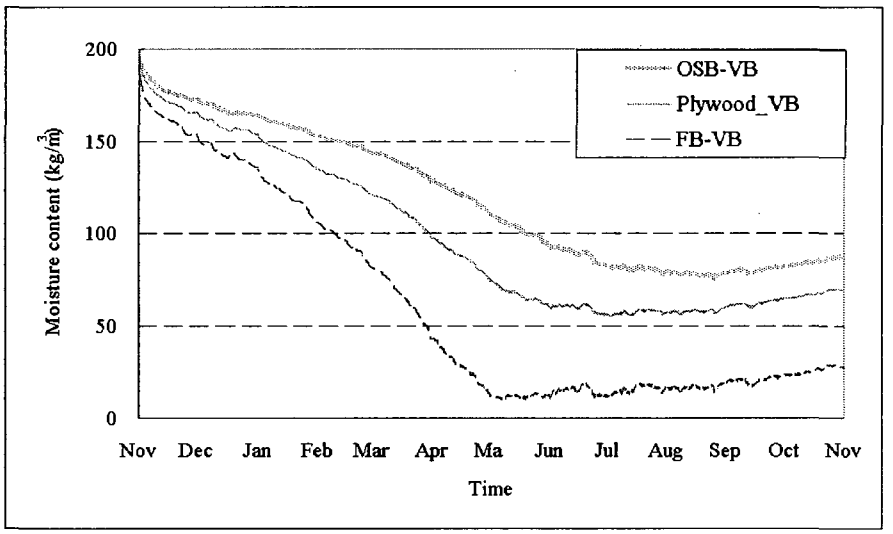

Figure 5.28 Drying of wet sheathing in wood siding wall under Vancouver climate, comparison between OSB, Plywood and FB, simulated by HAM-BE

5-3 Guidelines for moisture control in wood-frame wall

Wood-frame buildings dominate residential and low-rise commercial buildings in Canada and has proven long service lives. However, the organic materials in the wall systems, such as wood frame (studs, bottom and top plates), sheathing board, gypsum board and building papers, are sensitive to moisture intrusion. In various areas of North America, moisture-related failures of wood-frame buildings have been reported. The major deterioration mechanism is fungi growth and decay of building materials, other damage includes corrosion of metal fasters, stain of indoor finish, heat loss from thermal bridge, VOC issue and irritable reflection of occupants.

Rain leakage was firmly identified as the primary moisture source to induce

moisture-related damage. Other sources can be ground water, condensation of vapor diffusion and air leakage, wetting during construction and so on. The essential principle to prevent wood-frame walls from moisture-related failure is to prevent moisture intrusion of liquid phase (rain leakage) and vapor phase (air leakage and vapor diffusion) and allowing drying to either outdoor or indoor directions in case wetting occurs. Thus, as the essential and also last defending strategy to prevent moisture-related building failure, any wall systems composed of moisture-sensitive materials, should have certain drying capacity provided by appropriate design.

However, today's wood-frame wall systems generally do not have sufficient drying capacity, arising largely from the changed design criteria after the 1970's "Energy Crisis". To reduce energy consumption, today's building envelopes are designed with thick insulation and air/vapor-tight approach. With this approach, the drying capacity of the envelope can be largely restrained, since the materials at the outer/inner sides of the wood-frame usually have poor vapor permeance. As the result, drying of moisture absorbed in the wood-frame and surrounding materials is a slow process for several months or years and moisture-related damage can occur before the moisture dries out.

To improve the drying performance, in most cases the wood-frame wall systems could be designed in the "vapor-flow-through" pattern to facilitate drying and avoid high vapor resistance materials at either side of the wall. This concept was stated by Lstiburek (2006) as: "a classic flow-through wall assembly should have a permeable interior surface and finish and permeable exterior sheathing and permeable building paper drainage plane".

This permits drying to both the interior and exterior.

Unfortunately, to apply the "vapor-flow-thorough" approach requires case-by-case analysis and there is no definitive solution applicable for every wall system. The difficulties exist as: uncertainty of the moisture loading and vapor flow direction at the both side of the wall, the type of cladding and the material properties of the walls' components, and related issues of installation, maintenance and durability. A more detailed discussion of these difficulties is carried out.

Theoretically, the wall should have high vapor permeance at the side facing to an environment with lower vapor pressure to facilitate drying and have low vapor permeance at the side facing an environment with high vapor pressure to reduce moisture intrusion. However, for most areas of Canada, the vapor pressure gradient between indoors and outdoors switches in a year. That means that any attempt to keep vapor out by applying high vapor resistance material at one side of the wall can also trap vapor in during some season in the year.

The building materials also increase the uncertainty to reach a definitive drying strategy. Some cladding materials are moisture-absorptive and can function as a moisture source after rains. To control this moisture source (called "solar-driven wetting"), the sheathing membrane should have high vapor resistance. This means the wall system loses the ability to drying outward, which is considered as the major drying direction. In case a low vapor permeance membrane, e.g. polyethylene sheet, is used at the inner side of wood-frame as the vapor barrier, a "moisture trap" can create and the wall can be very

susceptive to any moisture intrusion. On the other side, the hygrothermal properties of the building materials have not been well studied and accurately measured. For example, the WRB is the critical element in the moisture defending strategy, but various measuring methods to evaluate the WRB's vapor/liquid resistance exist and can generate confusing information to judge one product's performance.

In the whole life of the building envelope, including design, manufacture, installation and maintenance, any mistake and default can result in disaster failure. For example, rain leakage due to improper design/installation can bring large amount of water behind the cladding and be a tough challenge the drainage and drying capacity of the system. Another example is that the life spans of sealant and caulking materials can be much shorter than the services life of the building, risk of leakage could largely increase without regular maintenance and replacement of these components, especially if the design does not provide a "second line defense".

Facing this complex situation, it is impossible to provide a single drying strategy for all wall systems, and the rational solution to design the wood-frame wall system with sufficient drying capacity to serve its working condition relies on the thorough consideration of the climate conditions, indoor conditions, expected moisture loading, layout of the systems and selected materials. This thesis focuses on the drying performance of two cladding systems (wood siding and 3-coating stucco) under two climatic regions (Montreal and Vancouver) by analysis of experimental data and numerical modeling. Observations and guidelines to reduce moisture-related failures in

the studied wood-frame walls can be outlined:

1. The climatic condition is the primary factor to affect the drying performance of the building envelope. The investigated climate regions in this thesis research are Montreal and Vancouver. In both climates, the vapor pressure gradient across the wall reverses direction in the summer and winter seasons. The main drying process occurs in the summer season when the outdoor air has lower humidity ratio; while in winter season, the vapor diffusion from indoor space should be controlled to avoid condensation. The climatic condition of Vancouver has a relatively lower drying potential through the year, comparing to Montreal's climate. The severe climate condition (frequent rainfall and humid air) of Vancouver accents the requirement of efficient moisture management and of avoiding of moisture intrusion in the building envelope.

2. The investigated exterior cladding systems are 20 mm stucco finish and 2 layers of asphalt impregnated papers and wood siding on furring with spun bonded polyolefin membrane with crinkled surface. The stucco has relatively higher vapor resistance and can restrain outward drying, when used as cladding material. The asphalt impregnated paper used in stucco cladding systems has very high vapor resistance when it is dry, but has much lower vapor resistance to allow drying when it is wet. Generally, the stucco wall has worse drying performance than wood siding wall. In cases where the polyethylene vapor barrier is installed in the wood-frame, a "moisture trap" can be created and the wall system has significantly lack of drying capacity; moisture intrusion

from exterior or interior should be strictly avoided, or extra drying mechanism, such as ventilation behind cladding, should be considered to improve the wall's drying performance. Wood siding wall represents cladding systems of high outward vapor permeance. The wood laps are air/vapor permeable and the spun bonded polyolefin membrane also has constant high vapor permeance. According to the numerical simulation, the cladding wall presents much better drying performance to release moisture in wet material. Even in the cases where the installation of polyethylene vapor barrier in the wood siding wall eliminates inward drying, the outward drying is still allowed.

3. To facilitate outward drying, the materials at the exterior side of the stud cavities should allow vapor diffusion through. Especially, the performance of sheathing membrane should be carefully considered. The sheathing membrane should be an effective capillary break to stop rain absorption and also have certain vapor permeance for drying. However, in case the cladding material receives moisture and absorbs water during rain, e.g. brick veneer, the air gap behind the cladding should be provided to enhance drying.

The most common types of sheathing membrane (or called weather resistance barrier, WRB for short) are asphalt-saturated felt, building paper and housewrap. The components, advantage and disadvantage of them are summarized in Table 5.7. There is

no definitive recommendation for the choice of sheathing membranes. All of the products have their strengths and weaknesses requiring specific consideration in a particular application. The sheathing membrane is one component of the envelope system and it should be determined and judged to achieve the successful performance of the whole system.

4. The sheathing board provides stiffness to prevent lateral movement of the frame and a base to fasten the cladding. The sheathing material with higher vapor permeance contributes to outward drying. In the investigated sheathing board, fiberboard presents fast drying and less moisture accumulation than OSB and plywood. However, the choice of sheathing board also needs to consider the type of wall system, stiffness, wet performance (ability to prevent water suction, swelling or delaminating) and cost; these aspects are not covered in the presented thesis.

Table 5.7 Features of sheathing membranes (source: Straube 2001)

	Asphalt-saturated felt	Building paper	Housewrap
Manufacturing	Felt is made of recycled paper (cardboard) or sawdust, and impregnated with asphalt.	Building paper is manufactured from Kraft paper and then impregnated with asphalt.	Housewrap is generally made from polyethylene or polypropylene, can be Non-perforated or perforated.
Physical features	Felt can be classified as#15 felt, weigh from 7.5 to 12.5 pounds/sq ft, and 30# felt, weigh between 16 and 27 pounds per square.	The longer fibers in the Kraft paper allow for a lighter weight product with similar and often better mechanical properties than felt.	The housewraps are significantly thinner and lighter than felts or papers, but are usually stronger, especially when wet.
Water and vapor control	None of the products is truly waterproof. Under long-term or extreme exposure, water will penetrate.		
	Better seal performance around nail/staple openings Better resistance to surfactant effects Can rot when wet, warm and long enough; Vapor permeance can increase dramatically when wet;		Easy and fast applied with minimum laps and joints; not rot; more susceptible to leaks at fastenings, partially solved by specifying plastic capped nails, or solved by taping over the fasteners; constant and high vapor permeance.

5. The application of polyethylene membrane as vapor battier should be judged

depending on the following factors: the climate condition, indoor humidity level, and the hygroscopic features of the cladding materials. In case the indoor humidity is kept at a high level throughout the year, for example, swimming pool, bathroom and manufactures with high moisture generation, it should be applied at the inner side of the wall to prevent vapor diffusion from indoor space. For the condition with reversing vapor pressure gradients between outdoor and indoor spaces in a year, there is no single correct location for the polyethylene vapor barrier. In summer time when outdoor vapor pressure is higher than the indoor vapor pressure, the existence of polyethylene sheet at the inner side of wall's frame can restrain inward drying and even cause vapor condensation on its surface. In case the materials on the inner side of the wall have certain vapor resistance, e.g. Kraft-faced fiberglass insulation or painted gypsum board, the polyethylene sheet is not necessary for indoor space with low to intermediate humidity levels. Products with changing vapor permeance according to environmental condition, such as smart vapor retarder (Kunzel 1999) or Kraft-faced fiberglass insulation, can be used to prevent cold condensation in winter and still provide drying capacity in summer.

Meanwhile, the complete moisture control strategy is the integration of methods to prevent moisture from getting into the stud cavity by deflection and drainage, drying of wet materials and elimination of air leakage and condensation. Beside the drying strategy discussed above, the following methods should be considered in the design of wood-frame walls for climate with significant amount and frequency of rainfall and concerned moisture-related building failure:

1. Reduce the exposure of cladding to rain (OAA 2005): rationally design building's shape and direction upon the site condition, to design the shapes of roof and overhangs to shade cladding from rain drops;
2. The exterior surface of the building envelope should have features to shed rain;
3. Apply the "rain screen principle" with three combined functions to stop rain penetration: pressure equalized compartments, capillary break and drainage path (Morrison Hershfield Limited 1990);
4. Install sheathing membrane as capillary break/drainage surface over sheathing substrates; for condition with severe rain exposure or contact cladding system, e.g. stucco or contact sidings, two layer of sheathing membranes can significantly reduce rain leakage at fasteners, and improve drainage by creating drainage space between the two membranes (Straube 2001);
5. Apply two-stage and drained joint to protect the inner sealant (Amstock 2000);
6. Provide sufficient flashing around joints between different materials and different components;
7. Air leakage through the wall can hardly be controlled as a design feature for drying, because of the symbiotic problems of heat loss and vapor condensation, especially caused by air exfiltration in heating season. Therefore, air leakage through the wall should be eliminated by a continuous air barrier system. The possible pattern of air convection to facilitate drying is natural ventilation in the air gap behind the exterior finish with feasible and practical design (Stovall & Karagiozis 2004;

Davidovica et al. 2006).

8. Install continuous air barrier systems composed of impermeable board or membrane, air-tight sealant or caulking, at either side of the stud cavity to eliminate air leakage;
9. Keep quality control in the manufacture and installation; regularly maintain the building envelope system.

6 Conclusion, Contribution and Future Work

6-1 Conclusion and Contribution

The objective of the thesis is to develop a numerical tool for the study of building envelopes' hygrothermal performance. For this purpose, research efforts in the study of building envelopes' hygrothermal performance through experimental and numerical simulation methods are surveyed. Features of the published hygrothermal tools and their application are analyzed. The state of the art knowledge of heat and moisture transport in building materials is applied to establish the conservation equations of the numerical tool. Air convection also is integrated in the conservation equations by Darcy-Boussinesq approximation. Two tasks are carried out to validate the numerical tool: inter-model comparison with the benchmarks of the HAMSTAD project, and comparison with measured results of the experiment of CRD project. The numerical tool is prone to be accurate and reliable. The presented numerical tool has the advanced feature as listed:

1. Handling transient and combined HAM transport in multi-dimension and multi-layer building envelopes;

2. Applying "phase-divided" equations for moisture transport, to obtain accurate calculation;

3. Coupling air convection as heat and moisture transport mechanism;

4. Material properties as moisture-dependent equations;

5. Hourly meteorological data as boundary condition;

6. Added moisture and heat sources in building components and their surfaces;

7. Flexibility for researchers to modify, maintain and transfer their modeling work.

An approach to investigate the drying performance of wood-frame walls by numerical modeling is established. The bottom part of the sheathing board is identified as the region with highest risk of moisture accumulation in case rain leakage occurs. High initial moisture load is added into this part of the sheathing board to simulate wetting due to rain leakage. The wall is exposed to hourly weather condition of selected area. The drying profiles of the wall's components are analyzed based on results of numerical modeling. Through adjustment of the numerical tool's input, the factors of interest to affect the drying performance of the wall system can be investigated. The factors studied in the presented thesis included two climatic conditions (Montreal and Vancouver), type of cladding, type of sheathing, and the function of polyethylene vapor barrier. Through comparison between drying profiles of wet components in the walls, this thesis has illuminated the influence of climatic conditions, indoor conditions, and material properties of the wall's components (moisture storage character and vapor permeance). The major conclusions based on this study are listed:

1. To avoid moisture trapped in moisture storage materials of the wall, drying process should be allowed to the inside of the building (inward drying) and outside of the building (outward drying). Meanwhile, the wall should have certain resistance to vapor diffusion from outside and inside spaces. Theoretically, the wall should have high vapor permeance at the side facing to environment with lower vapor pressure to facilitate drying and have low vapor permeance at the side facing to environment with high vapor pressure to reduce moisture intrusion. However, the vapor pressure gradient cross the wall usually does not keep a single direction in the whole year; rather, it switches between heating and hot seasons. Thus, vapor permeance of the components at the inner and outer side of the stud cavity should be selected to fulfill the requirement of drying

and also avoiding condensation due to vapor diffusion.

2. For both Montreal and Vancouver climates, the drying process occurs manly in the warm/hot season when outdoor air has lower humid ratio; and in cold (heating) season, the vapor diffusion from indoor space should be controlled to avoid cold condensation. The Montreal climate provides higher drying potential than the Vancouver climate.

3. The cladding with high vapor permeance can be beneficial for outward drying. Thus, the selection of appropriate sheathing membrane is critical to facilitate drying. The ideal sheathing membrane should have high water resistance as effective capillary break, and also high vapor permeance to allow vapor diffusion.

4. In the case material of the cladding absorbs water during rain, e.g. unpainted or aged wood siding, brick veneer and unsealed stucco, the sheathing membrane behind the cladding should be vapor tight to stop solar driven wetting; meanwhile, ventilation in the air gap behind the cladding should be utilized to dry the cladding materials.

5. The investigated sheathing boards, plywood board, OSB and fiberboard, are hygroscopic and sensitive to moisture problems. The location of the sheathing board exposes it to moisture intrusion in case rain leakage occurs. The sheathing material with higher vapor permeance presents lower moisture accumulation in the wall and faster drying.

6. The installation of exterior insulation sheathing can significantly reduce the drying capacity of the wall systems, since the vapor permeance of exterior insulation materials range between semi-impermeable (0.1 perm < permeance < 1 perm) and impermeable (permeance < 0.1 perm). In case an exterior insulation sheathing board is installed, a layer of sheathing membrane should be provided on the top or behind the exterior insulation sheathing to drain any rain leakage passing the cladding.

7. Polyethylene membrane is impermeable to vapor diffusion (Permeance < 0.1 perm). It

should only be used in cases where indoor moisture level is high. In case the materials on inner side of the wall have certain vapor resistance, e.g. Kraft-faced fiberglass insulation or painted gypsum board, the polyethylene sheet is not necessary for indoor space with low to intermediate moisture level.

8. In well insulated and airtight wall systems, drying of wet materials is a slow process and can take months or years to release moisture absorbed in building materials. Drying is the necessary solution after moisture intrusion, but the primary consideration in design should be sheltering the wall from wind-driven rain, reducing rain penetration by "rain-screen" principle, and providing sufficient drainage system.

6-2 Future Work

Comparing with hygrothermal tools coded with more traditional computer languages such as FORTRAN or C. The holder software of HAM-BE, COMSOL was developed with modular concept. The functions required to implement numerical modeling (drawing geometric objects, definition of variables and PDEs, mesh generation and solving algorithm) were built in as commands in script format or graphic user interfaces (GUIs). Thus, HAM-BE is an open and easy learned modeling surrounding for the users to build/modify/extend their modeling work. Further research work can be carried out in the following aspects to extend the capacity of the tool itself and also the application of numerical modeling in building science field.

1) Investigation of hygrothermal performance of other building envelope systems

The building envelope systems investigated in this thesis are wood-framed walls with wood siding or stucco as the cladding. HAM-BE also can be applied in the hygrothermal study of other wall systems, such as light-gauge steel stud wall and brick veneer wall. The light-gauge steel stud wall systems are widely used for multi-level residential

buildings, especially high-rise condominium buildings in the lower Mainland of British Columbia. Exposed to intense wind-driven rain and built with identical technique and components, e.g. cladding, insulation, windows, doors with lower wood-frame walls, the steel stud walls also face the threat of rain leakage and their hygrothermal performance should be studied to provide durable design. Brick veneer walls are the popular choice for residential buildings. The hygrothermal performance of the brick veneer wall presents different concerns for building science research. The bricks are hygroscopic and also capillary-active; the fine pores of bricks can absorb significant amount of water during rains. The solar driven wetting can cause moisture accumulation in sheathing board and induce premature failure. The presented numerical tool can be used to predict the hygrothermal response of various building envelope systems and to verify design practice under certain climatic condition. To fulfill the above mentioned tasks, HAM-BE should be adjusted and validated through field or laboratory experiments.

2) Study of hygrothermal-related phenomena

Moisture content and temperature profiles are the essential information to understand hygrothermal-related processes: such as material expansion/shrinkage and corresponding load redistribution of stress/tension and damage due to changing hygrothermal condition, mold growth and deterioration under certain hygrothermal conditions, salt migration driven by temperature and moisture content gradients, and so on. With the strong capacity to couple various physical/chemical phenomena governed by PDEs, HAM-BE can be extended to investigate the inter-action of these hygrothermal-related phenomena for the interest of building science research.

3) Study of air convection in building envelope systems

HAM-BE coupled air convection in the conservation equations of heat and moisture transport. However, the application of air flow format in this thesis was limited to buoyancy flow, and more complex air flow phenomena, e.g. air leakage through the

building envelope and forced convection in rain-screen are worthy of investigation. Since air flow can carry much more moisture than vapor diffusion, it can not be neglected as a damage mechanism and also can be utilized to facilitate drying by proper design. This work requires collection of data to adjust parameters in the applicable equation and the boundary conditions, and model validation through field and laboratory experiments.

4) Development of HAM tool for public users

User-friendly interfaces can be created to serve the presented numerical tool. The users can do all the modeling operation through well-organized drop-down menus. Help toolbar and user manual can also be provided for users. The numerical tool can be used by architects and engineers, without thorough training of modeling skills.

5) Extending numerical simulation of building system

HAM-BE is a simulation tool for building envelope systems. Since COMSOL can be used with MATLAB/SIMULINK tools, the HAM-BE can be used as a functional block in the systematic analysis of heat/moisture balance of whole building. This approach has been applied in the HAMLab and International Building Physics Toolbox (IBPT). Even the capacity of this approach is limited by the modeling surrounding. It promises raising of the standard modeling platform for HAM analysis and building science study in the wider range.

References

Adan O, Brocken H et al. "Determination of Liquid Water Transfer Properties of Porous Building Materials and Development of Numerical Assessment Methods: Introduction to the EC HAMSTAD Project", Journal of Thermal Envelope and Building Science 2004; 27: 253 - 260

Alturkistani A, Fazio P, Rao J, Mao Q. "A New Test Method to Determine the Relative Drying Capacity of Building Envelope Panels of Various Configurations", BAE2051, Journal of Building and Environment 43, pp. 2203-2215, 2008

Alvarez JC. "Evaluation of Moisture Diffusion Theories in Porous Materials", Master Thesis, Department of Mechanical Engineering, Virginia Polytechnic Institute and State University, USA, 1998.

Amstock JS. "Handbook of Adhesives and Sealants in Construction", McGraw-Hill Professional Sealing compounds, 2000.

ASTM C1498-01, "Test Method for Hygroscopic Sorption Isotherms of Building Materials", American Society for Testing and Materials, USA, 2001.

ASTM C177-04, "Standard Test Method for Steady-State Heat flux Measurements and Thermal Transmission Properties by Means of the Guarded-Hot-Plate Apparatus", American Society for Testing and Materials, USA, 2004.

ASTM C518, "Standard Test Method for Steady-state Thermal Transmission Properties

by means of the Heat Flow Meter Apparatus", American Society for Testing and Materials, USA, Sept 2002.

ASTM C522-03, "Standard Test Method for Airflow Resistance of Acoustical Materials", American Society for Testing and Materials, USA, 2003.

ASTM D4442-92, "Standard Test Methods for Direct Moisture Content Measurement of Wood and Wood-base Materials", American Society for Testing and Materials, USA, 1997.

ASTM Standard E96, "Test Methods for Water Vapor Transmission of Materials", American Society for Testing and Materials, USA, 1996.

ASTM UOP578-02, "Automated Pore Volume and Pore Size Distribution of Porous Substances by Mercury Porosimetry", American Society for Testing and Materials, USA, 2002.

Baker MC. "Canadian Building Digest-111: Decay of wood", National Resource Council of Canada, originally published in March 1969.

Barrett D. "The Renewal of Trust in Residential Construction: an Inquiry into the Quality of Condominium Construction in British Columbia", report prepared for the Province of British Columbia, Canada; 1998.

Beall C. "Thermal and Moisture Protection Manual: for Architects, Engineers, and Contractors", McGraw-Hill, New York, USA; 1999.

Beaulieu P, Cornick SM, Dalgliesh WA, Djebbar R, Kumaran MK, Lacasse MA et al. "MEWS Methodology for Developing Moisture Management Strategies: Application

to Stucco-clad Wood-frame Walls in North America", NRCC-45213, Institute for Research in Construction, National Research Council Canada, Canada; 2001.

Beaulieu P, Bomberg M, Cornick S, Dalgliesh A, Desmarais G, Djebbar R, Kumaran K, Lacasse M, Lackey J, Maref W et al. "Final Report from Task 8 of MEWS Project (T8-03) - Hygrothermal Response of Exterior Wall Systems to Climate Loading: Methodology and Interpretation of Results for Stucco, EIFS, Masonry and Siding Clad Wood-Frame Walls", IRC-RR-118, Institute for Research in Construction, National Research Council Canada, Canada; 2002.

Blocken B. "Wind-driven Rain on Buildings: Measurements, Numerical Modelling and Applications", Doctoral Thesis, Catholic University of Leuven, Belgium; 2004.

Bomberg MT, Brown WC. "Building Envelope and Environmental Control: Part 1- Heat, Air and Moisture Interactions", NRC publication, originally published in "Construction Canada" 1993; 35(1): 15-18.

Bomberg M, Onysko DM. "Heat, Air and Moisture Control in Walls of Canadian houses: a review of the historic basis for current practices", Journal of Thermal Envelope and Building Science 2002; 26(1): 3-31.

Bomberg M, Carmeliet J, Grunewald J, Holm A, Karagiozis A, Kuenzel H, Roels S. "Position Paper on Material Characterization and HAM Model Benchmarking", Proceeding of the 6th Symposium on Building Physics in the Nordic Countries, Trondheim, Norway; 2002.

Brunauer S, Emmett PH, Teller E. "Adsorption of Gases in Multimolecular Layers",

Journal of the American Chemical Society 1938; 60:309-19.

BSC. "Building Materials Property Table", Building Science Corporation, http://buildingscience.com/bsc/designsthatwork/buildingmaterials.htm, 2006.

BSC "Air Barriers vs. Vapor Barriers", Building Science Corporation, http://www.buildingscienceconsulting.com/resources/, 2007.

Burch DM, Thomas WC. "An Analysis of Moisture Accumulation in a Wood-frame Wall subjected to Winter Climate", Proceeding of the ASHRAE/DOE/BTECC Conference, Thermal performance of the exterior envelopes of building, Clearwater Beach, Florida, USA; 1992.

Burch DM, Rode C. "Empirical Validation of a Transient Computer Model for Combined Heat and Moisture Transfer", Proceeding of Thermal Performance of the Exterior Envelopes of Building VI, Clearwater Beach, Florida, USA; December 4-8, 1995.

Burch DM, Chi J. "MOIST: a PC Program for Predicting Heat and Moisture Transfer in Building Envelopes", National Institute of Standard and Technology, USA; 1997.

Candanedo L, Ge H, Derome D, Fazio P. "Analysis of Montreal 30-year Weather Data to Select Loading Conditions for Large-scale Tests on Wall Panel Systems", Proceeding of the 3th International Building Physics Conference, Montreal, Canada; Aug 27-31, 2006.

Carll CG, Highley TL. "Decay of Wood and Wood-Based Products above Ground in Buildings," Journal of Testing and Evaluation, 1999; 27(2): 150-158.

Carmeliet J, Roels S. "Determination of the Isothermal Moisture Transport Properties of Porous Building Materials", Journal of Thermal Envelope & Building Science, 2001; 24(3): 183-210.

Carmeliet J, Roels S. "Determination of the Moisture Capacity of Porous Building Materials", Journal of Thermal Envelope & Building Science, 2002; 25(3): 209-237.

Carmeliet J, Hens H, Roels S, Adan O, Brocken H, Cerny R, Pavlik Z, Hall C, Kumaran K, Pel L. "Determination of the Liquid Water Diffusivity from Transient Moisture Transfer Experiments", Journal of Thermal Envelope and Building Science 2004; 27(4): 277-305.

COMSOL. "Modeling Guide", COMSOL Inc., 2007.

Cornick S, Dalgliesh A, Said N, Djebbar R, Tariku F, Kumaran MK. "Report from Task 4 of MEWS Project: Environmental Conditions Final Report", Institute for Research in Construction, National Research Council Canada, October 2002.

Cornick SM, Dalgliesh WA. "A Moisture Index Approach to Characterizing Climates for Moisture Management of Building Envelopes", Proceedings of the 9th Canadian Conference on Building Science and Technology, pp. 383-398; Vancouver, BC, Canada; Feb. 27-28, 2003.

CWC. "Design with Wood", Canadian Wood Council, http://www.cwc.ca/DesignWithWood/, 2007.

Dacquisto DJ, Crandell JH, Lyons J. "Building Moisture and Durability--- Past, Present and Future Work", prepared by Newport Partners for Office of Policy Development

and Research, Department of Housing and Urban development, USA; 2004.

Dalton J. "Experimental Essays on the Constitution of Mixed Gases; on the Force of Steam or Vapour from Water and Other Liquids in Different Temperatures, Both in Torricellian Vacuum and in Air; on Evaporation; and on Expansion of Gases by Heat", Manchester Lit. and Phil. Soc. Mem. 1802, 5:535-602.

Davidovica D, Srebrica J, Burnett E. "Modeling Convective Drying of Ventilated Wall Chambers in Building Enclosures", International Journal of Thermal Sciences, February 2006; Volume 45, Issue 2, , Pages 180-189.

Desmarais G, Derome D, Fazio P. "Mapping of Air Leakage in Exterior Wall Assemblies", Journal of Thermal Envelope and Building Science, 2000; 24(2): 132-154.

Djebbar R, van Reenen D, Kumaran MK. "Indoor and Outdoor Weather Analysis Tool for Hygrothermal Modeling", Proceeding of the 8th Conference on Building Science and Technology, pp. 139-157; Toronto, Canada; Feb, 2001.

Drchalova J, Pavlik Z, Cerny, R. "A Comparison of Various Techniques for Determination of Moisture Diffusivity from Moisture Profiles", Proceeding of the 6th Symposium on Building Physics in the Nordic Countries, Trondheim, Norway; June 17-19, 2002.

Durner W. "Hydraulic Conductivity Estimation for Soils with Heterogeneous Pore Structure", Journal of Water Resources Research, 1994; 30: 211-223.

Edwards B. as editor. "Green Architecture", Wiley-Academy, London, UK; 2001.

Fazio P, Alturkistani A, Marsh C, Rao J. "Environmental Chamber for Investigation of Building Envelope Performance", Journal of Architectural Engineering 1997; 3(2): 97-103.

Fazio P, Bartlett K, Rao J, Yang DQ, Miao G. "Experimental Evaluation of Potential Movement of Mold Spores from Wall Cavities to Indoor Environment", Proceedings of the 10th Conference on Building Science and Technology, Ottawa, Canada; May 11-13, 2005.

Fazio P, Rao J, Alturkistani A, Ge H. "Large Scale Experimental Investigation of the Relative Drying Capacity of Building Envelope Panels of Various Configurations", Proceedings of the 3rd International Conference in building Physics (IBPC3), pp 361-368; Montreal, Canada; August 27-31, 2006a.

Fazio P, Mao Q, Vera S. "Establishing a Uniform and Measurable Moisture Source to Evaluate the Drying Capacity of Building Envelope Systems", Proceedings of the 3rd International Building Physics Conference (IBPC3), pp 369-377; Montreal, Canada; August 27-31, 2006b.

Fazio P, Ge H, Mao Q, Alturkistani A, Rao J. "A Test Method to Measure the Relative Capacity of Wall Panels to Evacuate Moisture from their Stud Cavity", Journal of Architectural Engineering 2007; 13(4): 194-204.

Funk M. Wakili KG. "Driving Potentials of Heat and Mass Transport in Porous Building Materials: a Comparison between General Linear, Thermodynamic and

Micromechanical Derivation Schemes", Journal of Transport in Porous Media 2007; 72(3): 273-294.

Gaur R.C. Bansal N.K. "Effect of Moisture Transfer across Building Components on Room Temperature", Journal of Building and Environment 2002; 37:11–17.

Gerbasi, Dino, "CONDENSE User's Manual", GES Technologies Inc., Montreal, Quebec, 2005.

Gowri K. "Knowledge-Based System Approach to Building Envelope Design", Ph.D. Dissertation, Centre for Building studies, Concordia University, Montreal, Canada; 1990.

Grunewald J. "Documentation of the Numerical Simulation Program DIM3.1, Volume 1: Theoretical Fundamentals. Delphin4.1", University of Technology, Dresden, German; 2000a.

Grunewald J. "Documentation of the Numerical Simulation Program DIM3.1, Volume 2: User's Guide. Delphin4.1", University of Technology, Dresden, German; 2000b.

Grunewald J, Bomberg M. "Towards an Engineering Model of Material Characteristics for Input to HAM Transport Simulation", Journal of Thermal Envelope and Building Science 2003; 26(4): 343-366.

Hagentoft CE "Introduction to Building Physics", Studnetlitteratur, Lund, Sweden, 2001.

Hagentoft CE. "HAMSTAD – WP2 Modeling, Version 4", Report R-02:9, Department of Building Physics, Chalmers University of Technology, Gothenburg, Denmark; 2002a.

Hagentoft CE. "HAMSTAD – Final report: Methodology of HAM-modeling", Report

R-02:8. Department of Building Physics, Chalmers University of Technology, Gothenburg, Denmark; 2002b.

Hagentoft CE, Sasic Kalagasidis A, Adl-Zarrabi B, Roels S, Carmeliet J, Hens H, Grunewald J, Funk M, Becker R, Shamir D, Adan O, Brocken H, Kumaran K, Djebbar R. "Assessment Method of Numerical Prediction Models for Combined Heat, Air and Moisture Transfer in Building Components: Benchmarks for One-dimensional Cases", Journal of Thermal Envelope and Building Science 2004; 27: 327 – 352.

Haverinen U, Vahteristo M et al., "Knowledge-based and Statistically Modeled Relationships between Residential Moisture Damage and Occupant Reported Health Symptoms", Journal of Atmospheric Environment 2003; 37: 577-585.

Hazleden DG, Morris PI. "Designing for Durable Wood Construction: the 4 Ds", Proceeding of the 8th International Conferences on Durability of Building Materials and Components, Vancouver, Canada; May 30 - June 3, 1999.

Hazleden DG, Morris PI. "The Influence of Design on Drying Rates in Wood-Frame Walls under Controlled Conditions", Proceedings of Performance of Exterior Envelopes of Whole Buildings VIII: Integration of Building Envelopes, Clearwater Beach, Florida, USA; December 2-7, 2001.

Hens H. "Annex 24, Heat, Air and Moisture Transfer in Insulated Envelope Parts, Final Report, Volume1, Task1: Modeling", International Energy Agency, 1996.

Hens H, Carmeliet J. "Performance Prediction for Masonry Walls with EIFS: Using

Calculation Procedures and Laboratory Testing", Journal of Thermal Envelope and Building Science 2002; 25(3): 167-187.

Hens H. "Annex 41 Whole Building Heat, Air and Moisture Response (MOIST-EN)", ongoing project of International Energy Agency, 2005.

Hens H, Janssens A, Depraetere W, Carmeliet J, Lecompte J. "Brick Cavity Walls: A Performance Analysis Based on Measurements and Simulations", Journal of Building Physics 2007; 31: 95-124.

Husman T. "Clusters of Autoimmune Diseases in Microbial Exposure in Moisture Damaged Buildings", Journal of Allergy & Clinical Immunology 2004; Volume 113 , Issue 2 , Page S59.

Hutcheon NB. "Fundamental Considerations in the Design of Exterior Walls for Buildings", Engineering Journal 1953; 36(1) 687-698.

Janssen H, Blocken B, Carmeliet J. "Conservative Modelling of the Moisture and Heat Transfer in Building Components under Atmospheric Excitation", International Journal of Heat and Mass Transfer 2007; 50(5-6): 1128-1140.

Janssens J, Hens H. "Interstitial Condensation due to Air Leakage: a Sensitivity Analysis", Journal of Thermal Envelope and Building Science 2003: 27(1): 15-29.

Janz M. "Methods of Measuring the Moisture Diffusivity at High Moisture Levels", Report TVBM-3076, Division of Building Materials, Lund Institute of Technology, Lund, Sweden; 1997.

JLC. "Window Leaks Rampant, Canadian Study Reports", edited by Ted Cushman, http://www.highbeam.com/doc/1G1-110807846.html, Journal of Light Construction, November 2003.

Kalagasidis AS. "HAM-Tools, International Building Physics Toolbox, Block documentation, R-02:6", Department of Building Physics, Chalmers University of Technology, Gothenburg, Sweden; 2002.

Kalagasidis AS. "HAM-Tools: an Integrated Simulation Tool for Heat, Air and Moisture Transfer Analyses in Building Physics", Doctoral thesis, Department of Building Technology, Chalmers University of Technology, Gothenburg, Sweden; 2004.

Karagiozis AN, Kuenzel H, Holm A, Desjarlais A. "An Educational Hygrothermal Model: WUFI-ORNL/IBP", Report of the Oak Ridge National Laboratory, USA; 1999.

Karagiozis AN. "Integrated Approaches for Moisture Analysis", Proceeding of Durability and Disaster Mitigation in Wood Frame Housing, Monona Terrace Convention Center, Madison, Wisconsin, USA; November 1999.

Karagiozis AN, Künzel HM. "WUFI-ORNL/IBP - A North American Hygrothermal Mode", Proceedings for Performance of Exterior Envelopes of Whole Buildings VIII: Integration of Building Envelopes, Clearwater Beach, Florida, USA; December 2-7, 2001.

Karagiozis AN. "Chapter 6: Advanced Numerical Models for Hygrothermal Research, Moisture Analysis and Condensation Control in Building Envelopes", pp90-106, edited by Trechsel HR, American Society for Testing and Materials (ASTM), USA;

2001.

Karagiozis AN. "A North American Research Approach to Moisture Design by Modeling", Proceeding of the 6th Symposium on Building Physics in the Nordic Countries, Trondheim, Norway; June 17-19, 2002.

Karagiozis AN. "Importance of Moisture Control in Building Performance", Canadian Conference on Building Energy Simulation, September, Montreal, Canada; September, 2003.

Karagiozis AN, Desjarlais A. "What Influences the Hygrothermal Performance of Stucco Walls in Seattle", Proceedings of the 9th Conference on Building Science and Technology, p. 32-44, Vancouver, British Columbia, Canada; February 27-28, 2003.

Kaviany M. "Principles of Heat Transfer in Porous Media, Mechanical Engineering series", Springer, New York; 1995.

Krus M, Sedlbauer K, Zillig W, Kunzel HM. "A New Model for Mould Prediction and its Application on a Test Roof", Proceeding of the Second Internal Scientific Conference: the Current Problems of Building Physics in the Rural Building; Cracow, Poland; Nov, 2001.

Kudder RJ, Erdly JL. Editors. "Water Leakage through Building Facades", American Society for Testing and Materials, 1998.

Kumaran MK. "Annex 24, Heat, Air and Moisture Transfer in Insulated Envelope Parts, Task 3: Material Properties", Acco, Leuven, Belgium, 1996.

Kumaran MK. "Interlaboratory Comparison of the ASTM Standard Test Methods for

Water Vapor Transmission of Materials (E 96 95)", ASTM Journal of Testing and Evaluation (USA) 1998: 26(2): 83-88.

Kumaran K, Lackey J, Normandin N, van Reenen D, Tariku F. "Thermal and Moisture Transport Property Database for Common Building and Insulating Materials", ASHRAE Research project 1018-RP, 2002.

Kunzel HM. "Simultaneous Heat and Moisture Transport in Building Components: One and two-dimensional Calculation Using Simple Parameters", Fraunhofer-Institut fur Bauphysic, Germany, 1995.

Kunzel HM. "The Smart Vapor Retarder: an Innovation Inspired by Computer Simulations", ASHRAE Transactions 1998; p. 903-907.

Kunzel, HM. "Flexible Vapor Control Solves Moisture Problems of Building Assemblies - Smart Retarder to Replace the Conventional PE-film", Journal of Thermal Envelope & Building Science, 1999: Vol. 23, pp. 95 - 102.

Lawton MD, Brown WC, Lang AM. "Stucco-Clad Wall Drying Experiment", CHMC Research Report, Vancouver, BC, Canada; 1999.

Li QR, Fazio P, Rao J. "Hygrothermal Simulation of Drying Performance of Typical North American Building Envelope", Proceedings of the 10th Conference of International Building Performance Simulation Association; Montreal, Canada; August 15-18, 2005.

Li QR, Fazio P, Rao J. "Applying Numerical Simulation to Extend Experiment Design on Drying Capacity of Light-frame Wall Systems", Proceedings of the 2006

Architectural Engineering National Conference: Building Integration Solutions; Omaha, Nebraska, USA; March 29 – April 1, 2006.

Li QR, Fazio P, Rao J. "Development of HAM Tool for Building Envelope Analysis", Journal of Building and Environment, 2008.

Lstiburek J. "Builders Guide to Cold Climates", Energy & Environmental Building Association, 2006.

Maref W, Lacasse M, Booth D. "Management of Exterior Wall System (MEWS) – Modeling, Experiments and Benchmarking", Institute for Research in Construction, National Research Council of Canada, 2002.

Maref W, Lacasse MA, Booth DG. "Benchmarking of IRC's Advanced Hygrothermal Model - hygIRC Using Mid- and Large-Scale Experiments", Research Report, Institute for Research in Construction, National Research Council Canada, 2002.

Mclean RC, Galbraith GH, Sanders CH. "Moisture Transmission Testing of Building Materials and the Presentation of Vapor Permeability Values", Building Research and Practice 1992; 18(2): 82-91.

McNeel SV, Kreutzer RV. "Fungi & Indoor Air Quality", Health & Environment Digest 1996; 10(2) 9-12.

Mendes N, Winkelmann FC, Lamberts R, Philippi PC. "Moisture Effects on Conduction Loads", Energy and Buildings 2003; 35: 631–644.

OAA. "OAA Rain Penetration Control Practice Guide", Ontario Association of Architecture, 2005.

Ojanen T. "Improving the Drying Efficiency of Timber Frame Walls in Cold Climates, by Using Exterior Insulation", Thermal Performance of the Exterior Envelopes of Buildings VII, Clear water Beach, Florida, USA; 1998.

Okland O. "Convection in Highly-insulated Building Structures", Doctoral thesis, Norwegian University of Science and Technology in Trondheim, Norway; 1998.

ORNL. "ORNL helping Seattle Solves Crumbling Building Mystery", Oak Ridge National Laboratory, USA; 2001.

Philip JR, De Vries DA. "Moisture Movement in Porous Material under Temperature Gradients", Transactions, American Geophysical Union 1957; Vol. 38 (2): 222-232.

Quirouette R, Marshall S, Rousseau J. "Design Considerations for an Air Barrier System", Technical series 01-129, Canada Mortgage and Housing Corporation (CMHC), 1991.

Rao J, Miao G, Yang DQ, Bartlett K, Fazio P. "Experimental Evaluation of Potential Movement of Airborne Mold Spores out of Building Envelope Cavities Using Full Size Wall Assemblies", Third International Conference in building Physics (IBPC3), Montreal, Canada; August 27-31, 2006.

Rivard H. "CONDENSE Version 2.0: User's Manual", Quebec Building Envelope Council, Montreal, Canada; 1993.

Rode C. "Combined Heat and Moisture Transfer in Building Constructions", Doctoral Thesis, Report No. 214. Department of Civil Engineering, Technical University of Denmark, Denmark; 1990.

Rode C. "Prediction of Moisture Transfer in Building Constructions", Building and Environment 1992, Vol. 27(3): 387-397.

Rode C. "Chapter 10: A Look to the Future, Moisture Analysis and Condensation Control in Building Envelopes", pp152-158, edited by Trechsel HR, American Society for Testing and Materials (ASTM), USA; 2001.

Rode C, Stang BD, Hansen MH. "Model for Multidimensional Heat, Air and Moisture Conditions in Building Envelope Components", Project description, Department of Civil Engineering, Technical University of Denmark, Denmark; 2006.

Roels S, Depraetere W, Carmeliet J, Hens H. "Simulating Non-Isothermal Water Vapor Transfer: An Experimental Validation on Multi-Layered Building Components", Journal of Building Physics1999; Vol. 23, No. 1, 17-40.

Rousseau J. "A Study of the Rainscreen Concept Applied to Cladding Systems on Wood Frame Walls", performed by Morrison-Hershfield Limited for CMHC (Canada Mortgage and Housing Corporation), Technical Series 96-214, 1990.

Rousseau M. "An Overview of the Survey of Building Envelope Failures in the Coastal Climate of British Columbia", performed by Morrison-Hershfield Limited for CMHC (1996). Journal of Building Physics 1999; 22(4): 364-367.

Salonvaara MH, Ojanen T, Kokko E, Karagiozis AN. "Drying Capabilities of Wood Frame Walls with Wood Siding", Thermal Performance of the Exterior Envelopes of Buildings VII, Clear water Beach, Florida, USA; 1998.

Salonvaara MH. "Development of Heat, Air, Moisture and Pollutant Transport Model,

BEESL/EQS Quality Assurance and Project Plan for CHAMPS Development", Building Energy and Environmental Systems Laboratory at Syracuse University, New York, USA; 2004.

Schellen HL, van Schijndel AWM. "Application of an Integrated Indoor Climate & HVAC Model for the Indoor Climate Performance of a Museum", the 7th Symposium on Building Physics in the Nordic Countries, Reykjavík, Iceland; June 13-15, 2005.

Sherman MH, Chan R. "Building Airtightness: Research and Practice", Energy Efficiency and Renewable Energy, Building Technology Program of the Department of Energy, USA; 2004.

Stovall TK, Karagiozis A. "Airflow in the Ventilation Space Behind a Rain Screen Wall," Performance of Exterior Envelopes of Whole Buildings IX International Conference, Clearwater, Florida, USA; December, 2004.

Straube, J. "The Influence of Low-permeance Vapor Barriers on Roof and Wall Performance", Proceedings of Performance of Exterior Envelopes of Whole Buildings VIII, December 2001a.

Straube, J. "Wrapping it Up: Building Paper and Housewraps", Canadian Architect, May 2001b.

Teasdale-St-Hilaire A, Derome D, Fazio P. "Approach for the Simulation of Wetting due to Rain Infiltration for Building Envelope Testing", the 9th Conference on Building Science and Technology, Vancouver, Canada; February 27-28, 2003.

TenWolde A. "Design tools, Chapter 11 in Moisture Control in Buildings", ASTM

Manual MNL 18. American Society for Testing and Materials, West Conshohocken, PA, USA; 1994.

TenWolde A, CoUiver DG. "Chapter 2: Weather Data, Moisture Analysis and Condensation Control in Building Envelopes", pp16-28, Edited by Trechsel HR. American Society for Testing and Materials (ASTM), USA; 2001.

Tom RW. "Wall Moisture Problems in Alberta Dwellings", Canada Mortgage and Housing Corporation (CMHC), Canada; 2001.

Van Schijndel AWM. "Solving Building Physics Problems Based on PDEs with FEWMLAB", the 6th Symposium on Building Physics in the Nordic Countries, in Trondheim, Norway; June 17-19, 2002.

van Schijndel AWM, Hensen JLM. "Integrated Heat, Air and Moisture Modeling Toolkit in MATLAB", Proceeding of the 9th International IBPSA Conference, Montreal, Canada; August 15–18, 2005.

Van Straaten RV. "Measurement of Ventilation and Drying of Vinyl Siding and Brick Clad Wall Assemblies", Master thesis, University of Waterloo, Canada; 2003.

Viitanen H, "Factors Affecting the Development of Mould and Decay in Wooden Material and Wooden Structures", Dissertation, The Swedish University of Agricultural Sciences Department of Forest Products, Uppsala; 1996.

Wang JK, Hagentoft CE. "A Numerically Stable Algorithm for Simplified Calculations of Combined Heat, Air and Moisture transport", 24th National Heat Transfer Conference, Pittsburgh, USA; Aug 2000.

Wang JK, Hagentoft CE. "A Numerical Method for Calculating Combined Heat, Air and Moisture Transport in Building Envelope Components", Nordic Journal of Building Physics 2001; Vol 2.

Watt D. "Building Pathology: Principles and Practice", Blackwell Science Inc, USA; 1999.

Weitzmann P, Kalagasidis AS, Nielsen TR, Peuhkuri R, Hagentoft CE. "Presentation of the International Building Physics Toolbox for Simulink", Proceeding of the Eighth International IBPSA Conference, Eindhoven, Netherlands; August 11-14, 2003.

Woloszyn, M. Carsten, R. "IEA Annex 41, MOIST-ENG Subtask 1 – Modelling Principles and Common Exercises. Energy Conservation in Buildings and Community Systems", International Energy Agency, July, 2007.

Wu Y. "Experimental Study of Hygrothermal Properties for Building Materials", Master thesis, Department of Building, Civil and Environmental Engineering, Concordia University, Montreal, Quebec, Canada: July 2007.

Wu Y, Kumaran M, Fazio P. "Moisture Buffering Capacities of Five North American Building Materials", Journal of Testing and Evaluation 2008; Vol. 36, No. 1: 7 pages.

Yang CS, Heinsohn PA. "Sampling and Analysis of Indoor Microorganisms", Published by Wiley-Interscience, 2007.

Zhang J. "Combined Heat, Air, Moisture, and Pollutants Transport in Building Environmental Systems", JSME International Journal Series B 2005; Vol. 48, No. 2: 182-190.